SHRP-C-365

Mechanical Behavior of High Performance Concretes, Volume 5

Very High Strength Concrete

Paul Zia
Shuaib H. Ahmad
Michael L. Leming
North Carolina State University
Raleigh, North Carolina

John J. Schemmel
Robert P. Elliott
University of Arkansas
Fayetteville, Arkansas

Strategic Highway Research Program
National Research Council
Washington, DC 1993

SHRP–C–365
ISBN 0-309-05624-1
Contract C-205
Product No. 2014, 2023, 2024

Program Manager: *Don M. Harriott*
Project Manager: *Inam Jawed*
Production Editor: *Cara J. Tate*
Program Area Secretary: *Carina S. Hreib*

November 1993

key words:
admixture
aggregate
compressive strength
concrete mixture
durability
fly ash
high performance concrete
portland cement concrete
early strength
high strength
silica fume

Strategic Highway Research Program
National Academy of Sciences
2101 Constitution Avenue N.W.
Washington, DC 20418

(202) 334-3774

1 5M/NAP/1193

Acknowledgments

The research described herein was supported by the Strategic Highway Research Program (SHRP). SHRP is a unit of the National Research Council authorized by section 128 of the Surface Transportation and Uniform Relocation Assistance Act of 1987.

The research was conducted by a consortium among researchers at North Carolina State University (prime contractor), the University of Arkansas, and the University of Michigan. The team included Paul Zia, Shuaib H. Ahmad, and Michael L. Leming at North Carolina State University; John J. Schemmel and Robert P. Elliott at the University of Arkansas; and A. E. Naaman at the University of Michigan.

The late Robert E. Philleo served as a project consultant during the initial stage of the project. He helped in defining the criteria for high performance concrete and in setting the direction of the research. The research team benefited greatly from his many stimulating discussions and guidance.

The research team also received valuable support, counsel, and guidance from the Expert Task Group. The support and encouragement provided by Inam Jawed, SHRP program manager, are deeply appreciated.

Special recognition is given to New York Department of Transportation, North Carolina Department of Transportation, Illinois Department of Transportation, Arkansas State Highway and Transportation Department, and Nebraska Department of Roads. The cooperation and assistance given by the staffs of these five state transportation agencies were critical to the field installations of pavements to demonstrate the use of high performance concrete.

A group of materials producers and suppliers donated the materials used for the laboratory studies of high performance concrete. These industrial partners included Blue Circle Cement, Inc.; Pyrament/Lone Star Industries, Inc.; Martin Marietta Company; Memphis Stone and Gravel Co.; McClinton-Anchor; Arkhola Sand and Gravel; Monex Resources, Inc.; Fly Ash Products; Elkem Chemicals; Cormix; Dow Chemical; and W. R. Grace. Their generous support of this research program is deeply appreciated.

The authors of this report would also like to acknowledge the contributions of many collaborators who participated in the various phases of this research program. They include former and present graduate research assistants William K. Chi, Wayne L. Ellenberger, M. R.

Hansen, Aykut Cetin, Kristina M. Hanes, Johnny D. Waycaster, Randy Maccaferri, and Dena Firebaugh and former undergraduate laboratory assistants Randall A. Boyd, Joseph B. Taylor, Wesley N. Denton, and Harold D. Ingram at North Carolina State University. The collaborators at the University of Arkansas include former and present graduate research assistants James R. Powell, Vikas Arora, and Mike Callahan and former undergraduate laboratory assistant Memory Rodgers.

Opinions expressed in this report reflect the views of the authors, who should be held accountable for any errors and omissions.

Contents

Acknowledgments iii

List of Figures vii

List of Tables ix

Preface xi

Abstract 1

Executive Summary 3

1 **Introduction** 7

1.1 Definition of Very High Strength Concrete 8
1.2 Potential Applications of VHS concrete 9

2 **Objective and Scope** 11

3 **Characterizations of Constituent Materials** 13

3.1 Cements 13
3.2 Coarse Aggregates 13
3.3 Fine Aggregates 15
3.4 Chemical Admixtures 16
3.5 Mineral Admixtures 17

4 **Mixture Proportions** 19

5 Mixing and Curing Procedures 21

5.1 Mixing Procedures 21
5.2 Curing Procedures 22

6 Laboratory Experiments 23

6.1 Compression Tests 23
6.2 Tension Tests 37
6.3 Freezing-Thawing Tests 47
6.4 Shrinkage Tests 59
6.5 Creep Tests 62
6.6 Rapid Chloride Permeability Tests 64
6.7 AC Impedance Tests 66
6.8 Concrete-to-Steel Bond Tests 70

7 Conclusions 75

References 79

Appendix 81

List of Figures

Figure 6.1 Stress-strain relationship of VHS (F) concrete at design age of 28 days.....28
Figure 6.2 Stress-strain relationship of VHS (S) concrete at design age of 28 days.....28
Figure 6.3a Effect of age on stress-strain curve for VHS (F) concrete with RG 30
Figure 6.3b Effect of age on stress-strain curve for VHS (S) concrete with RG 30
Figure 6.4a Variation of compressive strength with time for VHS (F) concrete 33
Figure 6.4b Variation of compressive strength with time for VHS (S) concrete 33
Figure 6.5a Variation of modulus of elasticity with time for VHS (F) concrete 34
Figure 6.5b Variation of modulus of elasticity with time for VHS (S) concrete 34
Figure 6.6a Comparison of observed versus predicted modulus of elasticity of VHS concrete considering all test ages 36
Figure 6.6b Average size effect of VHS (S) concrete at design age.....36
Figure 6.7 Comparison of observed versus predicted split cylinder strength of VHS concrete at design age.....42
Figure 6.8 Comparison of oberved versus predicted modulus of rupture of VHS concrete at design age 42
Figure 6.9a Variation of modulus of rupture with time for VHS (F) concrete 43
Figure 6.9b Variation of modulus of rupture with time for VHS (S) concrete 43
Figure 6.10a Load versus midspan deflection of VHS (F) concrete at design age of 28 days 44
Figure 6.10b Load versus midspan deflection of VHS (S) concrete at design age of 28 days 44
Figure 6.11a Load versus midspan deflection of VHS (F) concrete with MM.....45
Figure 6.11b Load versus midspan deflection of VHS (S) concrete with MM 45
Figure 6.12a Load versus tensile strain of VHS (F) concrete at design age of 28 days.....46
Figure 6.12b Load versus tensile strain of VHS (S) concrete at design age of 28 days.....46
Figure 6.13a Load versus tensile strain of VHS (F) concrete with MM.....48
Figure 6.13b Load versus tensile strain of VHS (S) concrete with MM.....48
Figure 6.14 Relative dynamic modulus versus number of freezing-thawing cycles for C/VH(F)/3 55
Figure 6.15 Relative dynamic modulus versus number of freezing-thawing cycles for C/VH(S)/3 56
Figure 6.16 Relative dynamic modulus versus number of freezing-thawing cycles for R/VH(S)/3 57
Figure 6.17 Relative dynamic modulus versus number of freezing-thawing cycles for M/VH(S)/3 58

Figure 6.18 Variation of shrinkage strain with time for VHS Concretes 61
Figure 6.19a Variation of creep strain with time for VHS (F) concrete 63
Figure 6.19b Variation of creep strain with time for VHS (S) concrete 63
Figure 6.20 Comparisons of results from AC impedance test and RCPT 71
Figure 6.21a Stress versus net slip for VHS (F) concrete in C-S bond test 73
Figure 6.21b Stress versus net slip for VHS (S) concrete in C-S bond test 73

List of Tables

Table 2.1 Types of coarse and fine aggregates 11

Table 3.1 Results of physical and chemical analyses of Type I cements compared with ASTM C 150 14
Table 3.2 Properties of coarse aggregates 15
Table 3.3 Properties of fine aggregates 16
Table 3.4 Chemical admixtures used in the test program 16
Table 3.5 Results of physical and chemical analyses of fly ash 17

Table 4.1 Mixture proportions of VHS (F) concrete 20
Table 4.2 Mixture proportions of VHS (S) concrete 20

Table 6.1 Test program for compressive strength and modulus of elasticity — Group 1 24
Table 6.2 Test program for modulus of rupture, tensile strain capacity, and split tensile strength — Group 2 24
Table 6.3 Test program for frost durability, shrinkage, creep, and chloride permeability — Group 3 25
Table 6.4 Test program for bond strength — Group 5 25
Table 6.5a Summary of test results for compressive strength and modulus of elasticity at different test ages for VHS (F) concrete 31
Table 6.5b Summary of test results for compressive strength and modulus of elasticity at different test ages for VHS (S) concrete 32
Table 6.6 Summary of test results for 4 x 8-in. and 6 x 12-in. cylinder strengths for VHS (S) concrete 35
Table 6.7a Summary of test results for modulus of rupture, tensile strain capacity, and split cylinder tensile strength for VHS (F) concrete 39
Table 6.7b Summary of test results for modulus of rupture, tensile strain capacity, and split cylinder tensile strength for VHS (S) concrete 40
Table 6.8a Mixture proportions, strength, and plastic properties of VHS (F) concrete used for freezing-thawing test specimens 51
Table 6.8b Mixture proportions, strength, and plastic properties of VHS (S) concrete used for freezing-thawing test specimens 52
Table 6.9 Results of freezing-thawing test of VHS concrete 54
Table 6.10 Summary of shrinkage test results for VHS (F) and VHS(S) concretes 60
Table 6.11 Results of rapid chloride permeability test (RCPT) of VHS concrete 67

Table 6.12 Results of AC impedance test of VHS concrete 69
Table 6.13 Summary of test results of concrete-to-steel bond tests for VHS (F) and VHS (S) concretes 72

Preface

The Strategic Highway Research Program (SHRP) is a 5-year, nationally coordinated research effort initiated in 1987 at a cost of $150 million. This highly focused and mission oriented program originated from a thorough and probing study* to address the serious problems of deterioration of the nation's highway and bridge infrastructure. The study documented the need for a concerted research effort to produce major innovations for increasing the productivity and safety of the nation's highway system. Further, it recommended that the research effort be focused on six critical areas in which the nation spends most of the $50 billion used for roads annually and thus technical innovations could lead to substantial payoffs. The six critical research areas were as follows:

- Asphalt Characteristics
- Long-Term Pavement Performance
- Maintenance Cost-Effectiveness
- Concrete Bridge Component Protection
- Cement and Concrete
- Snow and Ice Control

When SHRP was initiated, the two research areas of Concrete Bridge Component Protection and Cement and Concrete were combined under a single program directorate of Concrete and Structures. Likewise, the two research areas of Maintenance Cost-Effectiveness and Snow and Ice Control were also combined under another program directorate of Highway Operations.

* *America's Highways: Accelerating the Search for Innovation.* 1984. Special Report 202, Transportation Research Board, National Research Council, Washington, D. C.

Abstract

This report documents laboratory investigations of the mechanical behavior of high performance concrete for highway applications. High performance concrete is defined as concrete with much higher early strength and greatly enhanced durability against freezing and thawing compared with conventional concrete. Very high strength (VHS) concrete is one of the three categories of high performance concrete investigated in this program. The objective is to obtain information on the mechanical behavior of VHS concrete.

The laboratory investigation consisted of tests for both fresh or plastic concrete and hardened concrete. The plastic concrete tests included slump, air content, etc.; the results of these tests are presented in volume 2 of this report series, *Production of High Performance Concrete.* The hardened concrete tests include compression tests for strength amd modulus of elasticity, tension tests for tensile strength and flexural modulus, freezing-thawing tests for durability factor, shrinkage tests, creep tests, rapid chloride permeability tests, tests for AC impedance, and tests for bond between concrete and steel reinforcement.

Executive Summary

This report documents laboratory investigations of the mechanical behavior of high performance concrete for highway applications. High performance concrete (HPC) is defined as concrete with much higher early strength and greatly enhanced durability against freezing and thawing compared with conventional concrete. Very high strength (VHS) concrete is one of the three categories of high performance concrete investigated in this program. The objective is to obtain information on the mechanical behavior of VHS concrete.

For the purpose of this program, HPC is defined in terms of certain *target* strength and durability requirements as shown below:

Category of High Performance Concrete	Minimum Compressive Strength	Maximum Water/ Cement Ratio	Minimum Frost Durability Factor
Very early strength (VES)			
Option A (with Type III cement)	2,000 psi (14 MPa) in 6 hours	0.40	80%
Option B (with Pyrament PBC-XT cement)	2,500 psi (17.5 MPa) in 4 hours	0.29	80%
High early strength (HES) (with Type III cement)	5,000 psi (35 MPa) in 24 hours	0.35	80%
Very high strength (VHS) (with Type I cement)	10,000 psi (70 MPa) in 28 days	0.35	80%

In the above definition, the target minimum strength should be achieved in the specified time after water is added to the concrete mixture. The compressive strength is determined from 4 x 8-in. (100 x 200-mm) cylinders tested with neoprene caps. The water/cement ratio (W/C) is based on all cementitious materials. The minimum durability factor of 80% should be achieved after 300 cycles of freezing and thawing according to ASTM C 666, procedure A. This is in contrast to a durability factor of 60% for conventional concrete.

So that the research results would be applicable to different geographical regions, four different types of coarse aggregate were selected for producing VHS concrete. They included crushed granite and marine marl from North Carolina, dense crushed limestone from Arkansas, and washed rounded gravel from Tennessee. These aggregates were used with local sand from the three states. The characteristics of all constituent materials used for producing VHS concrete are described in detail in terms of their physical, chemical, and mineral properties. The normal laboratory mixing and batching procedures (ASTM C 192) were modified slightly to represent typical concrete dry-batch plant operations more closely.

The laboratory investigation consisted of tests for both fresh or plastic concrete and hardened concrete. The plastic concrete tests included slump, air content, etc.; the results of these tests are presented in volume 2 of this report series, *Production of High Performance Concrete.* The hardened concrete tests included compression tests for strength and modulus of elasticity, tension tests for tensile strength and flexural modulus, freezing-thawing tests for durability factor, shrinkage tests, creep tests, rapid chloride permeability tests, AC impedance tests, and tests for bond between concrete and steel reinforcement.

Based on the experience of the laboratory investigations, the following conclusions were drawn:

1. Using conventional materials and equipment, but with more care than needed for conventional concrete, VHS concrete with either fly ash or silica fume as the mineral admixture can be produced that will achieve a minimum compressive strength of 10,000 psi (70 MPa) in 28 days. Such concretes can be produced with either crushed granite or dense crushed limestone as coarse aggregate. However, with weaker aggregates such as marine marl and washed rounded gravel, the compressive strength would be slightly lower for comparable mixture proportions.

2. Because the demand for early strength gain is not critical for VHS concrete, it is not necessary to use insulation for curing under normal conditions.

3. Because of a larger amount of Type I cement plus fly ash or silica fume used in the VHS concrete mixtures along with a relatively low W/C, the strength development of the concretes is much more rapid in the first 7 days than predicted by the current recommendation of ACI Committee 209 (1993a) based on conventional concrete. The subsequent rate of strength growth is greatly reduced and is comparable to that predicted by the ACI method.

4. The modulus of elasticity increases with time in the same manner as the compressive strength. The same is true of the flexural modulus.

5. Because the design strength of VHS concrete is not too much higher than the upper ranges of the conventional concrete, the mechanical behavior of VHS concrete, such as the modulus of elasticity and the compressive and tensile strain capacities, is similar to that of conventional concrete. The modulus of elasticity, the flexural

modulus, and the splitting tensile strength can still be predicted reasonably well by the ACI Code equations (1993c).

6. As VHS concrete ages in time, its stress-strain relationship becomes more linear.

7. VHS concrete with silica fume [VHS (S)] appeared to be slightly stiffer than VHS concrete with fly ash [VHS (F)] as measured by the modulus of elasticity. The modulus of elasticity is lower for concrete with softer aggregates such as marine marl.

8. The observed compressive strain capacity ranged from 1,000 to 2,500 microstrains. The VHS (F) concrete exhibited slightly higher compressive strain capacity than the VHS (S) concrete. The tensile strain capacity varied from 120 to 180 microstrains. The VHS (F) concrete exhibited lower tensile strain capacity than the VHS (S) concrete. These strain capacities are comparable to those of conventional concrete.

9. Even with a very low W/C, VHS concrete should have an adequate amount of air entrainment to enhance its freezing-thawing resistance. The results of this investigation indicate that VHS concrete will meet the stringent requirement of a durability factor of 80% (in contrast to 60% commonly expected of quality conventional concrete) after 300 cycles of freezing and thawing according to ASTM C 666, procedure A, if the concrete contains at least 5% entrained air.

10. VHS concrete produced with washed rounded gravel from Memphis, Tennessee failed the freezing-thawing test according to ASTM C 666-90, procedure A, because of the deterioration of the aggregate, even though the concrete contained 8% entrained air. The aggregate had an absorption of about 5% and pore size of about 0.10 microns (as observed from scanning electron micrographs), the worst possible condition for freezing-thawing deterioration (Hansen 1993).

11. Shrinkage of VHS concrete follows the general trend of conventional concrete. The average shrinkage strain of VHS (F) concrete with crushed granite aggregate was 521 microstrains at 90 days, which is about 70% of the ultimate shrinkage strain recommended by ACI Committee 209 for the conventional concrete. On the other hand, the average 90-day shrinkage strains of VHS (S) concrete varied from -72 microstrains for concrete with washed rounded gravel aggregate to 361 microstrains for concrete with crushed granite aggregate, which indicates that VHS (S) concrete has even less shrinkage potential than VHS (F) concrete.

12. The observed creep strains of the different groups of VHS concrete ranged from 20% to 50% of that of conventional concrete. The creep strains were especially low for concretes with a 28-day strength in excess of 10,000 psi (70 MPa). The specific creep of the concrete with marine marl was much higher than that of the concrete with either crushed granite or washed rounded gravel.

13. With very low W/C and using silica fume or fly ash as mineral additive, VHS concrete after 14 days of moist curing exhibited fairly low chloride permeability based on the rapid chloride permeability test (RCPT).

14. The initial current (in amperes) flowing through the concrete specimen in the RCPT correlates consistently with the total charge measured in 6 hours. Therefore the initial current, which is an indirect measure of the concrete conductance, can be used as an alternate measurement for the RCPT. The total testing time can thus be shortened by 6 hours.

15. The AC impedance test measures the total resistance (in ohms) of a concrete specimen. This test method is simpler and faster than the RCPT and has the potential to be used as a substitute for the RCPT. The best correlation between the two test methods is to express the inverse impedance (reciprocal of impedance) in terms of the initial current measured in the RCPT.

16. A "beam" type concrete-to-steel bond test showed that by using the ACI 318 requirement for development length (1993c), sufficient bond strength was developed by VHS concrete that the steel reinforcement yielded before any significant bond slip occurred.

1

Introduction

SHRP's research on mechanical behavior of high performance concretes had three general objectives:

1. To obtain needed information to fill gaps in the present knowledge;
2. To develop new, significantly improved engineering criteria for the mechanical properties and behavior of high performance concretes; and
3. To provide recommendations and guidelines for using these concretes in highway applications according to the intended use, required properties, environment, and service.

Both plain and fiber-reinforced concretes were included in the study. The research findings are presented in a series of six project reports:

Volume 1 *Summary Report*

Volume 2 *Production of High Performance Concrete*

Volume 3 *Very Early Strength (VES) Concrete*

Volume 4 *High Early Strength (HES) Concrete*

Volume 5 *Very High Strength (VHS) Concrete*

Volume 6 *High Early Strength Fiber-Reinforced Concrete (HESFRC)*

This volume is the fifth of these reports. The readers will notice a certain uniformity in format and similarity in many general statements in these reports. This feature is adopted intentionally so that each volume of the reports can be read independently without the need to cross reference to other reports in the series.

1.1 Definition of Very High Strength Concrete

Very high strength (VHS) concrete is one of the three categories of high performance concrete (HPC) investigated in this research program. In volume 2 of this report series, *Production of High Performance Concrete*, the strength and durability criteria were defined for each of the three categories of HPC.

For VHS concrete, a minimum compressive strength of 10,000 psi (69 MPa) is required in 28 days with a maximum water/cement ratio (W/C) of 0.35. It must also achieve a minimum durability factor of 80% at 300 cycles of freezing and thawing according to ASTM C 666, procedure A. These criteria were adopted after several important factors pertinent to the construction and design of highway pavements and structures were considered. The rationale for the selection of the various limits is as follows.

The choice of a time requirement of 28 days for VHS concrete is based on conventional construction practice, in which time would not be a critical factor. It is considered unnecessary to extend this time requirement to a longer period, such as 56 days, as in many previous construction projects using moderately high strength concrete (Zia et al. 1991).

The use of 10,000 psi (69 MPa) as the strength criterion for VHS concrete is based in part on the results of previous research (Jobse and Moustafa 1984, Zia et al. 1989), which indicates that concrete strength of 8,000 to 10,000 psi (55.2 to 69 MPa) is optimal for the current AASHTO standard bridge girders, and in part on cost considerations indicating that concrete cost increases substantially when its strength level exceeds 10,000 psi (69 MPa).

The W/C specified is relatively low. For VHS concrete, a low W/C is needed to meet the high strength requirement. With low W/C, concrete durability may be improved in all exposure conditions. Since HPC is intended for highway applications where exposure to frost must be expected, it must be frost resistant.

The choice of an appropriate measure for frost durability is debatable and subjective. It is recognized that ASTM C 666, procedure A, which involves freezing and thawing in water, is a severe test. Therefore a durability criterion should not be unduly conservative. On the other hand, if HPC is to provide enhanced durability, it can be argued that higher standards are required. Since frost durability of concrete as measured by ASTM C 666, procedure A, is highly dependent on the air void system, and since freezing low-permeability concrete at the very high rate as required in the test procedure tends to discriminate against concrete of low W/C, the selected durability factor of 80% at 300 cycles of freezing and thawing is considered appropriate. This is in contrast to a durability factor of 60% commonly expected of quality conventional concrete according to ASTM C 666.

1.2 Potential Applications of VHS Concrete

VHS concrete is useful primarily for structural members for which construction time is not a critical factor. Little, if any, direct application of HVS concrete to pavement is anticipated. However, if including a mineral admixture such as silica fume or fly ash would improve abrasion resistance or prevent deleterious alkali-silica reactivity, VHS concrete might be chosen for application in a pavement or bridge deck. In addition, VHS concrete provides considerable structural advantages and economy when used in bridge girders, precast elements, prestressed piles, columns, and piers.

2

Objective and Scope

The objective of this investigation was to develop and analyze basic data on the mechanical properties of very high strength (VHS) concrete for highway applications. The concrete was produced using *only conventional constituent materials and normal production and curing procedures.* The laboratory experiments included eight different types of tests: compression, tension (both flexure and splitting), freezing-thawing, shrinkage, creep, rapid chloride permeability, AC impedance, and concrete-to-steel bond.

VHS concrete was produced in the laboratory with four different types of coarse aggregate and three kinds of sand, as summarized in Table 2.1.

Table 2.1 Types of coarse and fine aggregates

Type	Symbol	Source
Marine Marl	MM	Castle Hayne, North Carolina
Crushed Granite	CG	Garner, North Carolina
Dense Crushed Limestone	DL	West Fork, Arkansas
Washed Rounded Gravel	RG	Memphis, Tennessee
Sand		Lillington, North Carolina
Sand		Memphis, Tennessee
Sand		Van Buren, Arkansas

The studies using crushed granite, marine marl, and washed rounded gravel were conducted at North Carolina State University (NCSU); the studies using dense crushed limestone were conducted at the University of Arkansas. Lillington sand was used for the concretes made with crushed granite or marine marl, but Memphis sand was used for the concrete made with washed rounded gravel. Van Buren sand from the Arkansas River was used for the concrete made with dense crushed limestone.

3

Characterizations of Constituent Materials

3.1 Cements

Type I cement was used for the production of very high strength (VHS) concrete. The cement used at North Carolina State University (NCSU) was of low alkali content and met the requirements of ASTM C 150 specifications. It was supplied by Blue Circle Cement, Inc., from its plant in Harleyville, South Carolina. The cement used at Arkansas was supplied by the same manufacturer from its plant in Tulsa, Oklahoma.

The results of physical and chemical analyses of the cements are summarized in Table 3.1 along with the requirements of relevant ASTM specifications for comparison.

3.2 Coarse Aggregates

Four different types of coarse aggregates were used in this investigation. They were chosen as representative aggregates from a wide geographical area. Crushed granite (CG) is a strong, durable aggregate locally available in North Carolina; it was supplied by Martin Marietta Co. from its quarry in Garner. Marine marl (MM) is a weaker and more absorptive aggregate available in the coastal area of North Carolina; it was also supplied by Martin Marietta Co. from its quarry in Castle Hayne. Washed rounded gravel (RG) was provided by Memphis Stone and Gravel Co. from its Pit 558 in Shelby County, Tennessee. Dense crushed limestone (DL) was supplied by McClinton-Anchor from its West Fork quarry just outside Fayetteville, Arkansas.

The coarse aggregates used at NCSU met ASTM C 33 size #57 specifications, with most of the material passing the 1-in. (25-mm) sieve. The CG was a hard, angular aggregate of low absorption (0.6%). The MM was a cubical to subangular, relatively porous, and highly absorptive (typically more than 4.5%) shell limestone. The RG, drawn from a river, was primarily silicious and contained some crushed faces, but most of them were worn. The absorption was moderate (just under 3%), and hard chert particles were present. The maximum size of the DL used at Arkansas was slightly smaller and met ASTM C 33 size #67 specifications.

Table 3.1 Results of physical and chemical analyses of Type I cements compared with ASTM C 150

	ASTM C 150 Type I	Type I* NCSU	Type I+ Arkansas
Fineness			
Specific surface (Blaine)	2,800 cm^2/g	3,200 cm^2/g	3,970 cm^2/g
Soundness			
Autoclave expansion	0.80%	-0.01%	0.02%
Time of setting (Gillmore)			
Initial	1 hr	—	3 hr 2 min
Final	10 hr	—	4 hr 10 min
Water required			
1:2.75 mortar cubes	–	48.5%	—
Air temperature	–	73°F	—
Relative humidity	–	70%	—
Compressive strength (psi), 2-in. mortar cubes			
1 day	—	—	2,208
3 days	1,800	3,150	3,692
7 days	2,800	5,060	4,583
Silicon dioxide (SiO_2), %	–	20.81	19.35
Aluminum oxide (Al_2O_3), %	–	5.26	5.59
Iron oxide (Fe_2O_3), %	–	3.61	2.23
Calcium oxide (CaO), %	—	64.80	64.72
Magnesium oxide (MgO), %	6.0	0.92	2.30
Sulfur trioxide (SO_3), %	3.5	2.66	2.93
Loss on ignition, %	3.0	1.34	1.36
Sodium oxide (Na_2O),%	–	—	0.25
Potassium oxide (K_2O), %	—	—	0.63
Total equivalent alkali content, %	0.60	0.21	0.66
Tricalcium silicate, %	—	57.51	67.32
Dicalcium silicate, %	—	16.28	4.69
Tricalcium aluminate, %	—	7.84	11.04
Tetracalcium aluminoferrite, %	—	10.99	6.79
Insoluble residue, %	0.75	0.11	0.25

Note: 1 MPa = 145 psi

* Tests performed by the Materials and Tests Unit of North Carolina DOT

\+ Tests performed by the Materials Division of Arkansas DOT

Mineralogically, the CG consisted of approximately 35% quartz, 30% potassium feldspar, 25% sodium-rich plagioclase feldspar, and 10% biotite. The MM was a sandy fossiliferous limestone with about 60% calcite, 35% quartz, and 5% other oxide and hydroxide minerals. The RG consisted of 25% quartz, 10% quartzite, 60% chert, and 5% sandstone. The DL contained about 97% limestone and 3% clay minerals. It should be noted that the RG contained a large amount of chert, which could be a cause for alkali-silica reaction.

Physical analyses of the coarse aggregates were performed according to ASTM C 33, and the results are shown in Table 3.2.

Table 3.2 Properties of coarse aggregates

	CG	MM	RG	DL
Specific gravity (SSD)	2.64	2.48	2.55	2.72
% absorption	0.6	6.1	2.8	0.69
DRUW (pcf)	93.6	78.4	94.8	99.0
Fineness modulus	6.95	6.92	6.99	6.43
% Passing				
1 in.	100	98	95	100
3/4 in.	90	85	72	100
1/2 in.	31	43	56	82
3/8 in.	13	19	26	48
#4	2	4	1	6
#8	0	0	2	3
L.A. abrasion, %				
Grading A	—	—	17.6	—
Grading B	39.6	43.7	—	24
Sodium sulfate soundness, %	1.3	9.6	2.8	3
Less than 200 by washing, %	0.6	0.4	—	—

3.3 Fine Aggregates

Three different kinds of sand were used in this test program. The sand used with CG and MM was obtained from Lillington, North Carolina. The sand used with RG was shipped from Memphis, Tennessee, and Arkansas River sand from Van Buren, Arkansas was used with DL.

The Lillington sand contained 75% quartz, 22% feldspar, and 3% epidote. The finer material (passing #10 sieve) of the Memphis sand consisted of 95% quartz, 4% opaque minerals (oxide and hydroxide minerals), and 1% other miscellaneous minerals; the coarser material (retained on #10 sieve) consisted of 20% chert, 30% sandstone and shale fragments, and 50% quartz. The finer material of the Van Buren sand consisted of 85% quartz, 4% chert, 11% microcline, and

less than 1% rock fragments and heavy minerals; the coarser material consisted of 62% quartz, 16% chert, 11% microcline, and 5% rock fragments. The characteristics of the three kinds of sand are shown in Table 3.3.

3.4 Chemical Admixtures

Chemical admixtures used in the production of VHS concrete included a HRWR, an air-entraining agent (AEA), and a retarder. Their brand names, suppliers, and reference specifications are identified in Table 3.4.

Table 3.3 Properties of fine aggregates

	Lillington Sand	Memphis Sand	Van Buren Sand
Specific gravity (SSD)	2.57	2.62	2.62
% absorption	1.1	1.2	0.6
Fineness modulus	2.66	2.60	2.72
% passing			
#4	100	100	96
#8	97	93	88
#16	80	82	75
#30	47	55	55
#50	9	9	13
#100	1	1	0.4

Table 3.4 Chemical admixtures used in the test program

Admixture	Brand Name	Supplier	Reference Specifications
HRWR	PSI Super (naphthalene base)	Cormix	ASTM C 494, Type F
AEA	Daravair (neutral vinsol resin), 17% solids	W. R. Grace	ASTM C 260
Retarder	PSI 400R (lignin base)	Cormix	ASTM C 494, Type D

3.5 Mineral Admixtures

Mineral admixtures used for VHS concrete included fly ash (classes F and C) and silica fume. The class F fly ash used for the tests in North Carolina was supplied by Monex Resources, Inc., from its plant at Belews Creek, North Carolina. The class C fly ash used for the tests in Arkansas was supplied by Fly Ash Products in Pine Bluff, Arkansas. Class F fly ash typically contains much less calcium than class C fly ash. Therefore, although both are pozzolanic, class C fly ash usually has cementitious properties. The results of physical and chemical analyses of the fly ash are given in Table 3.5 along with the requirements of ASTM C 618 for comparison.

The silica fume used for the tests in North Carolina was EMSAC, Type F-100, supplied by Elkem Chemicals, Pittsburgh, Pennsylvania (now a subsidiary of Cormix). It was in slurry form, containing approximately 50% solids. In contrast, the silica fume for the tests in Arkansas was in powder form supplied by Cormix.

Table 3.5 Results of physical and chemical analyses of fly ash

	ASTM C 618 Class F	Class F* NCSU	ASTM C 618 Class C	Class C+ Arkansas
Fineness: Retained on no. 325 sieve, %	34	26.5	34	12.06
Soundness: Autoclave expansion, %	0.8	—	0.8	—
Specific gravity	—	2.20	—	2.58
Silicon dioxide plus iron and aluminum oxides, %	70	96.0	50	63.3
Calcium oxide, %	—	—	—	29.70
Magnesium oxide, %	—	—	—	5.1
Sulfur trioxide, %	5	0.5	5	1.9
Moisture content, %	3	0.4	3	0.05
Loss on ignition, %	6	1.1	6	0.1

* Analyses performed by the Materials and Tests Unit of North Carolina DOT
\+ Analyses performed by the Materials Division of Arkansas DOT

4

Mixture Proportions

In the early stage of this investigation, extensive development work involving a total of 360 trial batches of concrete was conducted to determine appropriate mixture proportions for the various types of high performance concrete. A detailed discussion of this development work can be found in volume 2 of this report series, *Production of High Performance Concrete.* For VHS concrete, the development work included 75 trial batches using four different kinds of coarse aggregate.

Proportioning of the concrete mixtures was based on the methods recommended by ACI Committee 211 (1993b). Selections of W/C, workability, and air content requirements were made first and these constraints were incorporated in accordance with the ACI Committee 211 guidelines, as was selection of aggregate quantities. Trial batches were formulated for several different percentages of mineral admixtures with several different amounts of portland cement.

At NCSU, a nominal maximum size (NMSA) of 1 in. (25 mm) (ASTM C 33, size #57) for the coarse aggregate was selected as being the most appropriate for a variety of applications. This aggregate size could be used for many structural members. The coarse aggregate used at Arkansas was slightly smaller (ASTM C 33, size #67).

Although the quantity of coarse aggregate (volume of coarse aggregate per unit volume of concrete) could have been increased by about 10% for paving applications, the quantity initially selected was at or near the recommended value in ACI Committee 211. These values were adjusted slightly in subsequent trial batches. The purpose of selecting a less coarse mixture was to provide a more general-purpose mixture.

Following evaluation of the results of the trial batches, the mixture proportions for VHS concrete with fly ash [VHS (F)] and VHS concrete with silica fume [VHS (S)] concretes with four different types of aggregate were selected, and they are summarized in Tables 4.1 and 4.2.

Table 4.1 Mixture proportions of VHS (F) concrete

Aggregate type:	CG	MM	RG	DL
Source of sand:	Lillington	Lillington	Memphis	Van Buren
Type of fly ash:	F	F	F	C
Cement (Type I), pcy	830	830	830	830
Fly ash, pcy	200	200	200	200
Coarse aggregate, pcy	1,720	1,570	1,650	1,680
Sand, pcy	937	900	860	1,020
HRWR (Naphthalen-based), oz/cwt	26	20	20	18
Retarder, oz/cwt	3.0	3.0	3.0	3.0
AEA, oz/cwt	3.5	1.3	1.2	2.5
Water, pcy	240	240	240	240
W/(C+FA)	0.23	0.23	0.23	0.23
Slump, in.	3.5	10	7.0	3.75
Air, %	5.5	8.0	2.0	4.8
Strength at 28 days, psi	12,200	7,620	8,970	9,833
Concrete temperature at placement, ^{o}F	80	72	69	76

Table 4.2 Mixture proportions of VHS (S) concrete

Aggregate type:	CG	MM	RG	DL
Source of sand:	Lillington	Lillington	Memphis	Van Buren
Cement (Type I), pcy	760	760	760	770
Silica fume, pcy	35	35	35	35
Coarse aggregate, pcy	1,720	1,570	1,650	1,680
Sand, pcy	1,206	1,140	1,150	1,250
HRWR (Naphthalene-based), oz/cwt	14	12	14	17
Retarder, oz/cwt	2.0	2.0	3.0	3.0
AEA, oz/cwt	0.9	0.6	0.9	1.5
Water, pcy	230	240	240	230
W/(C+SF)	0.29	0.30	0.30	0.29
Slump, in.	2.75	4.25	3.0	2.75
Air, %	5.0	5.6	7.3	5.1
Strength at 28 days, psi	11,780	8,460	9,120	10,010
Concrete temperature at placement, ^{o}F	80	77	80	75

5

Mixing and Curing Procedures

5.1 Mixing Procedures

Concretes made with crushed granite (CG), marine marl (MM), or washed rounded gravel (RG) were produced in the Concrete Materials Laboratory at North Carolina State University (NCSU) using a tilt-drum mixer with a rated capacity of 3.5 ft^3 (0.1 m^3). Concretes using dense crushed limestone (DL) were produced also in an identical mixer in the Concrete Laboratory at the University of Arkansas. The normal laboratory mixing and batching procedures (ASTM C 192) were modified slightly to represent typical concrete dry-batch plant operations more closely. Whether the concrete was produced at NCSU or Arkansas, the same general mixing procedures were followed.

VHS concrete used Type I portland cement and either fly ash or silica fume as pozzolan. The mixing procedure followed these steps:

1. Butter the mixer with a representative sample of mortar composed of approximately 3 lb (1.36 kg) cement, 6 lb (2.73 kg) sand, and 2 lb (0.91 kg) water. Turn on the mixer to coat the interior completely. (At Arkansas, only water was used to butter the mixer.) Empty the mixer and drain it for 1 minute.

2. Charge the mixer successively with approximately 25% of the coarse aggregate, 67% of thesand, 50% of the water, and 100% of the air entraining agent (AEA) added with the sand. Mix for 1 minute to generate air bubbles. The amount of water may be varied slightly to obtain a thick slurry. (At Arkansas, the mixer was charged with 0.33% of the coarse aggregate, 50% of the sand, and 67% of the water.)

3. Stop the mixer and add the remaining coarse aggregate, sand, water, and retarder. Mix for 10 seconds to coat sand and rock with water. If silica fume is used, add it with the sand.

4. Add cement (and fly ash, if used). Record the time as the beginning of the total mixing time. Mix for 1 minute. Stop the mixer and add the high-range water reducer

(HRWR). Mix for a minimum of 10 minutes, until a homogeneous mass of acceptable workability has been achieved. During all mixing, cover the mixer with a lid to minimize evaporation.

5. Discharge the concrete into a wheelbarrow; measure unit weight, air content, slump, and temperature; and fabricate test specimens.

5.2 Curing Procedures

Curing procedures differed for different categories of high performance concrete. For VHS concrete, the demand for early strength gain was not as critical as for very early strength (VES) concrete, thus it was not necessary to use insulation for curing.

VHS concrete specimens were cast in steel molds except in Arkansas, where plastic molds were used. The specimens were maintained for the first 20 to 24 hours at 60° to 80°F (15.6° to 26.7°C) and were protected from evaporation; they were then removed from their molds and placed in an atmosphere with 100% RH at 71° to 75°F (21.7° to 23.9°C) until testing. Some of the specimens with DL were soaked in limewater. After the specimens were removed from the moist curing room or limewater bath, they were allowed to dry in the laboratory for at least 1 hour before they were tested for strength. The drying was necessary to permit adhesion of linear voltage differential transducer (LVDT) connections during testing.

6

Laboratory Experiments

The laboratory investigation consisted of tests for both fresh or plastic concrete and hardened concrete. Plastic concrete were tested for slump, air content, etc.; the results of these tests are presented in volume 2 of this report series, *Production of High Performance Concrete*. The tests for hardened concrete included compression tests for strength and modulus of elasticity, tension tests for tensile strength and flexural modulus, freezing-thawing tests for durability factor, shrinkage tests, creep tests, rapid chloride permeability tests, tests for AC impedance, and tests for bond between concrete and steel reinforcement.

The testing program for the mechanical properties of hardened concrete is outlined in Tables 6.1 through 6.4*.

6.1 Compression Tests

The compression tests were conducted on 4 x 8-in. (101 x 202-mm) cylinders at different ages to obtain stress-strain, strength-time, and modulus-time relationships for VHS concrete with the four different types of coarse aggregates (MM, CG, DL, and RG). These tests were conducted for VHS concrete with fly ash [VHS (F)] and VHS concrete with silica fume [VHS (S)] as mineral additives. A limited number of compression tests were also conducted on 6 x 12-in. (152 x 304-mm) cylinders to investigate the size effect.

6.1.1 Test Setup and Procedure

The tests were conducted in a 2,000 kip (8,900 kN) compression testing machine with a hydraulic feedback system and an MTS 436 controller unit. The machine was capable of both load and displacement control modes; the tests for strength and modulus of elasticity were done using the load control option.

* Testing for the fatigue properties of plain concrete (Group 4) was not conducted due to the change of the scope of the project.

Table 6.1 **Test program for compressive strength and modulus of elasticity — Group 1**

Category of HPC	Aggregate Type	No. of 4 x 8-in. Cylinders Tested				No. of 6 x 12-in. Cylinders Tested
		1 Days	3 Days	7 Days	28 Days	28 Days
VHS (F)	MM	—	3	3	3	—
	CG	3	3	3	3	—
	DL	—	—	3	3	—
	RG	3	3	3	3	—
VHS (S)	MM	3	3	3	3	2
	CG	3	3	3	3	2
	DL	—	—	3	3	2
	RG	3	3	—	3	—

Table 6.2 **Test program for modulus of rupture, tensile strain capacity, and split tensile strength — Group 2**

Category of HPC	Aggregate Type	No. of Rupture Specimens Tested			No. of Split Tensile Specimens Tested	No. of 4 x 8-in. "Control" Cylinders Tested
		3 Days	7 Days	28 Days	28 Days	28 Days
VHS (F)	MM	2	2	2	—	2
	CG	2	2	2	2	2
	DL	—	2	2	2	2
	RG	2	2	2	2	2
VHS (S)	MM	2	2	2	2	2
	CG	2	2	2	2	2
	DL	—	—	2	2	2
	RG	2	2	2	2	—

Table 6.3 Test program for frost durability, shrinkage, creep, and chloride permeability — Group 3

Category of HPC	Aggregate Type	No. of Freezing - Thawing Specimens Tested at 14 Days	No. of Shrinkage Specimens Tested from Design Age to 90 Days	No. of Creep Specimens Tested from 1 Day to 90 Days	No. of Chloride Permeability Specimens Tested at 14 Days	No. of 4 x 8-in. "Control" Cylinders Tested at 1 Day
VHS (F)	MM	—	—	3	2	2
	CG	3	3	3	2	2
	DL	—	—	—	—	—
	RG	—	—	3	2	2
VHS (S)	MM	3	3	3	2	2
	CG	3	3	3	2	2
	DL	—	—	—	—	—
	RG	3	3	3	2	2

Table 6.4 Test program for bond strength — Group 5

Category of HPC	Aggregate Type	No. Specimens of Concrete-to-Steel Bond Test at 28 Days	No. of 4 x 8-in "Control" Cylinders Tested at 28 Days
VHS (F)	CG	2	2
VHS (S)	CG	2	2

The tests were conducted according to AASHTO T-22-86 and ASTM C 39, with minor modifications. The modifications were the use of an unbonded capping system, such as steel caps lined with neoprene pads, and the use of a deformation measuring fixture that included linear voltage differential transducers (LVDTs). The two LVDTs used in the compressive tests were Lucas Schaevitz MHR 050, with a sensitivity of 2.500 mV/V/0.001 in. The voltage was converted by a National Instruments AT-MIO-16 12-bit analog-to-digital converter.

An aluminum mounting jig was built to facilitate the mounting of the LVDTs on the test cylinder. The jig ensured that the LVDTs were placed 180 degrees apart and in the central 4 in. (101 mm) of the test cylinders. The device for mounting the transducers on the 4 x 8-in. (101 x 202-mm) cylinders is shown in Figure A.1. First the specimens were placed in the device and the bottom of the cylinder was placed so as to align with the alignment mark. A line of super-glue was applied at each of the four locations where the transducers were to be attached. The metallic contact area of the LVDT holder was sprayed with a zip kicker (a product for speeding up the reaction between the metal and the concrete surface with super-glue), and the LVDT holders together with LVDTs were attached with the wires of the LVDT protruding toward the bottom of the cylinder. After about a minute, the cylinder was removed from the transducer mounting device. To ensure a good bond between the LVDT holders and the concrete surface, additional super-glue was applied all around the contact surface and sprayed with the zip kicker. The unbonded caps were put on the cylinders and the specimen was placed in the compression testing machine.

The LVDTs used to measure the axial deformation of the cylinders had a maximum range of ±0.05 in. (1.27 mm) and the gage length for the axial deformation measurements was 4 in. (101 mm). The core of the LVDTs could be moved up or down by a specially designed screw-thread mechanism (which was machined to become a part of the core of the LVDT) so as to adjust the output voltage to zero or near zero.

The test specimen with the two mounted LVDTs was placed inside a protective steel jacket that rested between the two platens of the compression testing machine (Figure A.2). The steel jacket prevented damage to the transducers from the brittle failure of the specimens at the maximum load.

The test cylinders were loaded and unloaded up to a load of 5,000 lb (22.2 kN) at least twice before the cylinders were loaded to failure. This initial loading and unloading was done for seating purposes and the properly zero out the LVDTs. After the initial loading and unloading, the cylinders were loaded to failure. For 4 x 8-in. (101 x 202-mm) cylinders, a loading rate of 26,500 lb/min (118 kN/min) was used; for the 6 x 12-in. (152 x 303-mm) cylinders, a loading rate of 59,400 lb/min (264 kN/min) was used. The loading rates were within the range of 20 to 50 psi/sec (0.14 to 0.34 MPa/sec) as specified in AASHTO T 22-86 and ASTM C 39 revised.

The data acquisition system used was an OPTIM system (Megadec 100) capable of recording up to 40 channels of output. The load output and the output from the two displacement transducers were recorded using LabWindows software in conjunction with the OPTIM data acquisition system. A view of the compression test setup is shown in Figure A.3.

6.1.2 Specimen Preparation

The specimens were prepared according to ASTM C 192. Specimens used specifically for determining the compressive strength and modulus of elasticity were 4 x 8-in. (101 x 202-mm) cylinders and were cast in plastic molds. Companion 6 x 12-in. (152 x 304-mm) cylinders were also cast in plastic molds to investigate the size effect.

After casting, the specimens inside the molds were covered with plastic sheets for about 24 hours to prevent moisture loss. After 24 hours, the specimens were stripped and placed in sealed plastic bags to be tested at different ages. Before the tests, the specimens were air-dried for 10 to 15 minutes before the LVDTs were mounted on the sides of the specimens.

6.1.3 Test Results and Discussion

There are three categories of test results. They include stress-strain relationships, strength-time and modulus-time relationships, and strength comparisons of 4 x 8-in. (101 x 202-mm) cylinders with 6 x 12-in. (152 x304-mm) cylinders.

6.1.3.1 Stress-Strain Relationships

The stress-strain curves were obtained from the load-deformation curves by dividing the load by the nominal area of the cylinders and the axial deformation by the gage length. Figure 6.1 shows typical stress-strain curves of VHS (F) concrete at the design age of 28 days with different types of coarse aggregates. From Figure 6.1, it appears that the slope of the stress-strain curve for VHS (F) concrete with RG is relatively steeper than those for VHS (F) concretes with MM, CG and DL. The strain capacity corresponding to the maximum strength varies from about 1,200 microstrains for VHS (F) concrete with RG to about 2,000 to 2,500 microstrains for VHS (F) concrete with MM, CG, and DL.

Figure 6.2 shows typical stress-strain curves of VES (S) concrete at the design age of 28 days with different types of coarse aggregates. From Figure 6.2, it appears that the slope of the stress-strain curve for VHS (S) concrete with RG is relatively steeper than those for VHS (S) concretes with MM, CG, and DL. The strain capacity corresponding to the maximum strength is about 1,600 microstrains for the VHS (F) concrete with MM, RG, and DL, compared to about 1,900 microstrains for VHS (S) concrete with CG.

Examination of Figures 6.1 and 6.2 shows that softer coarse aggregates such as MM exhibit softer response in the initial portion of the curve, which translates into a lower modulus of elasticity.

The effect of age on the stress-strain curve for VHS (F) and VHS (S) concretes with one type of coarse aggregate (MM) is shown in Figures 6.3a and 6.3b. The initial portion of the stress-strain curve becomes more linear as the concrete matures, and there is a slight increase in the strain capacity during early age (up to 3 days), after which there is an insignificant effect on the strain

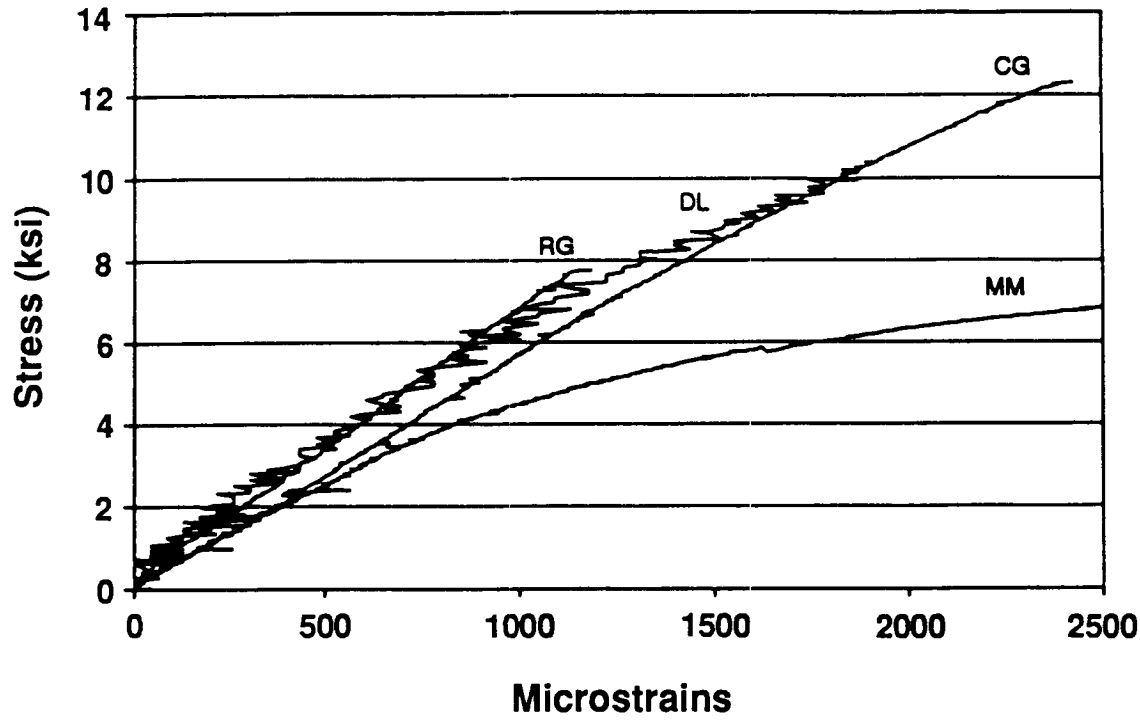

Figure 6.1 Stress-strain relationship of VHS (F) concrete at design age of 28 days

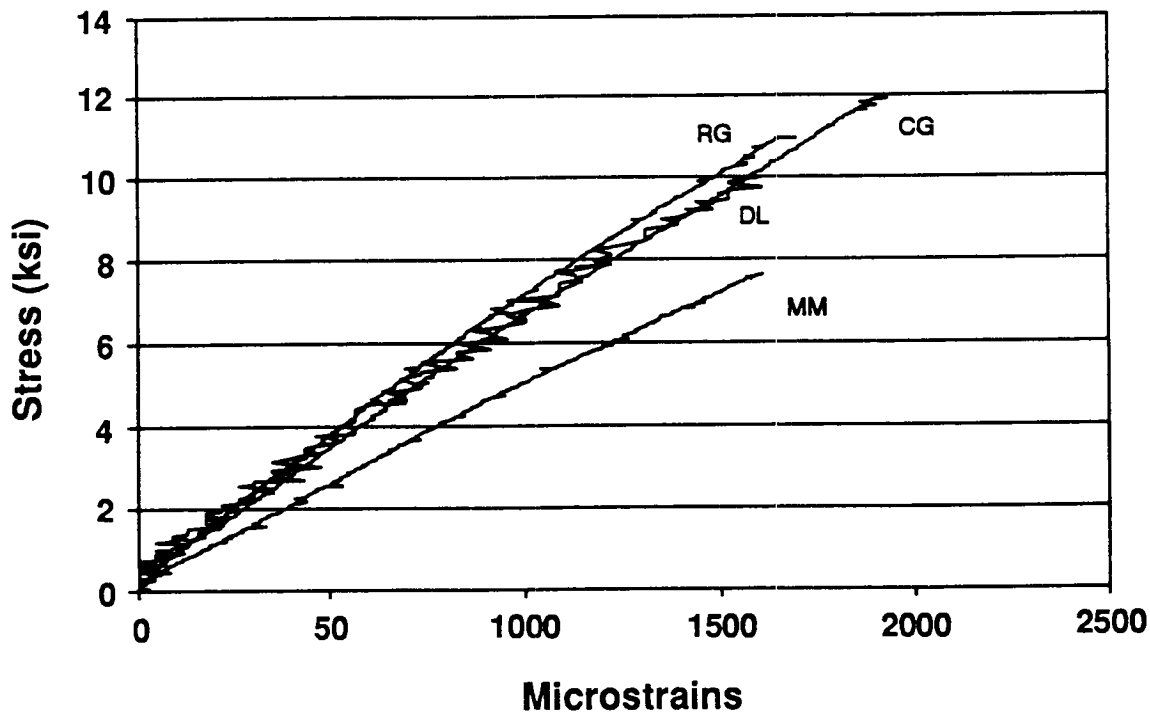

Figure 6.2 Stress-strain relationship of VHS (S) concrete at design age of 28 days

capacity due to the age of the concrete. For VHS (S) concrete, the strain capacity during early ages (up to 3 days) decreases as the concrete matures; at 28 days, the strain capacity is about 50% of the strain capacity at 3 days. Figures 6.3a and 6.3b also show that for VHS (S) concrete, the initial stiffness of the stress-strain curve at early ages less than 7 days is noticeably less than at later ages, whereas for VHS (F) concrete, the initial stiffness at early ages is comparable to that at later ages. Note that the stiffening of the behavior in the initial portion of the stress-strain curve with time results in an increase in the modulus of elasticity with time.

6.1.3.2 Strength-Time and Modulus-Time Relationships

The strength and modulus of elasticity test results for VHS (F) and VHS (S) concretes are summarized in Tables 6.5a and 6.5b. The values shown in the table are averages of three replicate specimens. The strength-time relationships for VHS (F) and VHS (S) concretes with different types of coarse aggregate in a nondimensional form are shown in Figures 6.4a and 6.4b. Each point on the curve is based on an average of three replicate specimens. From Figure 6.4a, it can be seen that for VHS (F) concrete, the strength gain with time for different types of coarse aggregates is similar. At 3 days, the strength achieved is about 55% to 75% of the 28-day strength and that during the early age (up to 3 days), the concrete with softer aggregate reaches a higher fraction of its 28 day strength. Figure 6.4a also compares the observed strength-time relationships of VHS (F) concrete with the prediction of ACI Committee 209 (1993a). The strength gain for VHS (F) concrete compares well with this prediction. Note that the equation of ACI Committee 209 was developed from a large number of experimental data for concretes with strengths up to 6,000 psi (42 MPa) at 28 days.

The nondimensional strength-time relationship for VHS (S) concrete shown in Figure 6.4b indicates that at 3 days, the strength achieved is about 70% to 80% of the 28-day design strength and that the strength gain with time for VHS (S) with CG is lower than for VHS (S) with MM, RG, and DL. Comparison with the prediction of ACI Committee 209 shows that strength gain is much faster in the first 7 days for VHS (S) concrete than the prediction indicates. Comparison of Figure 6.4a and Figure 6.4b shows that strength-time relationship is dependent on the type of coarse aggregate, and the general shape of the strength-time relationship is similar for VHS (F) and VHS (S) concretes.

The modulus-time relationships for the different types of coarse aggregate for VHS (F) and VHS (S) concretes are shown in Figures 6.5a and 6.5b. Each point on the curve is an average of three replicate specimens. The results for VHS (F) concrete indicate lower modulus for the softer coarse aggregate such as MM; however, the rate of increase in the modulus with time is comparable to VHS (F) concrete with other types of coarse aggregates. For VHS (S) concrete, the variation of the modulus with time for RG is different than those for CG, MM, and DL. The VHS (S) concrete with RG shows a nearly linear increase in the modulus with age after the first 3 days, which is not a typical response. At 3 days, the modulus of elasticity of VHS (S) concrete with RG is about 55% of the modulus of VHS (S) with CG; however, at the design age of 28 days, the modulus of VHS concrete with RG is slightly greater than the modulus of VHS concrete with CG.

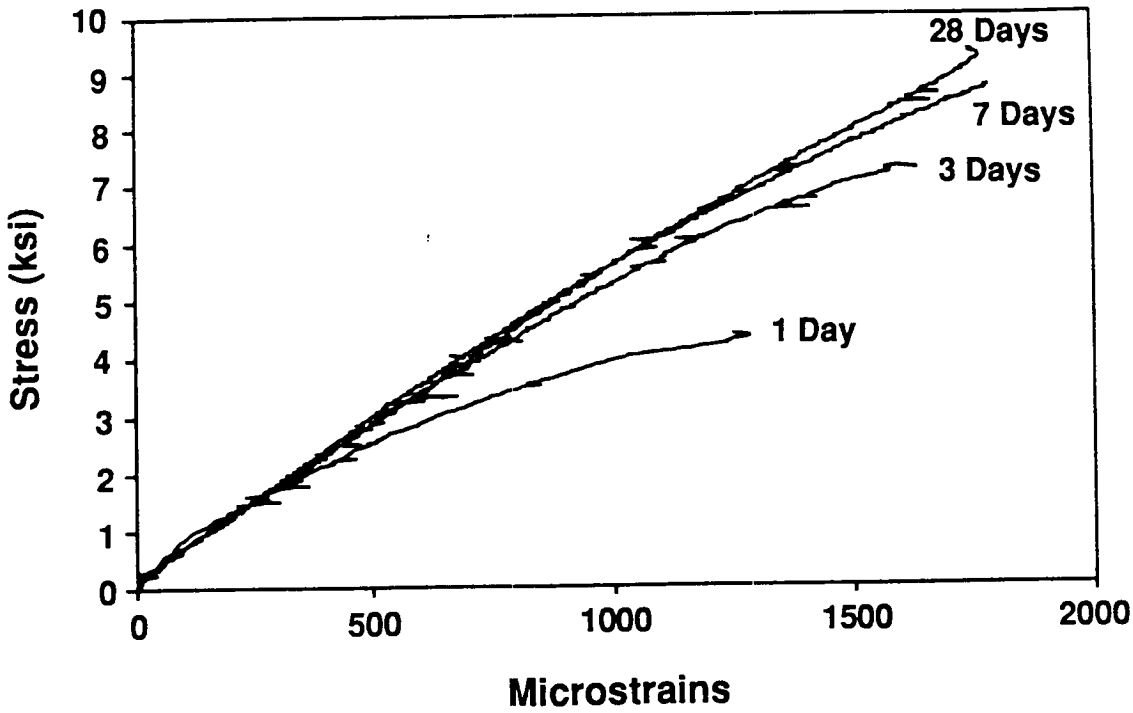

Figure 6.3a Effect of age on stress-strain curve for VHS (F) concrete with RG

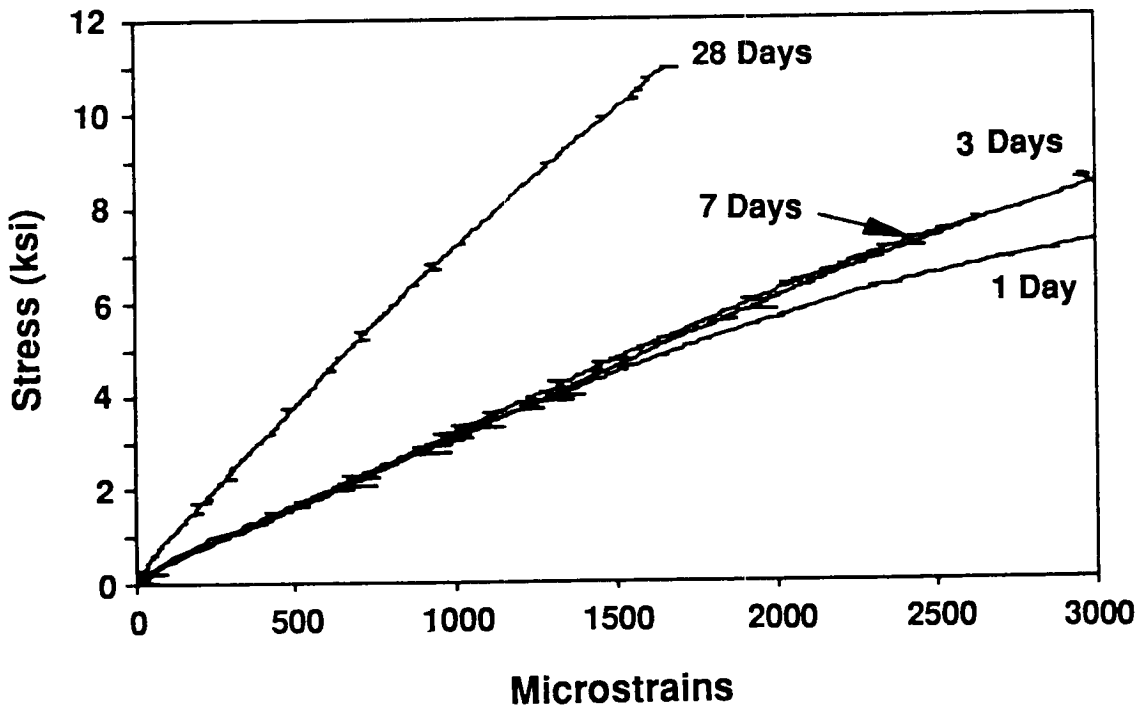

Figure 6.3b Effect of age on stress-strain curve for VHS (S) concrete with RG

Table 6.5a Summary of test results for compressive strength and modulus of elasticity at different test ages for VHS (F) concrete

Age (days)	MM	CG	DL	RG
	Compressive Strength (psi)			
1	—	4,920	—	4,550
3	6,590	8,300	—	7,200
7	7,470	9,940	8,660	8,050
28[1]	5,600	11,430	9,040	8,690
28[2]	—	—	—	—
28[3]	8,510	12,200	10,500	9,700
	Modulus of Elasticity (10^6 psi)			
1	—	3.40	—	4.25
3	4.85	5.30	—	5.45
7	5.30	5.60	6.91	5.40
28[1]	4.85	6.25	6.19	6.60
28[2]	5.12	5.45	—	6.20

[1] 4 x 8-in. companion cylinders of flexural strength testing.
[2] 6 x 12-in. companion cylinders of compressive strength testing.
[3] 4 x 8-in. cylinders of compressive strength testing.

Table 6.5b Summary of test results for compressive strength and modulus of elasticity at different test ages for VHS (S) concrete

Age (days)	MM	CG	DL	RG
	Compressive Strength (psi)			
1	4,730	7,720	—	7,920
3	6,460	9,360	—	8,810
7	7,110	11,060	8,690	9,920
28[1]	5,380	8,330	10,100	9,120
28[2]	7,910	12,230	10,310	—
28[3]	8,080	13,420	10,480	11,080
	Modulus of Elasticity (10^6 psi)			
1	3.65	3.96	-	2.95
3	4.40	5.55	-	3.15
7	4.70	5.75	6.88	4.00
28[1]	4.23	4.45	7.61	5.33
28[2]	5.05	6.45	-	7.00

[1] 4 x 8-in. companion cylinders of flexural strength testing.
[2] 6 x 12-in. companion cylinders of compressive strength testing.
[3] 4 x - in. cylinders of compressive strength testing.

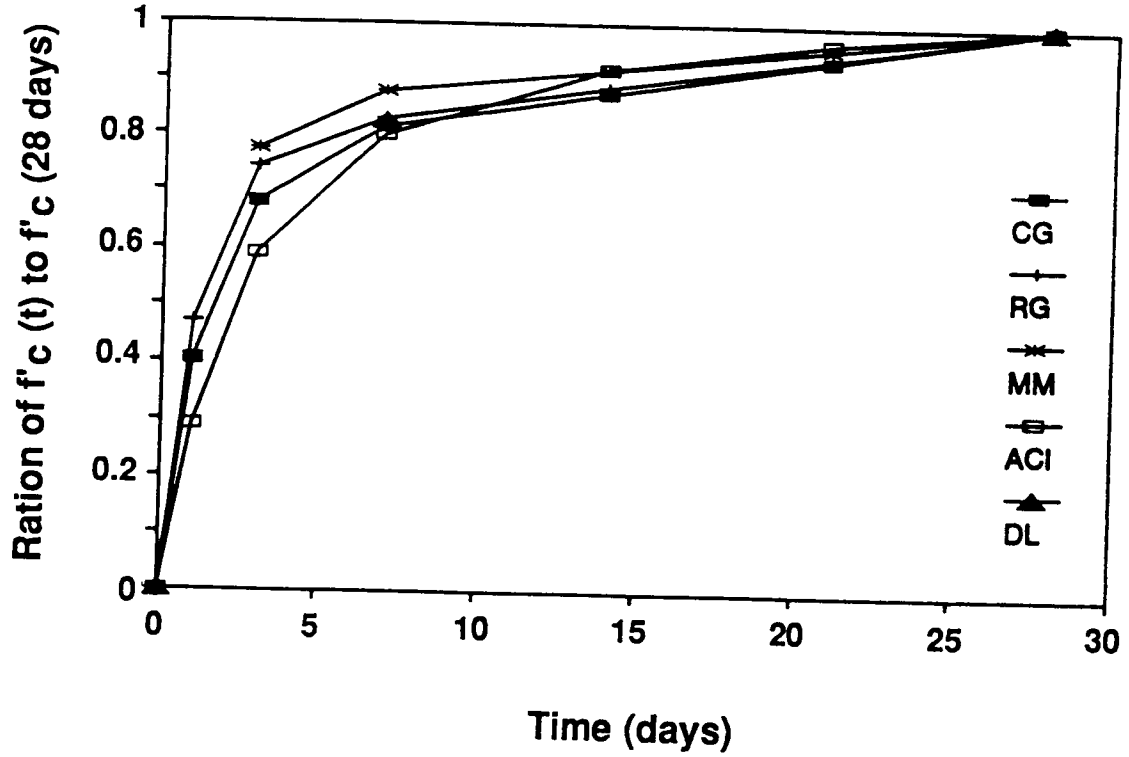

Figure 6.4a Variation of compressive strength with time for VHS (F) concrete

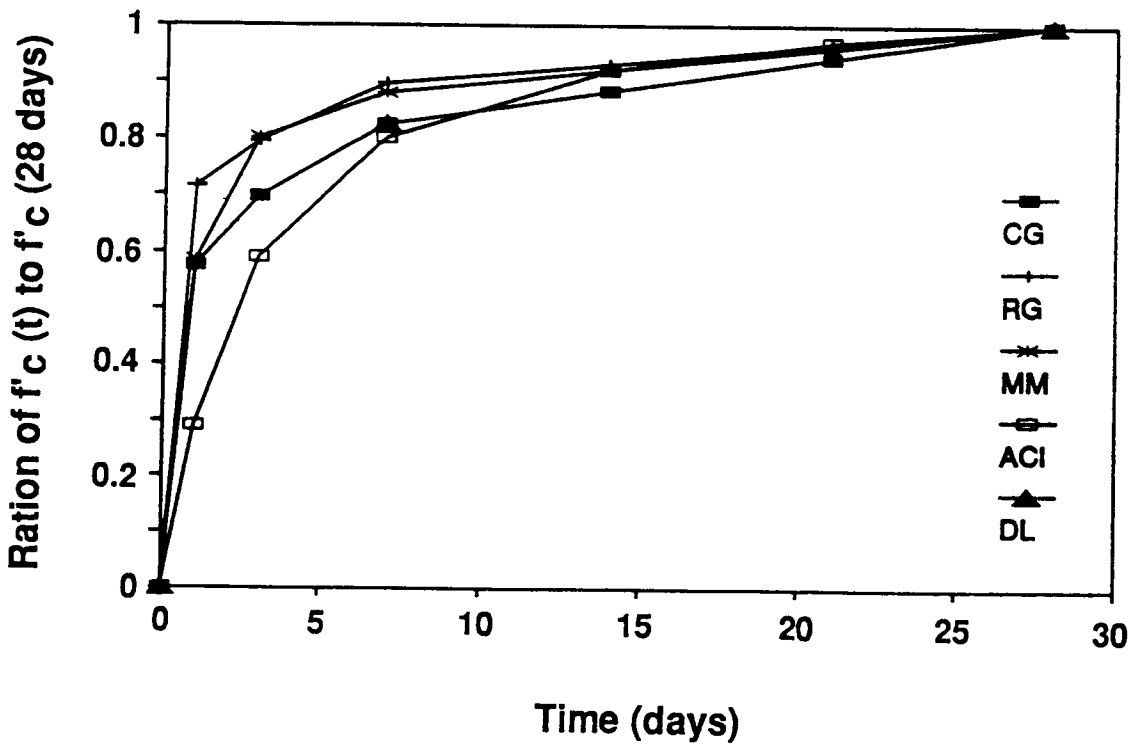

Figure 6.4b Variation of compressive strength with time for VHS (S) concrete

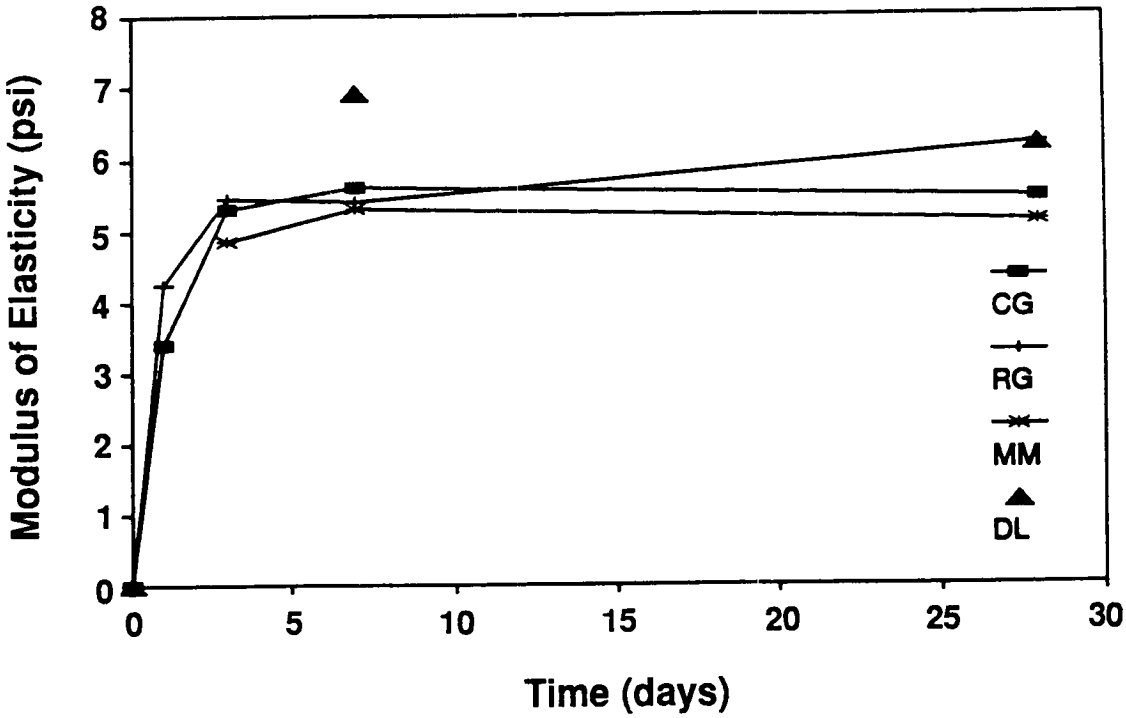

Figure 6.5a Variation of modulus of elasticity with time for VHS (F) concrete

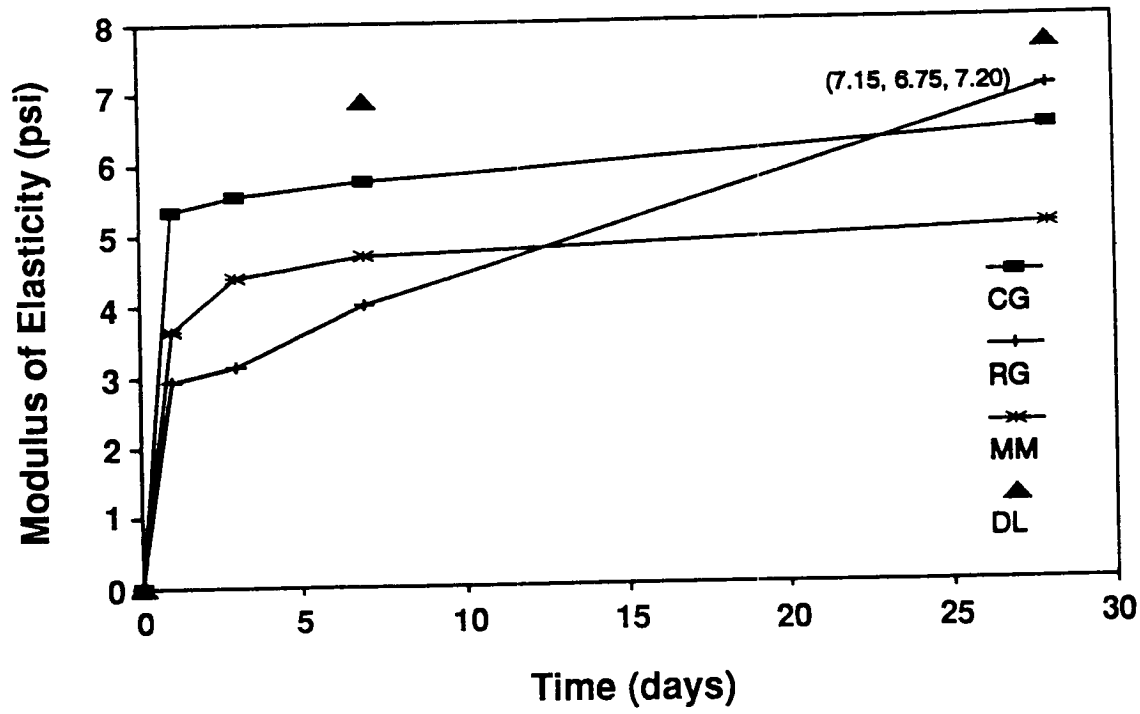

Figure 6.5b Variation of modulus of elasticity with time for VHS (S) concrete

The predictions by the various published equations for the modulus of elasticity by ACI 318 (1993c), ACI 363 (1993d), and Ahmad and Shah (1985) were compared with the observed modulus of elasticity of VHS concrete at different ages up to 28 days (Figures 6.6a). The ACI 318 equation uses a premultiplier of 57,000 to the square root of the compressive strength in psi units. It can be seen that for VHS concrete, the prediction by the ACI equation (1993c) is in close agreement with the experimental results, underpredicting the observed values by only 2%. The equations of ACI 363 (1993d), Ahmad and Shah (1985), and Cook (1989) overpredict the experimental results by 10%, 5%, and 15% respectively. Note that the ACI 318 equation was developed for lower strength concretes up to 6,000 psi (42 MPa) at 28 days, whereas the other equations were developed primarily for concretes with strengths exceeding 10,000 psi (70 MPa) at 28 days.

6.1.3.3 Strength Comparisons of 4 x 8-in. and 6 x 12-in. Cylinders

A summary of the strength comparisons between the 4 x 8-in. (101 x202-mm) cylinders and the 6 x 12-in. (152 x 304-mm) cylinders for VHS (S) concrete is presented in Table 6.6 and shown in Figure 6.6b. The results indicate that the ratio of the 6 x 12-in. (152 x 304-mm) cylinder strengths to the 4 x 8-in. (101 x 202-mm) cylinder strengths varies with the type of coarse aggregate used. The ratio of 6 x 12-in. (152 x 304mm) cylinder strength to 4 x 8-in. (101 x 202-mm) cylinder strength is 0.91 for the VHS (F) concrete with CG and 0.98 for VHS (F) concrete with MM and DL. Values reported in the literature for concretes with 28-day strength ranging from 5,000 psi (35 MPa) to 12,000 psi (84 MPa) vary from 0.90 to 0.95 (Carrasquillo et al. 1991, Leming 1988, Moreno 1990).

Table 6.6 Summary of test results for 4 x 8-in. and 6 x 12-in. cylinder strengths for VHS (S) concrete

Specimen Size	No. of Specimens	Test Age (days)	Strength (psi) MM	CG	DL	RG
A: 4 x 8 in.	3	28	8,880	13,420	10,480	11,080
B: 6 x 12 in.	2	28	7,910	12,230	10,310	—
A/B			0.98	0.91	0.98	—

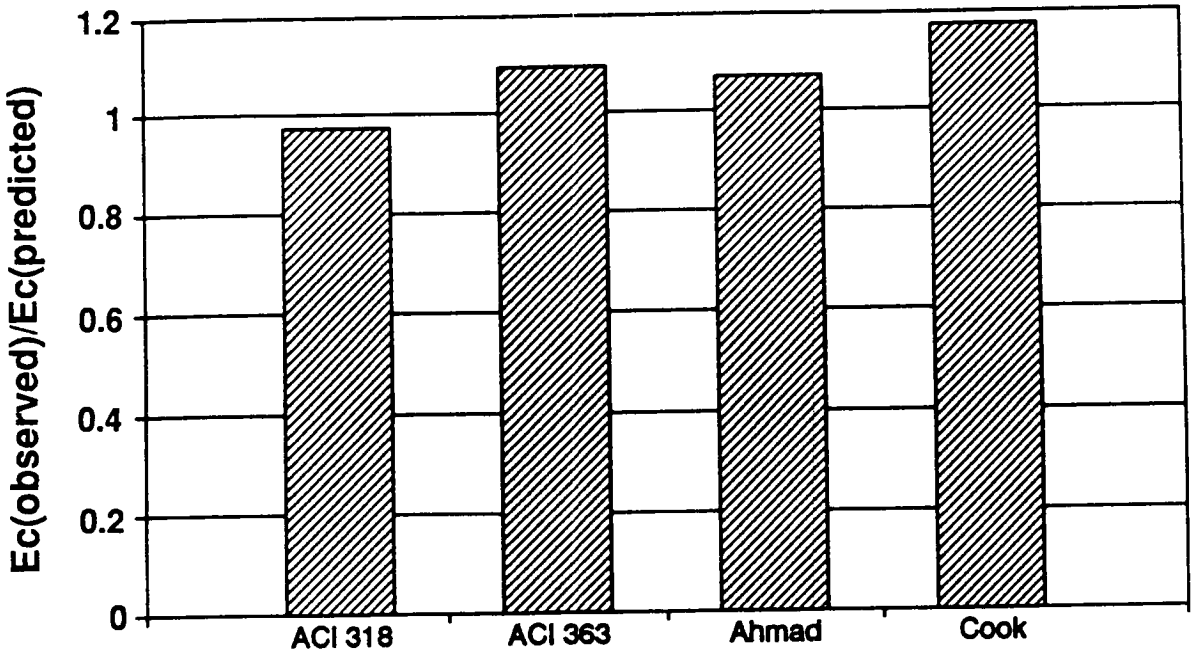

Figure 6.6a Comparison of observed versus predicted modulus of elasticity of VHS concrete considering all test ages

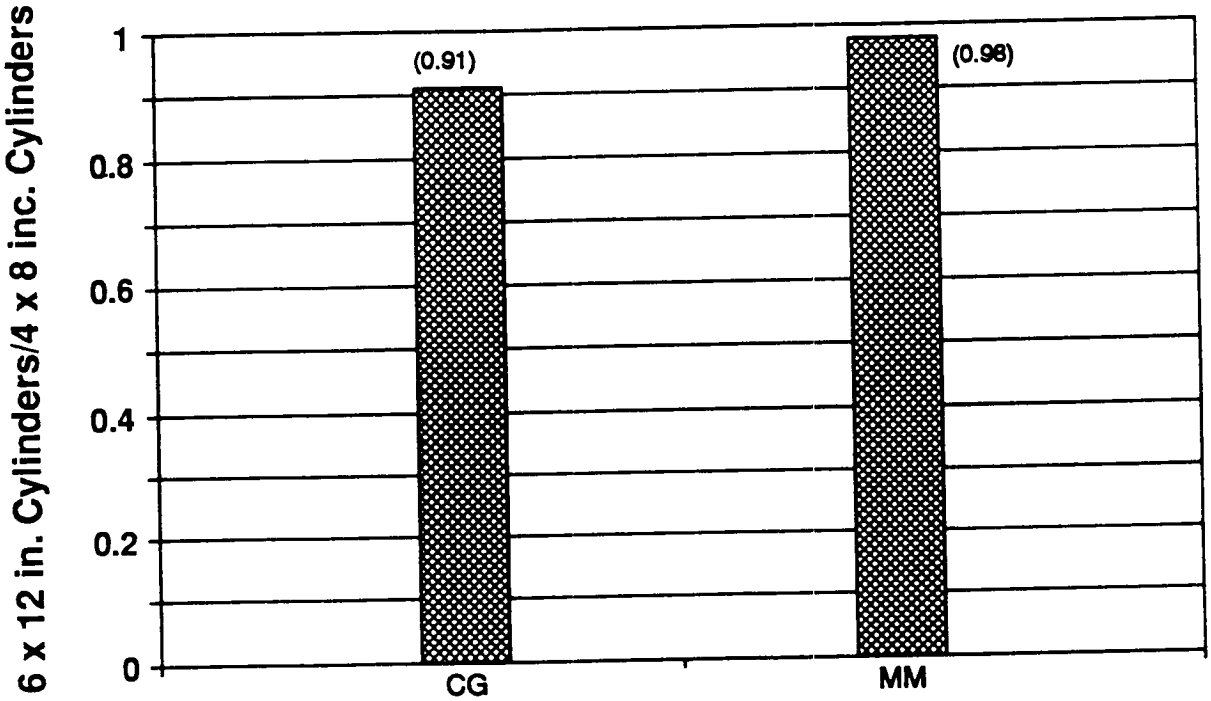

Figure 6.6b Average size effect of VHS (S) concrete at design age

6.2 Tension Tests

Two types of tensile strength tests were conducted: split cylinder tests and flexural tests. The split cylinder tests were conducted on 4 x 8-in. (101 x 202-mm) cylinders, and the flexural tests were conducted on 4 x 4 x 17.5-in. (101 x 101 x 444-mm) beams.

6.2.1 Test Setup and Procedure

6.2.1.1 Split Cylinder Tests

The split cylinder tests were conducted according to ASTM C 496. The cylinders were loaded at a rate of 7,500 lb/min (33.4 kN/min) until failure. This rate of loading was within the ASTM specified range of 100 to 200 psi/min (0.69 to 1.38 MPa/min). The split cylinder tests were conducted on a 300 kip (1335 kN) compression testing machine.

6.2.1.2 Flexural Tests

The flexural tests were conducted on a universal testing machine with a capacity of 120 kip (534 kN). The machine was equipped with a SATEC System Inc. M120BTE automated control system for programming the loading rate. The flexural tests were conducted in accordance with AASHTO T 97-86 and ASTM C 78, with some modifications. The modifications were necessary to incorporate the capability of monitoring the tensile strain capacity and the load-deflection response of the test specimen during testing. To measure the tensile strain and the midspan deflection of the test specimen, a mounting frame (fixture) was designed and fabricated. The mounting frame is capable of holding four LVDTs (two on each side of the beam) and an additional one for measuring the midspan deflection. To prevent damage to the transducers, a No. 2 smooth reinforcing bar was placed along the centroidal axis of the beam. This prevented the sudden collapse of the specimen upon reaching the maximum load and protected all the transducers.

Several preliminary tests indicated that the use of a No. 2 smooth reinforcing bar along the centroidal axis did not have any detectable effect on the strength and behavior of the test specimens. The test specimens were first placed in a transducer mounting device to facilitate the mounting of the four transducers to monitor the tensile and compressive strains during the flexural test. The device for mounting the transducers is shown in Figure A.4.

Preliminary testing revealed that the combination of slight imperfections in the steel molds for the beams and the rigid supports introduced a torsional effect that changed the mode of failure of the test specimen. A special beam support unit that could accommodate these imperfections was then designed and fabricated. In the beam support unit, both of the supports are restrained against motion along the centroidal axis of the beam; however, in the transverse direction, one of the supports is allowed to rotate (Figure A.5).

The mounting frame on the flexural test beams for monitoring the midspan deflections is shown in Figure A.6. The beams were tested in third point loading over a clear span of 12 in. (304 mm) according to AASHTO T 97-86 and ASTM C 78. The loading arrangement for the flexural testing is shown in Figure A.7.

The beams were tested at different ages, and companion 4 x 8-in. (101 x 202-mm) cylinders were tested at the same time. The test beams were loaded and unloaded up to a load of 500 lb (2.3 kN). This process was done twice for seating and zeroing the LVDTs. After the initial loading and unloading process, the test beams were loaded to failure. A loading rate of 800 lb/min (3.6 kN/min) was used.

The four LVDTs used to measure displacements in the flexural tests were Trans-Tek, Inc. #0270-0000, with a sensitivity of 3.189 VAC/ Inch/ Volt Input. A gage length of 4 in. (101 mm) was used for monitoring the compressive and tensile deformation near the extreme fibers. The voltage output from the LVDTs was converted by an OPTIM data acquisition system (Megadec 100). This system was used to eliminate electronic noise in order to record accurately the small displacements encountered. An aluminum jig was used for mounting the four LVDTs in the middle third of the beam and 5/8 in. (15.9 mm) from the top fiber and bottom fiber on the front and back of the beam. A view of the test setup is shown in Figure A.8.

6.2.2 Specimen Preparation

Specimens used for flexural tests were 4 x 4 x 17.5-in. (101 x 101 x 444-mm) beams, cast in steel molds with a No. 2 smooth bar placed along the centroidal axis. The smooth No. 2 bar was placed in the specimen to keep it from collapsing at failure in order to avoid damaging LVDTs. The concrete was placed into molds and vibrated internally with a needle vibrator. The finish was completed with a magnesium float. Companion 4 x 8-in.(101 x 202-mm) cylinders were cast in plastic molds. After casting, the specimens inside the molds were maintained at 60° to 80°F and protected from moisture evaporation by a plastic sheet cover for 20 to 24 hours. Then they were stripped of their molds and either tested immediately or placed in sealed plastic bags for testing at later ages. Since the tests involved the measurements of tensile strains and midspan deflections, transducers were mounted on the test specimens. The specimens were air dried for 10 to 15 minutes before the LVDTs were mounted on the two sides of the specimens. Figure A.4 shows the device for mounting the transducers on the specimen for flexural testing.

6.2.3 Test Results and Discussion

6.2.3.1 Split Cylinder Tests

The results of the split cylinder tests are shown in Tables 6.7a and 6.7b. The values shown in the table are the averages of two replicate specimens. The ratio of the observed to the predicted split cylinder strength for VHS (F) and VHS (S) concretes with different types of coarse aggregates is shown in Figure 6.7. The equation suggested by ACI Committee 318 (1993c) uses 6.7 as a premultiplier to the square root of the compressive strength in psi units. It appears that the ratio

of the observed to the predicted split cylinder strength is higher for VHS (S) concrete than for VHS (F) concrete. For VHS (F) concrete, the equations of ACI Committee 318 (1993c), ACI Committee 363 (1993d), and Ahmad and Shah (1985) underpredict the observed values by 5%, 14%, and 8% respectively. For VHS (S) concrete, the equations of the ACI Committee 318 and Ahmad and Shah overpredict by 8% and 5% respectively, whereas the equation of ACI Committee 363 underpredicts by 3%. Note that the equation of ACI Committee 318 was developed for concretes with strengths up to 6,000 psi (42 MPa) at 28 days age, whereas the equations of ACI Committee 363 and Ahmad and Shah were primarily for concretes with compressive strengths more than 6,000 psi (42 MPa) at 28 days.

Table 6.7a Summary of test results for modulus of rupture, tensile strain capacity, and split cylinder tensile strength for VHS (F) concrete

Coarse Aggregate Type	Age (days)	Modulus of Rupture (psi)	Tensile Strain Capacity (microstrains)	Split Cylinder Strength (psi)	4 x 8-in. "Control" Cylinder Strength (psi)
MM	3	450	-125	—	—
	7	620	-120	—	—
	28	600	-120	—	5600
CG	3	660	-150	—	—
	7	550	-200	—	—
	28	750	-140	620	11,430
DL	3	—	—	—	—
	7	110	-180	670	—
	28	590	-130	810	9,040
RG	3	230	-130	—	8,690
	7	380	-125	—	—
	28	430	-160	660	—

Table 6.7b Summary of test results for modulus of rupture, tensile strain capacity, and split cylinder tensile strength for VHS (S) concrete

Coarse Aggregate Type	Age (days)	Modulus of Rupture (psi)	Tensile Strain Capacity (microstrains)	Split Cylinder Strength (psi)	4 x 8-in. "Control" Cylinder Strength (psi)
MM	2	410	-200	—	—
	7	550	-200	—	—
	28	670	-200	520	5,380
CG	1	550	—	—	—
	7	630	-150	—	—
	28	800	-180	640	8,350
DL	3	—	—	—	—
	7	—	—	—	—
	28	—	—	720	10,100
RG	1	480	-100	—	—
	7	610	-140	—	—
	28	780	-175	710	9,120

6.2.3.2 Flexural Tests

The test results for the flexural modulus are presented in Tables 6.7a and 6.7b. The comparison of the experimental results with some of the empirical equations is shown in Figure 6.8. The equation suggested by the ACI Committee 318 (1993c) uses 7.5 as a premultiplier to the square root of the compressive strength in psi units. It can be seen that for VHS (F) and VHS (S) concretes, the ACI Code equation overpredicts the results by 6% and 15% respectively. The equation of Ahmad and Shah (1985) underpredicts the results of VHS (F) and VHS (S) concretes by 21% and 15% respectively. The equation recommended by ACI Committee 363 (1993d) underpredicts the results by as much as 32% and is the least satisfactory, since the equation was developed for concretes with strengths well over 10,000 psi (70 MPa) at 28 days.

The variation of the modulus of rupture with time for VHS (F) and VHS (S) concretes is shown in Figures 6.9a and 6.9b. For VHS (F) concrete with RG, the modulus of rupture increases rapidly up to 7 days, after which it increases gradually up to 28 days. For VHS (F) concrete with MM, the modulus of rupture increases rapidly up to 7 days, after which it essentially remains the same up to 28 days. For VHS (F) concrete with CG, the test results show a decrease in the modulus of rupture from 3 days to 7 days; this apparent decrease is due to inconsistent higher values obtained at 3 days, the results at 28 days seem to be consistent with the results of the VHS (F) concrete with other types of aggregates. For VHS (S) concrete with different types of aggregates, the modulus of rupture increases rapidly up to 7 days, after which it increases gradually up to 28 days (see Figure 6.9b). The modulus of rupture for the VHS (S) concrete with MM is lower than for VHS (S) concrete with CG and RG.

The load versus midspan deflection for VHS (F) and VHS (S) concretes with different types of coarse aggregates at the design age of 28 days is shown in Figures 6.10a and 6.10b. The figures show that the aggregate type has an appreciable effect on the initial stiffness of the load versus midspan deflection response for VHS concrete beams when tested in flexure. VHS concretes with RG exhibit the stiffest response and VHS concretes with MM exhibit the softest response for the load-deflection behavior of beams in the beam flexural test.

The effect of age on load versus midspan deflection for VHS (F) concrete with one type of coarse aggregate (MM) is shown in Figure 6.11a. With age, the response tends to become stiffer in the initial stage; the flexural deformation capacity at 7 days is significantly smaller than at 3 days, and at 28 days it is slightly smaller than at 3 days. The effect of age on the load versus midspan deflection for VHS (S) concrete with one type of coarse aggregate (MM) is shown in Figure 6.11b. The flexural deformation capacity shows essentially no change up to 7 days, after which there is a slight reduction at 28 days.

The load vs. tensile strain for VHS (F) and VHS (S) concretes with different types of coarse aggregates at the design age of 28 days is shown in Figures 6.12a and 6.12b. The results for VHS (F) concrete indicate that at 28 days, the tensile strain capacity depends on the type of coarse aggregate used. The tensile strain capacity is lowest for VHS (F) concrete with MM and highest for VHS (F) concrete with RG. The results for VHS (S) concrete show that at 28 days,

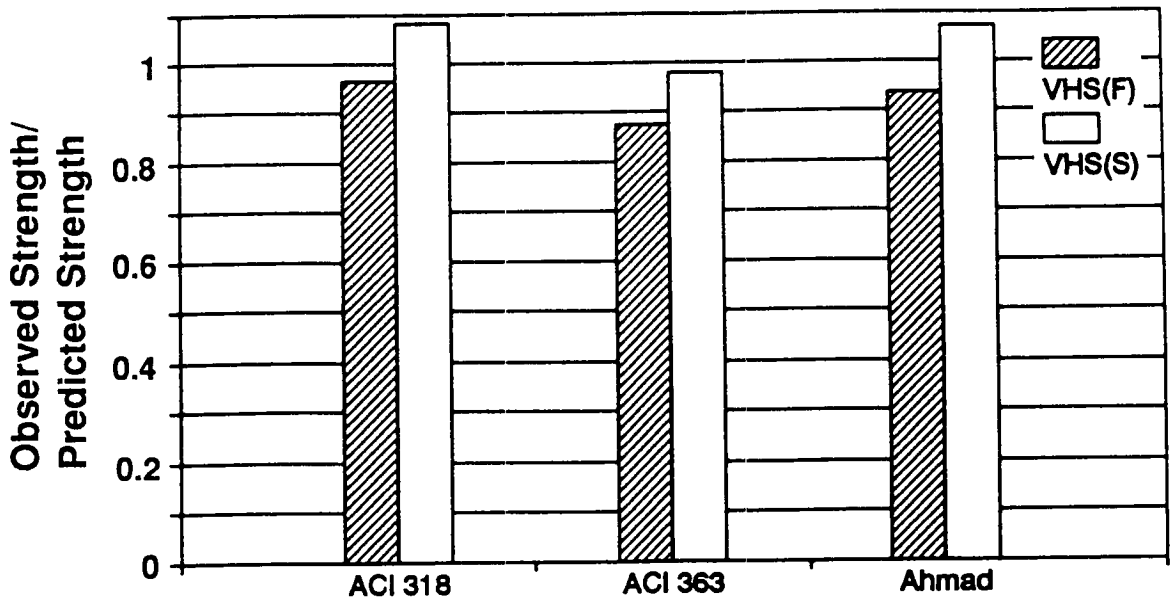

Figure 6.7 Comparison of observed versus predicted split cylinder strength of VHS concrete at design age

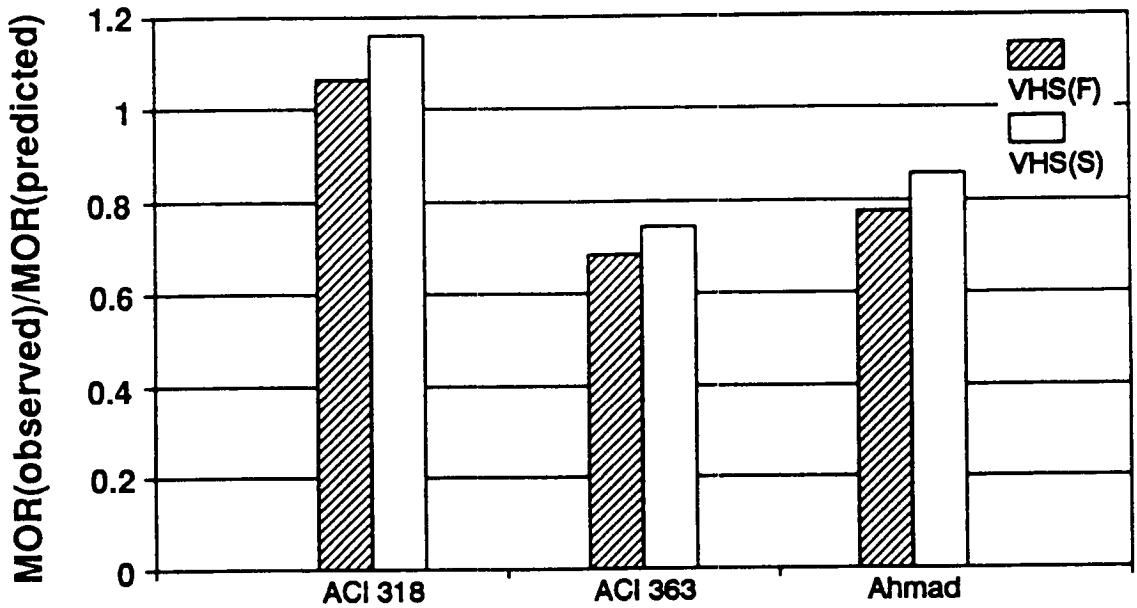

Fgiure 6.8 Comparison of observed versus predicted modulus of rupture of VHS concrete at design age

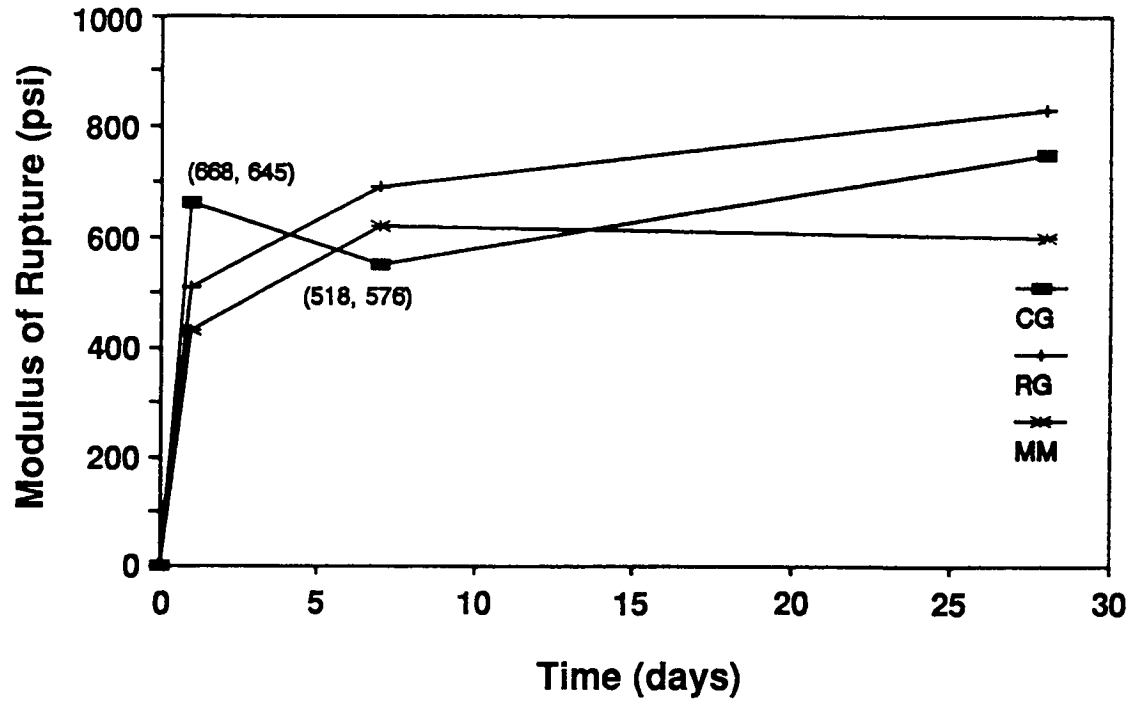

Figure 6.9a Variation of modulus of rupture with time for VHS (F) concrete

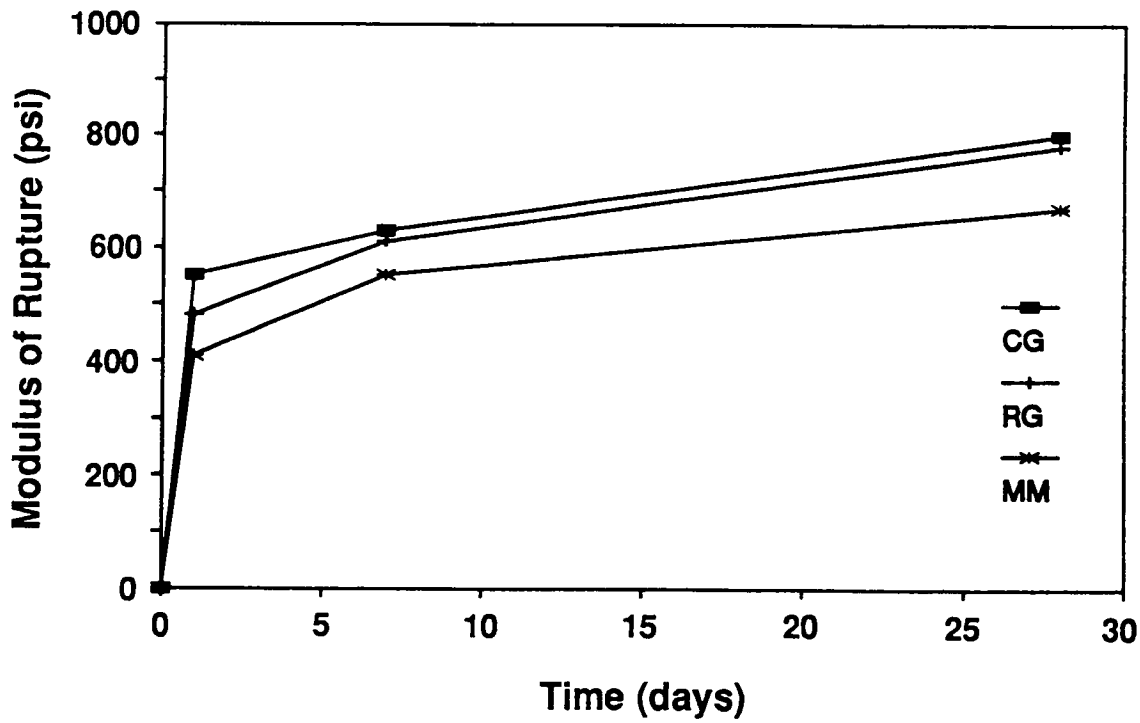

Figure 6.9b Variation of modulus of rupture with time for VHS (S) concrete

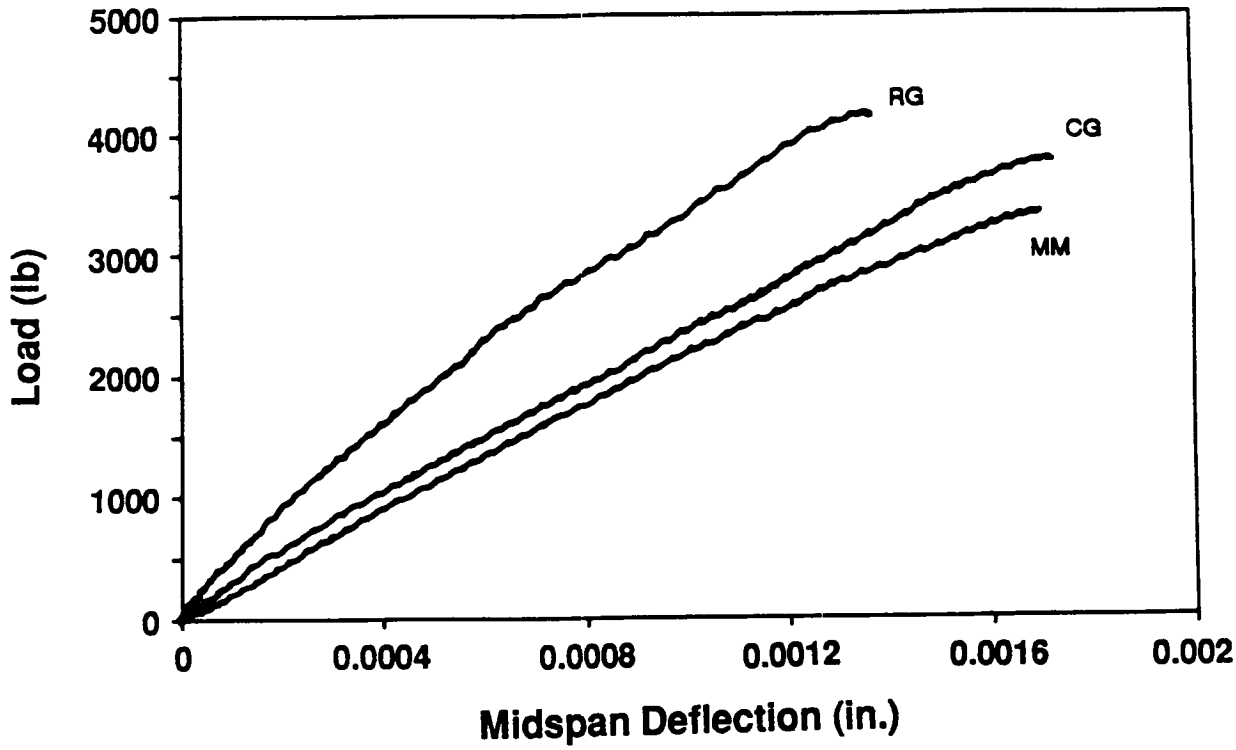

Figure 6.10a Load versus midspan deflection of VHS (F) concrete at design age of 28 days

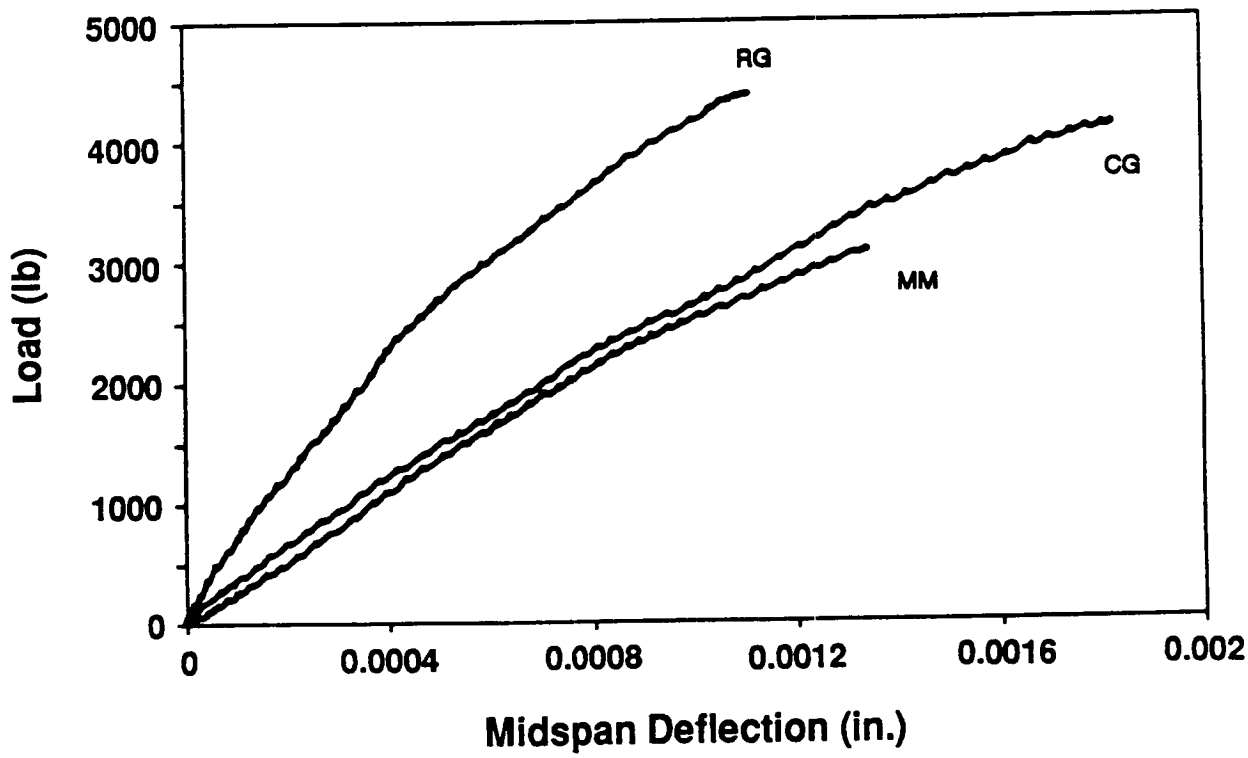

Figure 6.10b Load versus midspan deflection of VHS (S) concrete at design age of 28 days

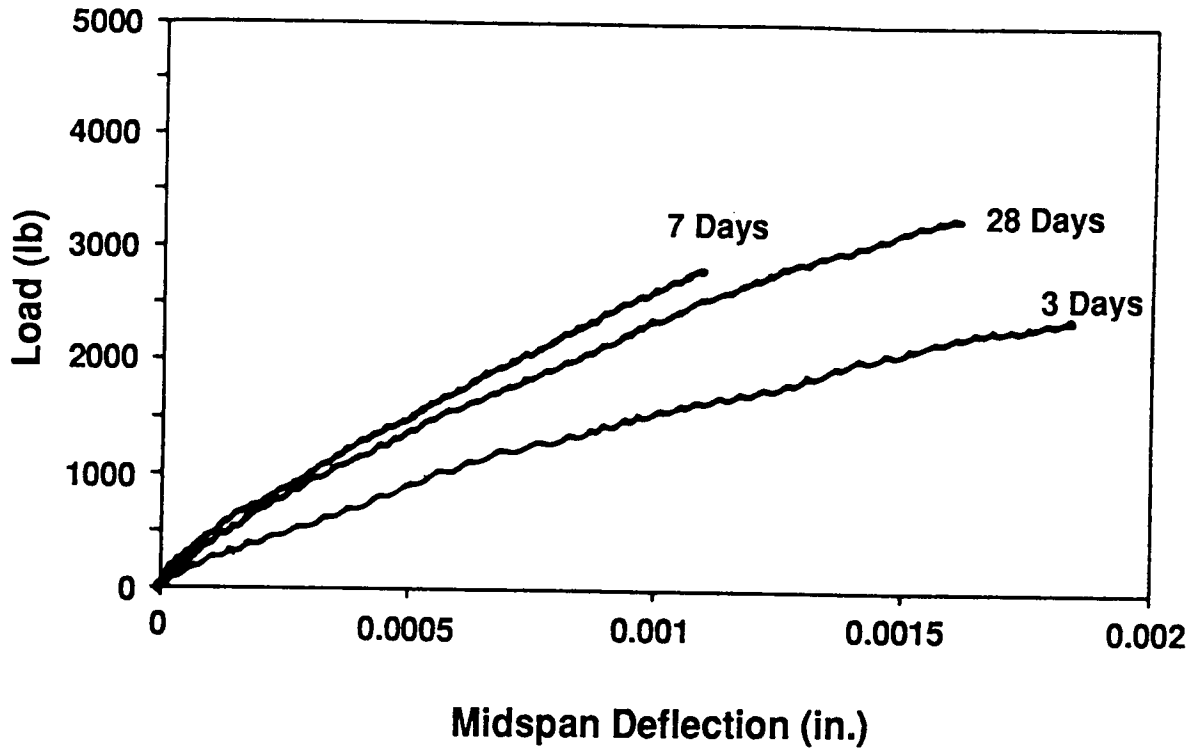

Figure 6.11a Load versus midspan deflection of VHS (F) concrete with MM

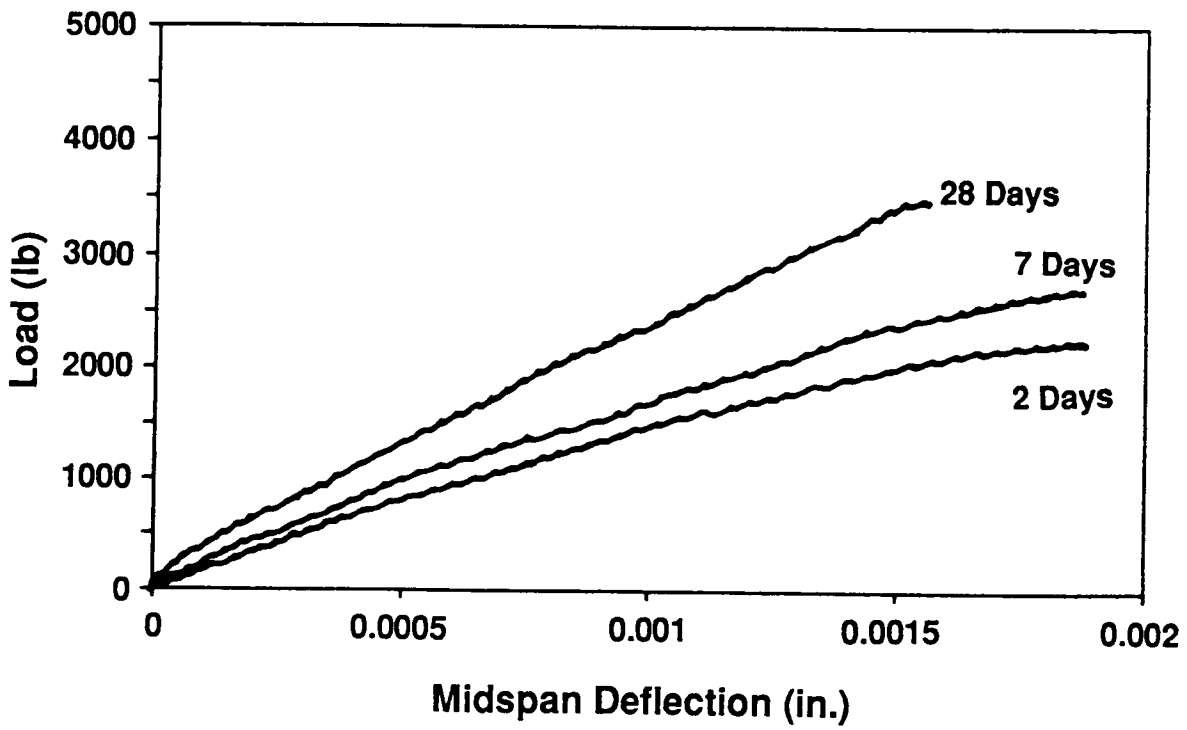

Figure 6.11b Load versus midspan deflection of VHS (S) concrete with MM

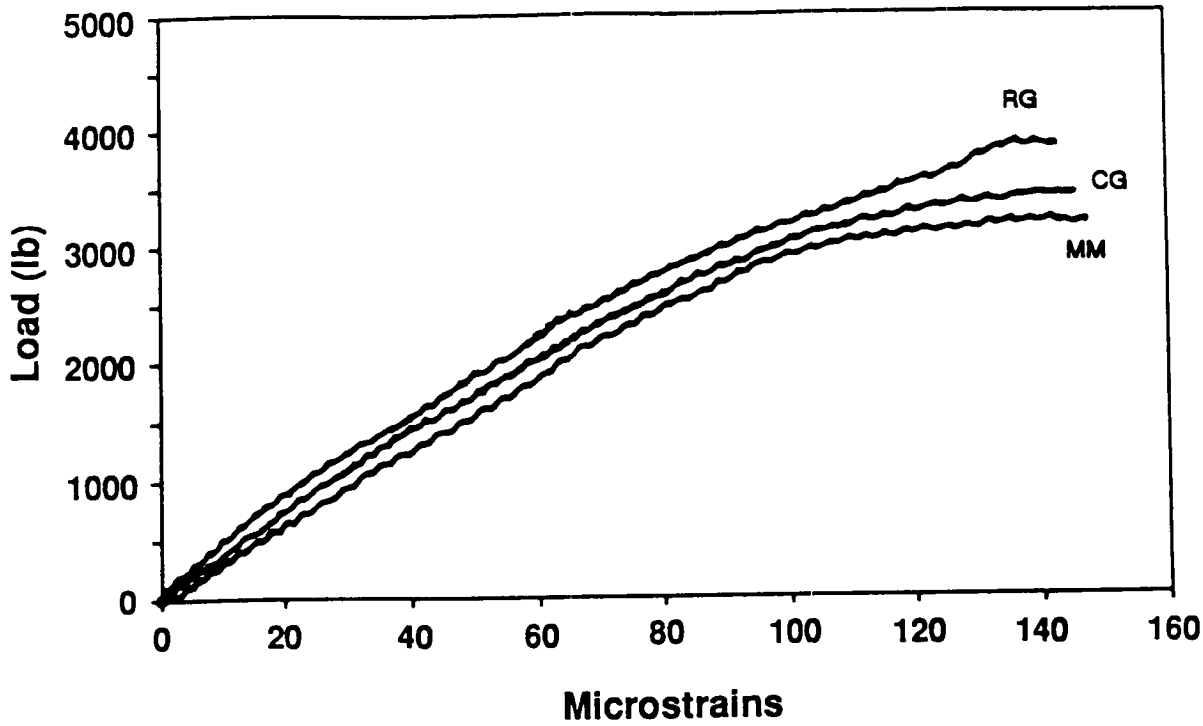

Figure 6.12a Load versus tensile strain of VHS (F) concrete at design age of 28 days

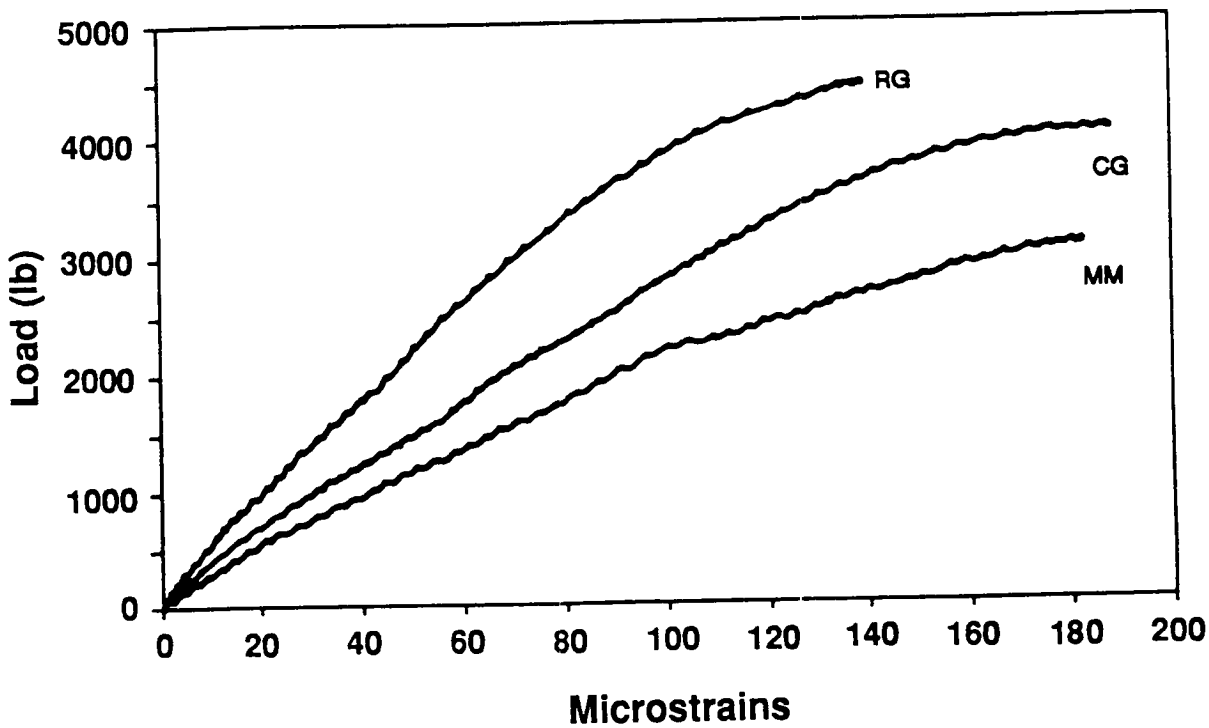

Figure 6.12b Load versus tensile strain of VHS (S) concrete at design age of 28 days

the tensile strain capacity is significantly affected by the type of coarse aggregate used (see Figure 6.12b). The tensile strain capacity is lowest for VHS (S) concrete with RG and is highest for VHS (S) concrete with MM.

The load versus tensile strain for VHS (F) concrete with MM (see Figure 6.13a) shows that at 3 days, the tensile strain capacity is about 125 microstrains and that it does not change significantly with age up to 28 days. The load versus tensile strain for VHS (S) concrete with MM (see Figure 6.13b) shows that at 2 days, the tensile strain capacity is about 200 microstrains and that it essentially remains constant with age up to 28 days.

6.3 Freezing-Thawing Tests

6.3.1 Test Setup and Procedure

The freezing-thawing tests were performed in accordance with ASTM C 666, procedure A, using a programmable freezing-thawing chamber as shown in Figure A.9. The chamber housed 12 rectangular aluminum containers 4 1/4 in. (106 mm) wide, 16 1/4 in. (413 mm) long, and 6 in. (150 mm) deep, surrounded by an antifreeze liquid that served as a heat exchange medium for the freeze-thaw cycle.

Two narrow vertical slits were cut in each side of the container to reduce its rigidity. The slits were then filled with silicon to make the container water-tight. Inside the container, small strips of Plexiglas were adhered to the two longitudinal side walls and the bottom to serve as supports for the specimen so that the specimen would be completely surrounded by water. The thickness of the side supports was 1/16 in. (1.6 mm), and that of the bottom supports was 1/8 in. (3.2 mm). These supports ensured proper spacing and clearance of the submerged specimens. The size of the specimen was 3 x 4 x 16 in. (75 x 100 x 400 mm). The specimens were placed inside plastic bags that were filled with water, then placed in the containers. This was to prevent aluminum from reacting with the lime (CaOH) in the concrete.

When the specimens were 14 days old, they were placed, with the finished surface up, in the freezing-thawing chamber and subjected to freezing and thawing between 0° and 40°F (± 3°F), or −17.8° to 4.4°C (±1.7°C). Each freezing-thawing cycle required approximately 2.5 hours to complete. The exact amount of time was somewhat influenced by the ambient temperature in the laboratory.

At intervals of not more than 36 freezing-thawing cycles, the specimens were removed from the freezing-thawing chamber, brought to saturated surface dry condition, and weighed in grams. The weight was later automatically converted to pounds by the computer program used for data analysis. The dimensions of each specimen were measured to the nearest 1/8 in. (3.2 mm). Each specimen was then tested for its fundamental transverse frequency.

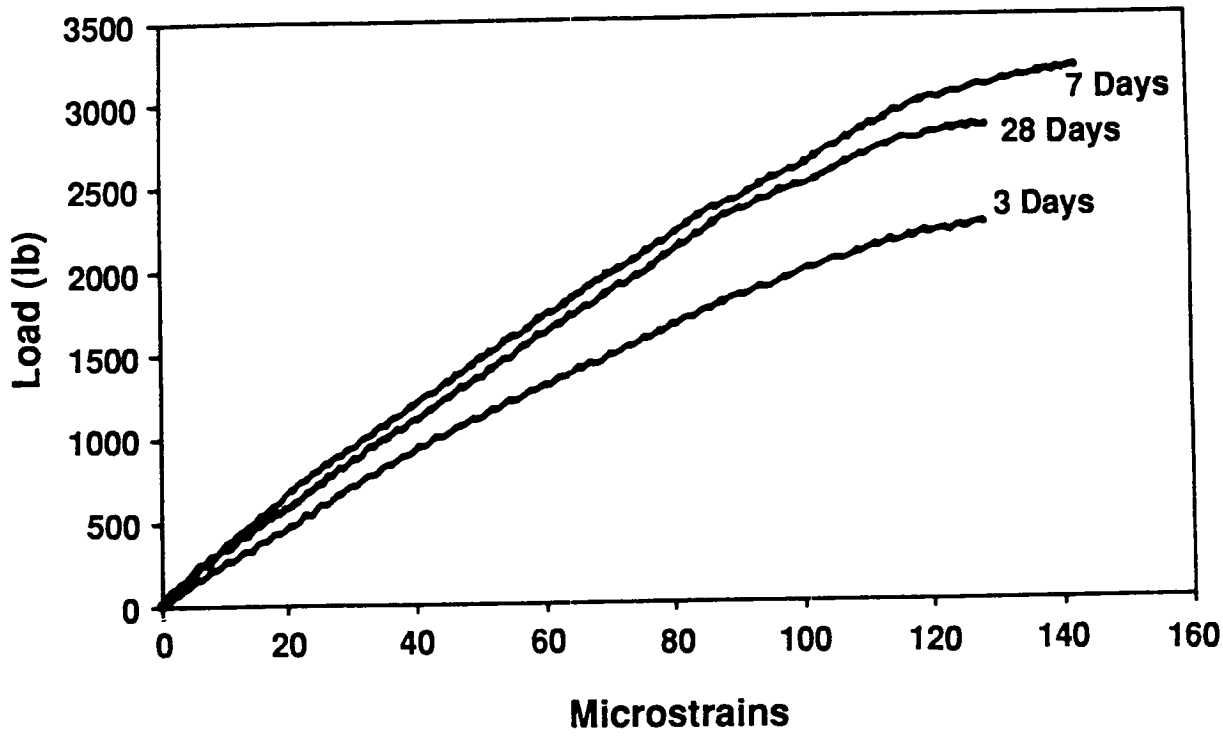

Figure 6.13a Load versus tensile strain of VHS (F) concrete with MM

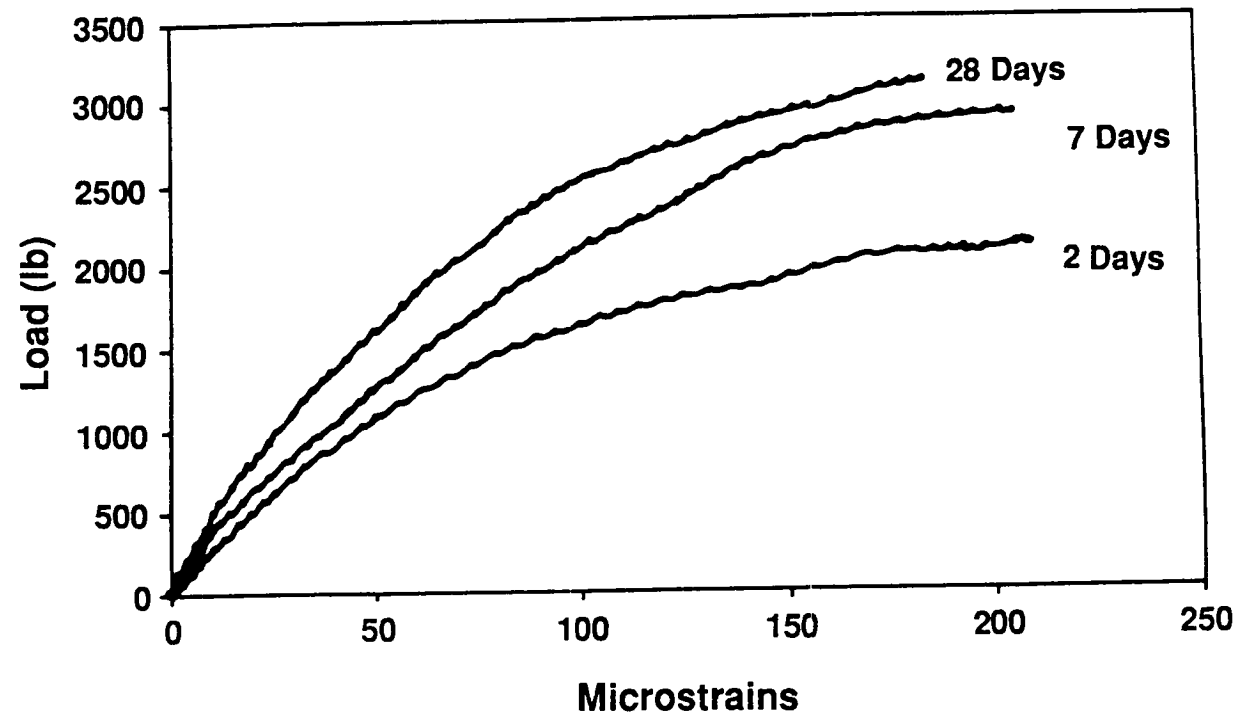

Figure 6.13b Load versus tensile strain of VHS (S) concrete with MM

The fundamental transverse frequency of the specimen was determined using an impact resonance device in accordance with the proposed revision of ASTM C 215. The equipment used for the test is shown in Figure A.10. The impactor used to excite the specimen for frequency measurement was a 1 x 0.5 x 7.75-in. (25 x 13 x 197-mm) steel bar with a weight of 1.034 lb (469 g). The steel bar was used instead of a spherical impactor for practical convenience. Results obtained using both spherical and prismatic impactors were compared beforehand, and no appreciable difference was found.

Soft rubber pad supports were placed at the estimated nodal points of the specimen, at approximately 0.224 of the length of the specimen from each end, to allow the specimen to vibrate freely. A small piezometric accelerometer (Model 303A02, PCB Piezotronics, Inc., Depew, New York) weighing 0.113 oz was placed at mid-height on the specimen near one end. The accelerometer had a calibrated operating frequency range of 10 to 10,000 Hz, a self-resonant frequency of 100 kHz, and a voltage sensitivity in excess of 10 mV/g. Amplitude deviation was within 3% full range.

Since the specimen was moist and adhesion to its surface was difficult, the accelerometer was held tightly against the specimen with a rubber band. Soft wax with good acoustic properties was used between the accelerometer and the specimen surface, which frequently was rough, to ensure good mechanical contact. The soft wax also provided some adhesion and kept the accelerometer from slipping.

The specimen was struck lightly at mid-height near its middle in the same direction as the primary axis of the accelerometer. The accelerometer was connected to a power unit supplied by the same manufacturer. The output signal from the power unit was sent to a digital acquisition (DAQ) board in a PC computer. The board (Model AT-MIO-16L-9, National Instruments, Austin, Texas) is a 12-bit, multipurpose, multiple-gain, 16 single-ended or 8 differential channel, input-output, plug-in board, with a 9 μs analog-to-digital converter, permitting sampling rates of up to 90,000 to 100,000 samples per second. The board was used within an 80386-based 20 MHz stand-alone microcomputer.

The software used to set up and operate the DAQ board was also provided by National Instruments. This software, LabWindows version 2.0 with the Advanced Analysis Library option, permitted standard programming languages to be used (together with special function calls provided with the software) to control or program data acquisition and to optionally perform analysis on the data and save the data or analysis to computer files. The programming language used in this application was Microsoft QuickBASIC version 4.0.

The program was written so that data acquisition of the output from the accelerometer was self-initiating (i.e., a jump in voltage from the accelerometer would initiate data acquisition). The sampling rate was 50 kHz with 2,048 sample points collected. The program transformed the data to time-based values and, using a LabWindows function call, conducted a fast Fourier transform (FFT) on the first 1,024 data points. The program examined the FFT output and selected the frequency with the largest amplitude as the fundamental or resonant frequency.

The program then used the resonant frequency, in combination with the mass of the specimen, to compute the dynamic modulus of elasticity of the specimen based on the following equation given in ASTM C 215:

$$E = CWn^2$$

where W = weight of specimen, lbs
n = fundamental transverse frequency, Hz
C = 0.00245 (L^3T/bt^3), sec^2/in^2, for a prism
L = length of specimen, in.
t, b = dimensions of cross-section of prism, in. (t is the direction in which the prism is driven)
T = a correction factor obtained from a table given in ASTM C 215 = 1.4 (T depends on the ratio of the radius of gyration to the length of the specimen, and on Poisson's ratio).

The resonant frequency test was conducted three times to observe the repeatability of the results. If any one reading deviated from the average of three measurements by more than 10%, the reading was ignored and the test was repeated. The average of the three final readings was then recorded.

After all the specimens were tested, they were returned to the freezing-thawing chamber and placed at different locations before the freezing-thawing cycles were resumed. Each specimen was subjected to the freezing-thawing test for 300 cycles or until its dynamic modulus became less than 80% of its original value, whichever occurred first.

A set of control specimens kept in water at room temperature was also tested for resonant frequency at the same time as the freeze-thaw specimens. The change in dynamic modulus of the control specimen reflected the effect of strength variation of the concrete.

6.3.2 Specimen Preparation

Six groups of specimens of VHS concrete using Type I cement with CG, MM, DL, or RG as aggregates were produced for the freezing-thawing tests. Silica fume was used with each of the four aggregate types, but fly ash was used only with the concrete mixtures containing CG and DL. Each group consisted of a set of three freezing-thawing specimens and one or two control specimens. In addition to the freezing-thawing specimens, a 6 x 6 x 24 in. (150 x 150 x 600 mm) prism was also cast from which the specimens for rapid chloride permeability and AC impedance tests were later obtained.

The mixture proportions, strength, and plastic properties of the concrete used for the test specimens are detailed in Tables 6.8a and 6.8b. The concrete was placed in the molds, vibrated with a needle vibrator, and finished with a magnesium float. A thermocouple wire was placed in one of the freezing-thawing specimens to measure the concrete temperature in the freezing-

Table 6.8a Mixture proportions, strength, and plastic properties of VHS (F) concrete used for freezing-thawing test specimens

Reference No.*	**523**	**657**
Batch ID	**C/VH(F)/3**	**VHFAG3B1**
Cement type	**I**	**I**
Aggregate type	**CG**	**DL**
Sand source	**Lillington**	**Van Buren**
No. of freezing-thawing specimens	**3**	**3**
No. of control specimens	**1**	**1**
Cement, pcy	830	830
Fly ash, pcy	200	200
Coarse aggregate, pcy	1,720	1,684
Sand, pcy	870	1,018
HRWR (naphthalene-based), oz/cwt	30	18
Retarder, oz/cwt	3.0	3.0
AEA, oz/cwt	2.9	2.5
Water, pcy	240	240
W/C	0.23	0.23
Slump, in.	2.5	5.0
Air, %	6.8	6.3
Strength in psi at: 1 day	—	—
14 days	10,070	8,160
28 days	—	9,810
Concrete temperature at placement, ^{0}F	72	76

* Reference No. relates to tables in appendix of volume 2 of this report series.

Table 6.8b Mixture proportions, strength, and plastic properties of VHS (S) concrete used for freezing-thawing test specimens

Reference No.*	518	608	556	667
Batch ID	**C/VH(S)/3**	**R/VH(S)/3**	**M/VH(S)/3**	**VHSFT08**
Cement type	**I**	**I**	**I**	**I**
Aggregate type	**CG**	**RG**	**MM**	**DL**
Sand source	**Lillington**	**Memphis**	**Lillington**	**Van Buren**
No. of freezing-thawing specimens	**3**	**3**	**3**	**3**
No. of control specimens	**1**	**1**	**1**	**1**
Cement, pcy	760	760	760	770
Silica fume, pcy	35	35	35	35
Coarse aggregate, pcy	1,720	1,650	1,570	1,684
Sand, pcy	1,206	1,160	1,140	1,252
HRWR (naphthalene-based), oz/cwt	14	14	12	17
Retarder, oz/cwt	2	3	2	3
AEA, oz/cwt	0.9	0.9	0.6	1.5
Water, pcy	230	220	240	230
W/C	0.29	0.28	0.30	0.29
Slump, in.	2.75	--	4.25	3.5
Air, %	5	8	5.6	5.8
Strength in psi at: 1 day	5,750	--	—	—
14 days	11,780	7,420	6,700	8,620
28 days	—	8,000	—	9,810
Concrete temperature at placement, °F	80	69	77	76

* Reference No. relates to tables in appendix of volume 2 of this report series.

thawing chamber. All specimens were moist-cured for 14 days before they were subjected to the feezing-thawing test.

6.3.3 Test Results and Discussion

The results of the freezing-thawing tests expressed in terms of durability factor are summarized in Table 6.9. Durability factor is defined as

$$D.F. = (E/E_0) \times (N/300)$$

where E_0 = initial dynamic modulus of specimen
N = number of cycles of freeze-thaw up to 300
E = dynamic modulus of specimen after N cycles of freezing-thawing

Figures 6.14 through 6.17 show the typical behavior of selected groups of test specimens in terms of the effect of freezing-thawing on the relative dynamic modulus of each specimen.

Table 6.9 shows that only one group of test specimens failed the freezing-thawing test. The three specimens of R/VH(S)/3 failed completely after only 42 cycles of freezing and thawing. Their failure was due to the weakness of the coarse aggregate used in the concrete. There was clear evidence of disintegration of the coarse aggregate at failure. The RG coarse aggregate from Memphis, Tennessee had an absorption of about 5% but pore sizes of about 0.10 microns (as observed in scaning electron micrographs), the worst possible situation for freezing-thawing deterioration (Hansen 1993).

The results of these tests indicate that VHS concrete can be produced with enhanced durability if it has a minimum air content of 5% and the coarse aggregate used is not susceptible to freezing-thawing damage.

Table 6.9 Results of freezing-thawing test of VHS concrete

Reference No.*	Batch ID	Air) Content (%)	No. of Cycles Completed	Durability Factor (%)		
				Specimen 1	Specimen 2	Specimen 3
523	C/VH(F)/3	6.8	300	100	99	100
657	VHFAG3B1	6.3	310	95	98	95
518	C/VH(S)/3	5.0	300	97	80	95
608	R/VH(S)/3	8.0	42	0	0	0
556	M/VH(S)/3	5.6	300	83	91	71
667	VHSFT08	5.8	300	90	95	92

* Reference No. relates to tables in appendix of volume 2 of this report series.

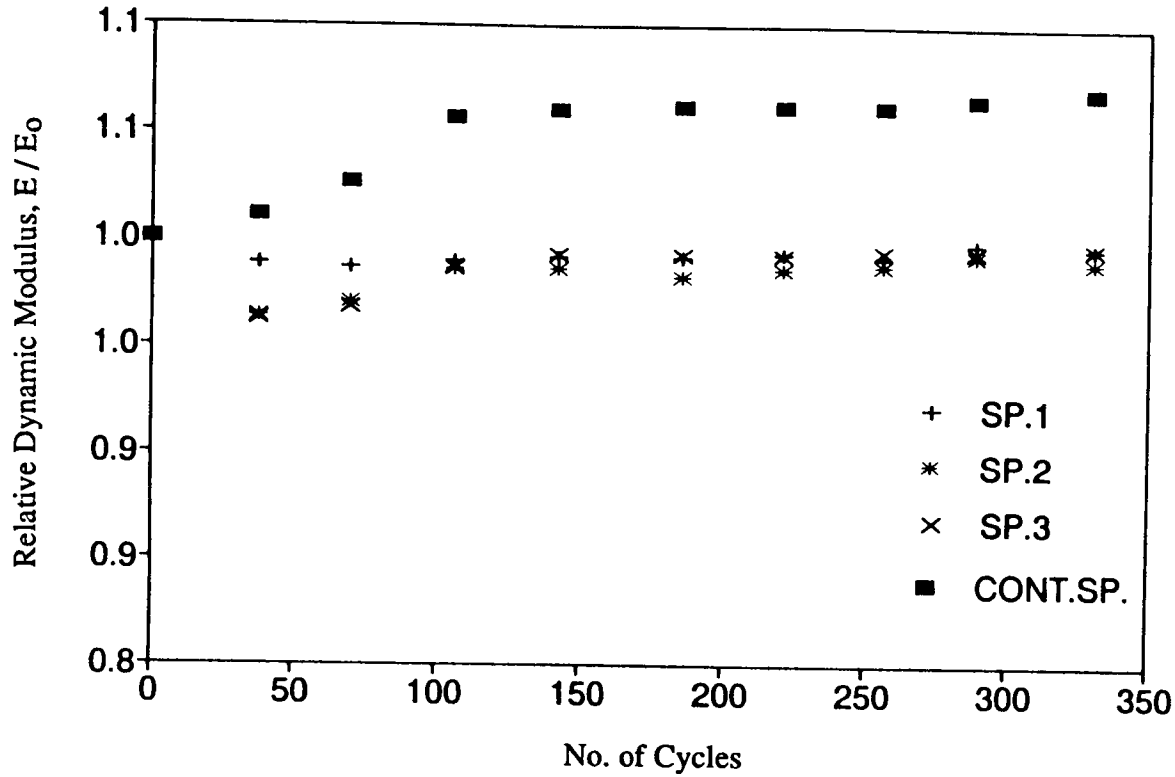

Figure 6.14 **Relative dynamic modulus versus number of freezing-thawing cycles for C/VH(F)/3**

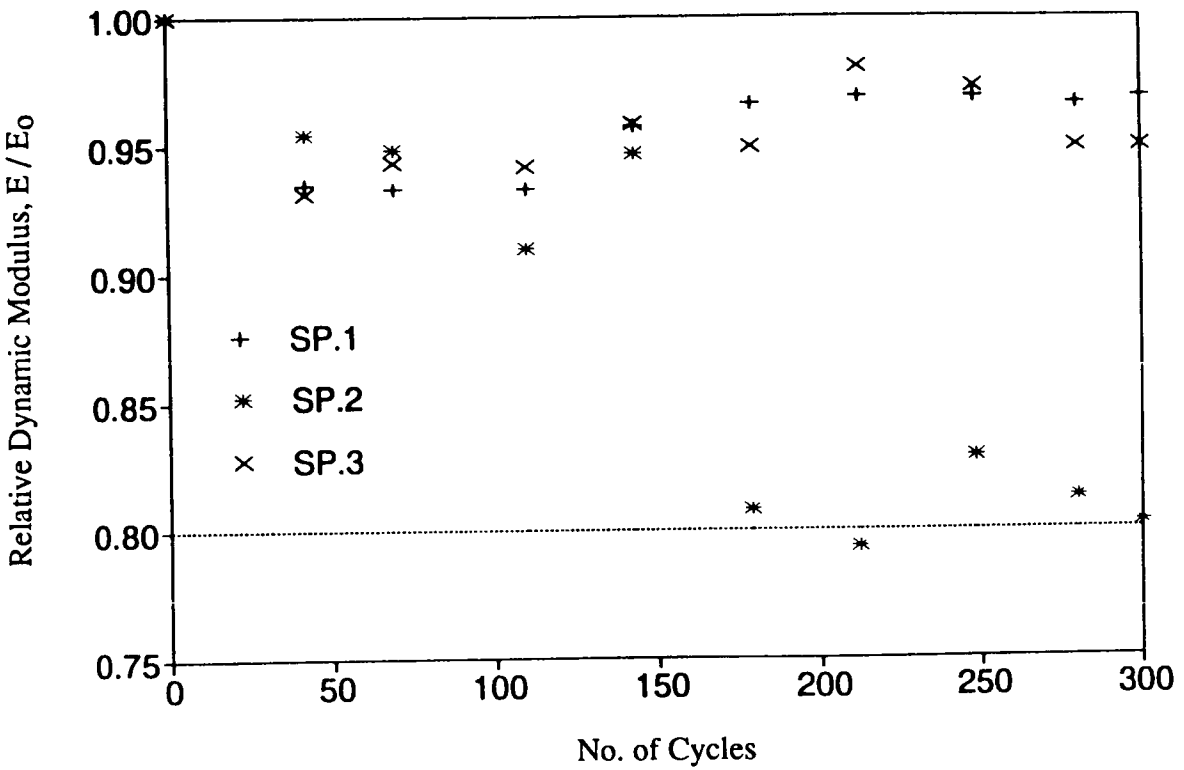

Figure 6.15 **Relative dynamic modulus versus number of freezing-thawing cycles for C/VH(S)/3**

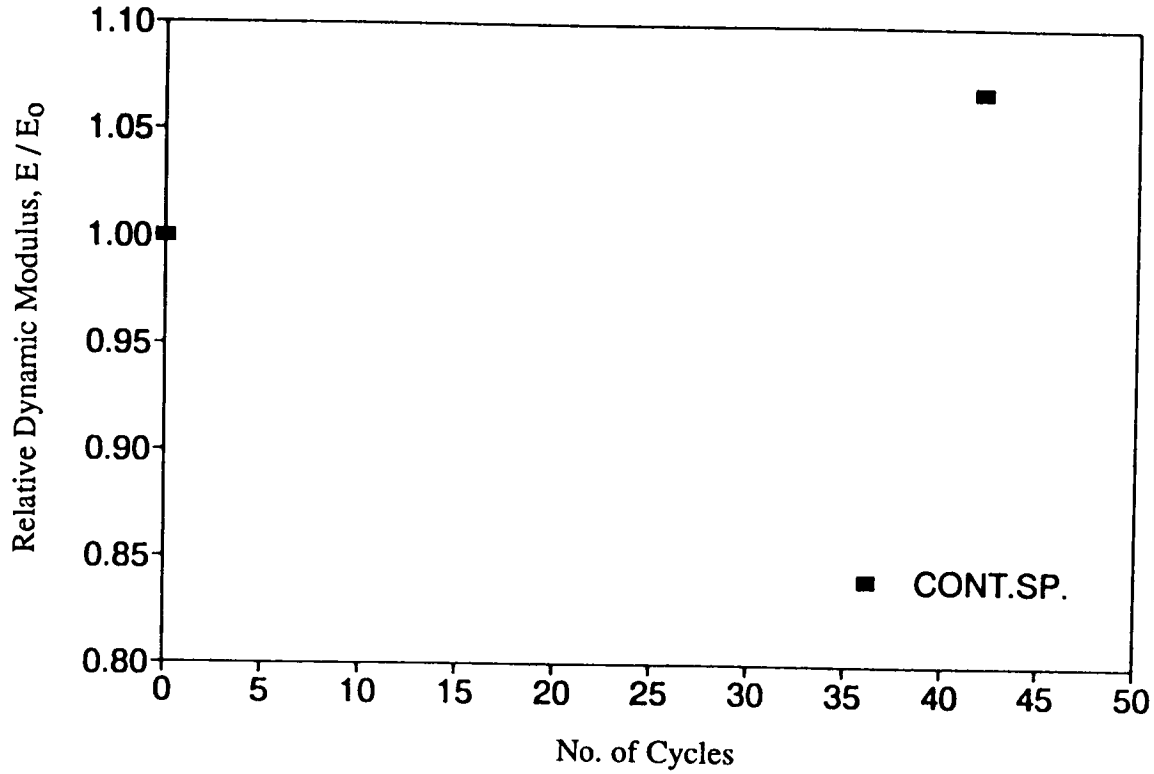

Figure 6.16 **Relative dynamic modulus versus number of freezing-thawing cycles for R/VH(S)/3**

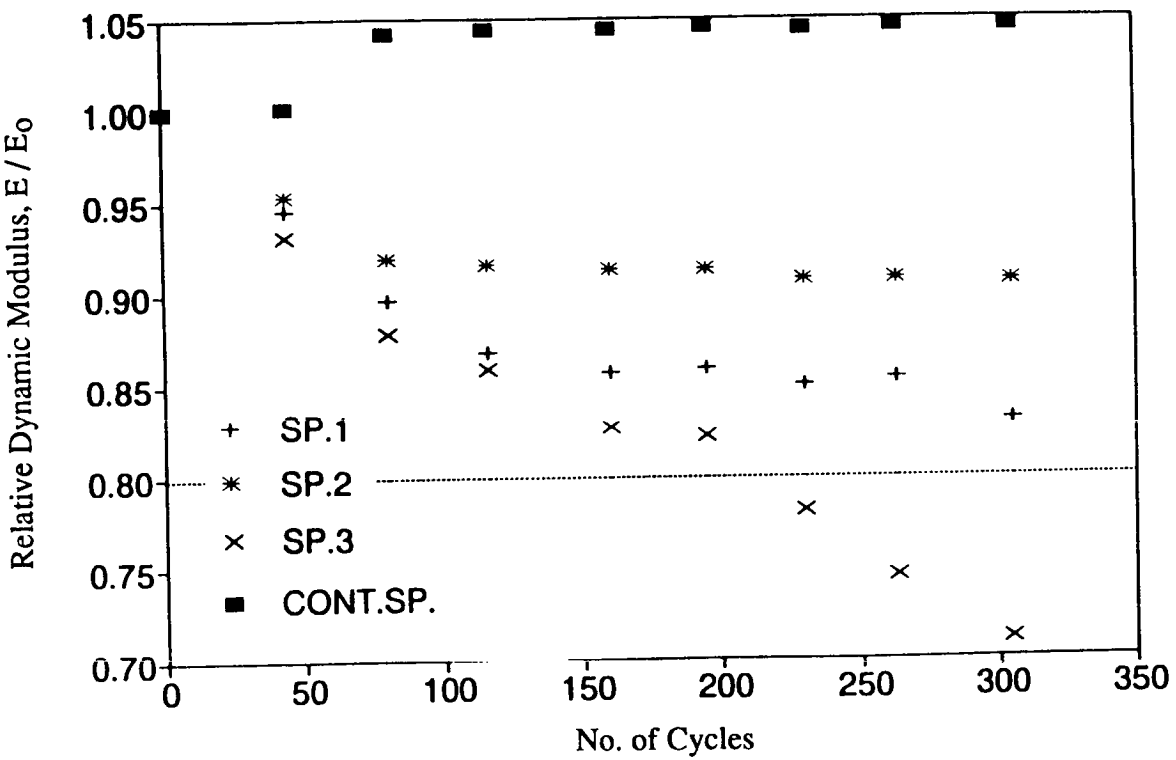

Figure 6.17 **Relative dynamic modulus versus number of freezing-thawing cycles for M/VH(S)/3**

6.4 Shrinkage Tests

The shrinkage tests were conducted on test specimens of 4 x 4 x 11.25-in (100 x 100 x 281-mm) prisms for a period of up to 90 days. Three replicate specimens were tested for each type of coarse aggregate. The overall program for the shrinkage tests is outlined in Table 6.3.

6.4.1 Test Setup and Procedure

The shrinkage tests were conducted in accordance with ASTM C 157. A digital dial gage (OKO SOKKI model DG 154) was used to measure length changes. The gage had a range of 2 in. (50 mm). A view of the shrinkage test is shown in Figure A.11.

6.4.2 Specimen Preparation

The 4 x 4 x 11.25-in. (100 x100 x 281-mm) prisms were cast in steel molds, internally vibrated with a needle vibrator, and finished with a magnesium float. The specimens with molds were protected from moisture loss by covering them with plastic sheets. The specimens were stripped at 24 hours. Upon removal of the specimens from the molds, the specimens and the standard calibration bar were placed in water maintained at 73°F for a period of 30 minutes before being measured for length. This was done to equalize the temperature of the specimens and the bar.

After the initial readings, the specimens were cured in lime-saturated water for 28 days. During this period, the specimens were removed from the water only for measurements. Subsequently, they were stored in air under normal laboratory conditions.

6.4.3 Test Results and Discussions

The results of the shrinkage tests for VHS (F) and VHS (S) concretes are summarized in Table 6.10. The results for VHS (F) concrete indicate that at 90 days, the average shrinkage strain was 521 microstrains for the concrete with CG. The variation of the shrinkage strains with time for VHS (F) concrete with CG and for VHS (S) concrete with three types of coarse aggregates is shown in Figure 6.18. These curves are based on average measurements of three replicate specimens. It can be seen that the curves for VHS (F) concrete with CG and for VHS (S) concrete with MM and RG show an initial expansion where readings were taken at early ages. This phenomenon is common for shrinkage specimens stored in water, according to ACI Committee 209 (1993a). For VHS (S) concrete with MM and RG, the shrinkage strains at 90 days were much smaller (-72 to 124 microstrains) than the generally accepted values (700 to 800 microstrains) for conventional concretes. However, for VHS (S) concrete with CG the average shrinkage strain at 90 days was 361 microstrains, which is about 50% of the generally accepted value for conventional concrete. The general trend of variation of shrinkage strains with time for VHS concretes was similar to that generally accepted for conventional concrete.

Note that the coarse aggregate in a concrete provides a restraining effect on the drying shrinkage of pure cement paste. The amount of restraint provided by the aggregate depends on the amount

Table 6.10 Summary of shrinkage test results for VHS (F) and VHS (S) concretes

Concrete Type	Coarse Aggregate Type	Batch ID	Age (days)	Shrinkage Strain (microstrains)	Avg. of No. of Specimens
VHS (F)	CG	C/VH(F)/3	1	0	3
			14	39	
			28	-120	
			70	512	
			90	521	
			113	531	
			172	486	
VHS (S)	MM	M/VH(S)/3	1	0	2
			14	-240	
			28	-170	
			66	98	
			90	124	
			113	148	
			168	256	
VHS (S)	CG	C/VH(S)/3	1	0	3
			14	45	
			37	217	
			56	361	
			90	361	
			100	361	
			223	505	
			278	538	
VHS (S)	RG	R/VH(S)/3	1	0	3
			30	-66	
			90	-72	
			99	-72	
			154	65	

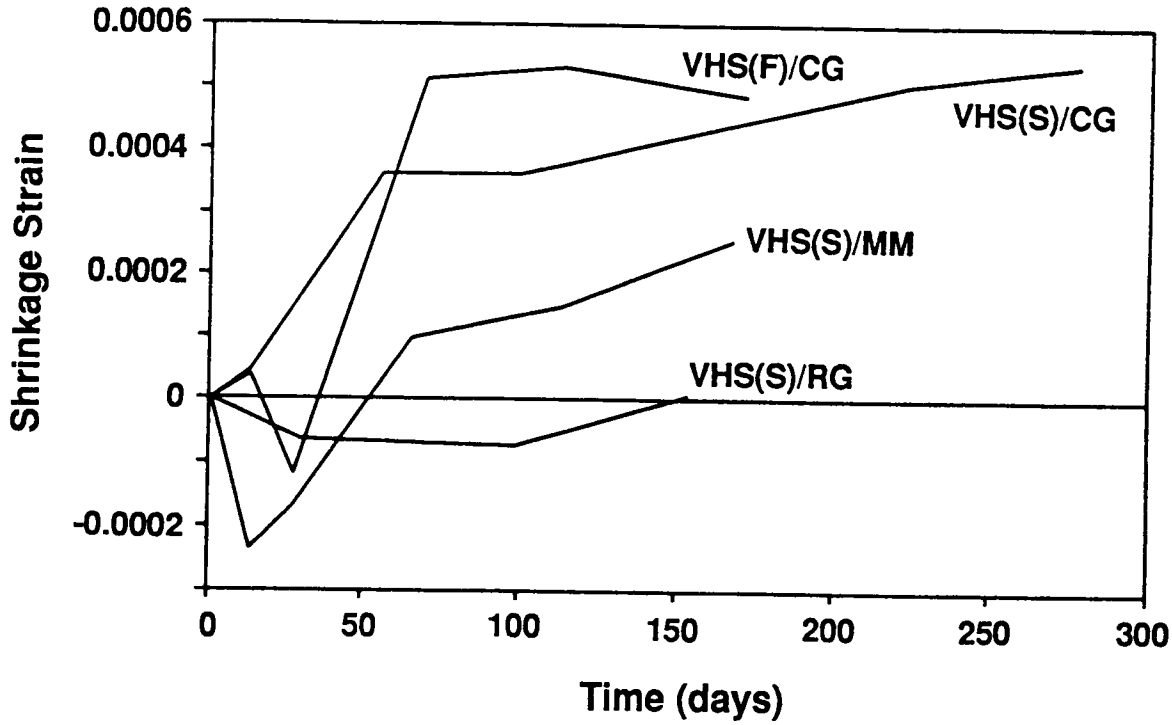

Figure 6.18 Variation of shrinkage strain with time for VHS concretes

of coarse aggregate, the stiffness of the concrete; and the maximum size of the coarse aggregate (Mindess, 1981). The stresses due to drying shrinkage at the interface between cement paste and aggregate increase as the maximum aggregate size increases (Mindess, 1981). The size and shape of a concrete specimen determine the rate of moisture loss and hence the rate and magnitude of drying shrinkage. The absorption characteristics of the coarse aggregate also influence the shrinkage characteristics of the concrete, especially during early ages. The length of diffusion path also has a strong influence on the rate of moisture loss, which in turn affects the shrinkage characteristics.

ACI Committee 209 (1993a) recommends a set of empirical equations that allow shrinkage strains to be estimated as a function of drying and relative humidity. The value of the ultimate shrinkage strain recommended by ACI Committee 209 is 730 $x10^{-6}$ in./in. The magnitude of ultimate shrinkage strain is difficult to estimate accurately because it depends on a number of factors including W/C, degree of hydration, presence of admixtures, and cement content. The average shrinkage strain at 90 days for VHS (F) concrete with CG was 521 microstrains. The average strains at 90 days for VHS (S) concrete varied from an expansion strain of 172 microstrains for concrete with RG to a shrinkage strain of 361 microstrains for concrete with CG.

6.5 Creep Tests

The creep tests were conducted on 4 x 8-in. (100 x 200-mm) cylinders for a period of 90 days. Three replicate specimens were tested for each type of coarse aggregate. The test program is outlined in Table 6.3.

6.5.1 Test Setup and Procedure

The tests were conducted in accordance with ASTM C 512-87. A special creep frame was fabricated to accommodate three 4 x 8-in. (100 x 200-mm) cylinders along with 4 x 4-in. (100 x100-mm) cylinders at each end to minimize the end effects.

6.5.2 Specimen Preparation

The 4 x 8-in. (100 x 200-mm) cylinders were cast in plastic molds, internally vibrated in accordance with section 5.2 of ASTM C 512. Along with three specimens for the creep tests, four additional specimens were also cast. Three of the four additional specimens, referred to as "control" cylinders, were tested for strength; the fourth 4 x 8-in. (100x200-mm) cylinder was used to obtain the 4 x 4-in. (100 x 100-mm) end cylinders to be used in the creep frame. The specimens with molds were protected from moisture loss by covering them with plastic sheets. The specimens were removed from the molds after 24 hours. Upon removal, the specimens were moist-cured in a curing room with 100% relative humidity for a period of 28 days. At the age of 28 days, the three control 4 x 8-in. (100 x 200-mm) cylinders were tested for strength. The three specimens for the creep tests were capped with sulfur capping and placed in the creep frame along with the 4 x 4-in. (100 x 100-mm) end cylinders. The creep frame was located in a room with controlled temperature and humidity. During the creep tests, the temperature and relative humidity were maintained at 73°F and 50% respectively. In placing the creep specimens in the creep frame, special care was taken in aligning the specimens to avoid eccentric loading. The creep specimens were loaded to 40% of the average compressive strength determined from the strength tests of the control cylinders. A load cell was used to monitor the load. The creep deformations were recorded periodically by a Whitmore gage. The load level was also checked periodically, and necessary adjustments were made to ensure that the load level was maintained for the duration of the creep tests.

6.5.3 Test Results and Discussion

The results of the creep tests for VHS (F) and VHS (S) concretes are shown in Figures 6.19a and 6.19b. These curves are averages of three replicate specimens. Note that the total creep strain in each case was obtained by subtracting the initial elastic strain and the shrinkage strain of unloaded control specimens from the total measured strain of the creep specimens. Specific creep in each case was obtained by dividing the total creep strain by the applied stress.

The results for VHS (F) concrete indicate that the creep behavior of concrete is influenced by the type of coarse aggregate. The role of the aggregate in influencing creep behavior is similar to the

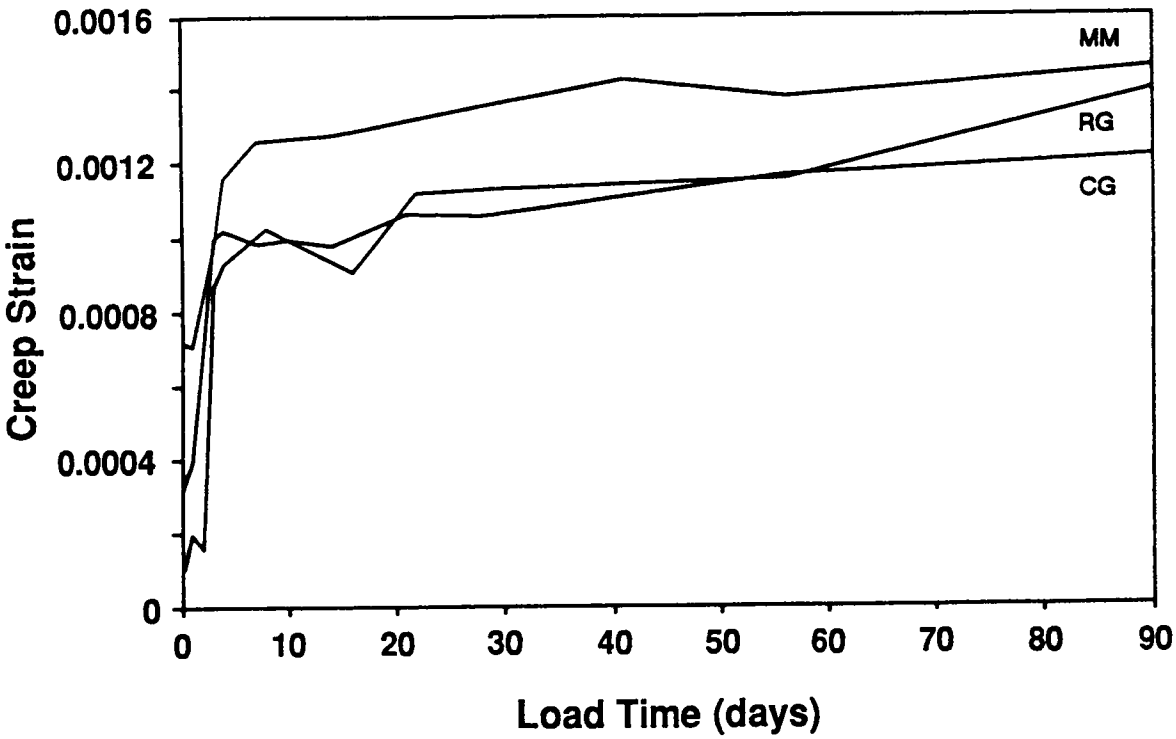

Figure 6.19a Variation of creep strain with time for VHS (F) concrete

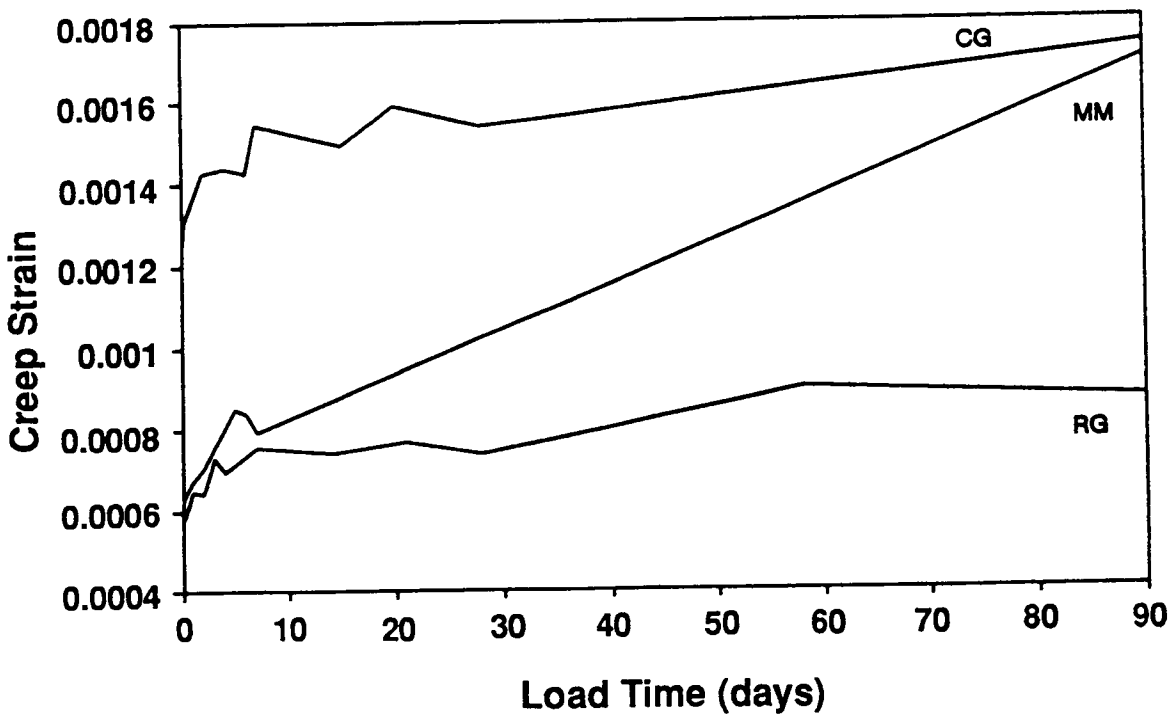

Figure 6.19b Variation of creep strain with time for VHS (S) concrete

role of aggregate in influencing shrinkage behavior. The coarse aggregate acts as a restraint to reduce the potential deformations of the paste. Thus, the aggregate content and the modulus of elasticity are the more important parameters affecting the creep of the concrete. Aggregate size, grading, and surface texture have little influence (Mindess, 1981). VHS (F) concrete with RG exhibits larger total creep strains as well as larger specific creep strains compared with VHS (F) concrete with CG and MM (see Figure 6.19a) Note that although MM is softer than the other aggregates, concrete with MM exhibits smaller total creep strains as well as smaller specific creep strains compared with the relatively stiffer aggregates.

For VHS (S) concrete, the creep strain at 90 days for concrete with MM is larger than for concretes with CG and RG. The variation of the creep strain with time is similar to that for VHS (F) concrete except for VHS (S) concrete with MM. The results (see Figures 6.19a and 6.19b) also indicate that addition of silica fume instead of fly ash to obtain VHS concrete appears to reduce both the total and the specific creep strains for concrete with RG and CG. For VHS concretes with MM, the results of specific creep strains for VHS (S) concrete appear to be inconsistently higher than for VHS (F) concrete with MM coarse aggregate. The results indicate that the specific creep strain for VHS concretes ranges from 20% to 50% of the specific creep strain of conventional concrete with a strength of 4,000 psi (28 MPa).

6.6 Rapid Chloride Permeability Tests

6.6.1 Test Setup and Procedure

The rapid chloride permeability test (RCPT) was performed in accordance with AASHTO T 277-83 and the identical ASTM C 1202. The typical specimen was a 2-in. (50-mm) thick slice sawed from the top of a 3.75-in. (94-mm) diameter core from a concrete prism cast at the same time as the freezing-thawing test specimens (Section 6.3.2). The top of the specimen was the finished surface that would be exposed to chloride ions.

The specimen was prepared by vacuum saturation and by soaking in water for 18 hours (Figure A.12). The specimen was then sealed in the test cells. The cell connected to the top surface of the specimen was filled with 3% sodium chloride (NaCl) solution, and the cell connected to the bottom surface of the specimen was filled with 0.3 N sodium hydroxide (NaOH) (Figure A.13). Two replicate specimens were always tested concurrently. Both specimens were energized continuously with 60 V DC between the cells (Figure A.14). The current flowing through the concrete specimen was measured and plotted on a strip chart recorder for 6 hours (Figure A.15). A switching unit was built to allow two measurements to be alternately plotted on one strip chart. The total time required to complete each test was about 33 hours. The test procedure followed these steps:

1. Obtain two 3.75-in. (94-mm) diameter concrete samples by coring through a 6 x 6-in. (150 x 150-mm) prism, oriented as cast, when the concrete is 12 days old. (Two days

are allowed for specimen preparation so that actual testing can be started at 14 days.) Keep the samples in a plastic bag.

2. Saw a 2-in. (50-mm) slice from the top of each core. Surface-dry the specimens for 10 minutes after cutting. Mark ID on each specimen and clearly identify its top surface. Keep the specimens in a plastic bag.

3. Boil 2 liters of water vigorously to de-air the water. Do not cap the boiling pot. Allow the water to cool.

4. Prepare clear epoxy; brush on side surface of each specimen. Allow the epoxy to cure as per manufacturer's instructions (use a type that will cure in 1 hour or less).

5. Place both specimens, separated slightly, in a tilted position in a beaker, then place the beaker in a *vacuum-type* desiccator and start vacuum (1 mm Hg abs.). Maintain vacuum for 3 hours.

6. While keeping the vacuum pump running, fill the beaker with the boiled water until it submerges the specimens.

7. Continue running the vacuum pump for 1 additional hour.

8. Turn the pump off and allow air to enter the desiccator.

9. Allow both specimens to remain in the beaker to soak in water for 18 hours.

10. Remove the specimens from the beaker, blot off water, and place the specimens in a plastic bag.

11. Place a small amount of silicon sealant on the brass shim around the inside perimeter of each cell. Place the specimen in the cell assembly with its top side toward the NaCl cell. Apply liberal amounts of silicon sealant around the specimen to seal it to the cells. Allow the sealant to cure as per manufacturer's recommendations (use a type that will cure in about 1 hour).

12. Fill (–) cell (top side) with 3% NaCl solution. Fill (+) cell with 0.3 N NaOH. Connect wires as marked with negative to NaCl and positive to NaOH. Turn on power, set to 60.0±0.1 v DC, and turn on plotter. Set plotter at 1 v full scale (this is actually 0.985 A full scale on NCSU's plotter) and 2 in./hr. Record time and ID number on plotter paper. Run the test for 6 hours.

13. Remove the specimens from the test cells. Rinse the cells and clean the assembly.

14. Integrate the area under the curve produced by the plotter in units of ampere-seconds (i.e., coulombs) and record results.

6.6.2 Test Results and Discussion

A total of seven groups of specimens of VHS concrete were subjected to the RCPT (Table 6.11). Each group consisted of two replicate specimens that were tested concurrently in two separate RCPT cells. A typical output strip chart from the RCPT is shown in Figure A.16. The abscissa represents time, obtained at a chart rate of 5 cm/hr for approximately 6 hours. The ordinate represents current (in amperes) flowing through the specimen, with a chart calibration of full scale being equal to 0.985 A for the particular plotter used.

As described above, two replicate specimens were tested together and both were energized continuously for 6 hours. However, the current flowing through each specimen was measured and plotted alternately on the strip chart. The average area under the curve in ampere-seconds (coulombs) is the total charge that passed through the specimen in 6 hours. The initial current in amperes is the average ordinate just after the test was started.

It can be seen that the amount of current flowing through the specimen tended to increase during the RCPT, due at least in part to the temperature increase in the specimen. This heating problem was, in turn, caused by the current. Thus the question was raised whether the initial current, which is also an indirect measure of the concrete conductance, could be used in lieu of the total charge as a more convenient way to obtain data for the RCPT. If so, 6 hours of testing time could be saved. It is encouraging to observe that a comparison of the initial current with the total charge for each of the seven groups of testing (Table 6.11) indicates a good correlation between the two measurements.

Note that both the freezing-thawing test and the RCPT were performed for six of the seven groups of specimens. As discussed in Section 6.3.3, only one of the six groups failed the freezing-thawing test because of deterioration of the coarse aggregate (i.e., RG). However, even though the specimens failed the freezing-thawing test, their coulomb values from the RCPT were reasonably low.

6.7 AC Impedance Tests

The objective of conducting the AC impedance test was to examine its potential as a reasonable alternative to the RCPT for more rapid determination of concrete permeability. The goal was to explore a faster method that could be more versatile and portable. The method would also avoid elaborate test setups and specimen preparation as well as expensive and time-consuming procedures. The use of external measurement terminals would allow more versatility than internal terminals used for the RCPT. A "point source" type of test such as the AC impedance test would be also more versatile since it could be adapted more easily to specimens of different shapes.

Table 6.11 Results of rapid chloride permeability test (RCPT) of VHS concrete

Reference No.*	Batch ID	W/C	Air (%)	Freezing-Thawing Cycles	Durability Factor (%)			RCPT	
					Sp. 1	Sp. 2	Sp. 3	Initial Current (A)	Total Charge (C)
523	C/VH(F)/3	0.23	6.8	300	100	99	100	0.087	2,366
563	M/VH(F)/3F1	0.23	10.6	--	--	--	--	0.186	6,500
657	VHFAG3B1	0.23	6.3	310	95	98	95	0.144	3,260
518	C/VH(S)/3	0.29	5.0	300	97	80	95	0.028	510
608	R/VH(S)/3	0.28	8.0	42	0	0	0	0.118	3,120
556	M/VH(S)/3	0.30	5.6	300	83	91	71	0.090	2,149
667	VHSFT08	0.29	5.8	300	90	95	92	0.140	3,155

* Reference No. relates to tables in appendix of volume 2 of this report series.

The RCPT measures total conductance of a specimen rather than conductivity. Similarly, the AC impedance test measures total resistance (in ohms), which may be more indicative of the gross concrete properties than resistivity. As long as the test could classify concrete as accurately as the RCPT, it would be a satisfactory alternative.

6.7.1 Test Setup and Procedure

Currently there are no AASHTO or ASTM standards for the AC impedance test. The test for this investigation was conducted using a Kohlrausch bridge instrument (Model 4000, AEMC Instruments, Boston). The Kohlrausch bridge uses 1,000 Hz AC with an accuracy of 1% on the impedance measurement. Eight impedance ranges can be selected using pushbuttons; usually the 1–10 kΩ range was used. The voltage actually placed across the specimen was measured to be about 0.20 v. Six 1.5 v AA batteries were used as power supply. The general setup is shown in Figure A.17.

A good electrical connection between the Kohlrausch bridge terminals and the concrete specimen was ensured by using potassium agar gel. The impedance (resistance) was measured at five random points on each specimen (see Figure A.18).

The AC impedance test was conducted in conjunction with the RCPT at three different stages:

1. after the RCPT specimens were cut, but before they were subjected to the vacuum saturation process;

2. after the specimens were vacuum-saturated, but before they were subjected to RCPT;

3. after the specimens were subjected to RCPT.

Therefore the specimens for the AC impedance test were prepared exactly in the same manner as for the RCPT. The AC impedance test procedure followed these steps:

1. After the specimen is cut from a 3.75 in. (95.3 mm.) concrete core, air-dry the specimen to avoid wet surfaces that may distort the electrical measurements.

2. Connect two electrode wires to the Kohlrausch bridge (which is similar to a Wheatstone bridge), with the sepecimen placed into one arm of the bridge. The free end of each wire should have a flattened piece of solder, about 0.25-in. (6.4-mm) diameter, as electrode. Virtually any type of electrical wire can be used to connect the concrete specimen into the bridge circuit since the current is very small. A wire length of about 18 in. (450 mm) is recommended.

3. Put a rubber glove on the hand that will press the electrodes onto the concrete specimen.

4. Dip the solder ends of the wires into potassium agar gel to obtain a small amount of gel, which ensures good conductivity between the electrodes and the concrete.

5. Press the solder flat ends against the two flat surfaces of the test specimen and hold them in place with the thumb and middle finger of one hand. With a little practice, a good connection can be made by feel. Also, the gel "fingerprint" should be kept small and consistent throughout the testing.

6. Balance the Kohlrausch bridge circuit and record the impedance measurement (in ohms).

7. Repeat the measurement at five random locations on the flat surfaces of each of the replicate specimens. Be careful not to allow the gel fingerprint to overlap, as this will affect the conductance.

6.7.2 Test Results and Discussion

AC impedance tests were conducted along with the RCPT on four groups of VHS concrete specimens (Table 6.12). (The AC impedance test was not conducted at Arkansas on concrete with DL.) As mentioned above, AC impedance was measured five times on each of two replicate

specimens, for a total of 10 measurements. Therefore each impedance value listed in Table 6.12 is the average of the 10 measurements.

Table 6.12 Results of AC impedance test of VHS concrete

Reference No.[1]	Batch ID	W/C	Air %	AC Impedance Test (Ω)			RCPT	
				Before Sat.[2]	After Sat.[3]	After Test[4]	Initial Current (A)	Total Charge (C)
523	C/VH(F)/3	0.23	6.8	2,785	2,750	2,616	0.087	2,366
563	M/VH(F)/3F1	0.23	10.6	--	1,592	1,222	0.186	6,500
556	M/VH(S)/3	0.30	5.6	3,921	2,320	2,766	0.090	2,149
608	R/VH(S)/3	0.28	8.0	2,351	2,354	2,839	0.118	3,120

[1] Ref. No. relates to tables in appendix of volume 2 of this report series.
[2] Test conducted before specimen was vacuum-saturated for RCPT.
[3] Test conducted after specimen was vacuum-saturated for RCPT.
[4] Test conducted after completion of RCPT.

The AC impedance was measured three times on the RCPT specimens: (1) just after the specimen was cut but before vacuum saturation, (2) after vacuum saturation of the specimen, and (3) after the RCPT was completed. Note that the degree of saturation is initially more varied in a specimen, so its conductance is lower and its impedance higher. After vacuum saturation, the degree of saturation of the specimen becomes more uniform, so its conductance is improved and its impedance reduced. After the RCPT is conducted on the specimen, its impedance again becomes slightly higher; this is because the test has affected the conductance of the specimen by driving some unknown amount of chloride ions into the concrete and driving out some of the ions originally in the pore water of the concrete. Furthermore, any heating of the specimen may accelerate further hydration of residual cement, thereby changing the electrical conductance pathways through the concrete. Because of these effects, vacuum saturation is regarded as the best preparation of the specimen for the AC impedance test.

As discussed before, chloride permeability (in coulombs) is essentially a conductance test whereas AC impedance (in ohms) is essentially a resistance test. Since the two properties are reciprocals, an inverse relationship could be expected between the data from these measurements. After evaluating the two sets of data in several ways, it was determined that the best way to correlate the two properties is by expressing the inverse impedance (reciprocal of impedance after saturation) in terms of the initial current as shown in Figure 6.20.

6.8 Concrete-to-Steel Bond Tests

Concrete-to-reinforcing steel (C-S) bond tests were conducted to determine the concrete-steel bond strength for VHS concrete. For these tests, the specimens were designed according to current ACI Code provisions for embedment length. The specimens had a cross-sectional area of 6 x 15 in. (150 x 375 mm) with an embedment length of 14 in. (350 mm) and a total length of 26 in. (650 mm). A No. 6 bar was centered 3 in. (75 mm) from the top and protruded from both ends of the specimen. The test program is outlined in Table 6.3.

6.8.1 Test Setup and Procedure

The test frame and general loading arrangement for the C-S bond test is shown in Figure A.19. A 120 kip (534 kN) center hole jack was used to apply the load to a No. 6 reinforcing bar embedded in the concrete specimen. The load was increased monotonically and the associated slip at the loaded and free ends of the bar was monitored. The reinforcing bar was axially attached to a 160 ksi (1,102 MPa) smooth prestressing rod of equal diameter. This smooth prestressing rod was instrumented with electrical resistance strain gages to act as a load cell.

Bar slip was measured using dial gages accurate up to 0.0001 in. (0.0025 mm). At the free end, the gages were mounted with the probe touching the end of the bar. At the loaded end, the gages were attached to the bar using a ring and set screws.

Loads were applied to the bar in increments of 2 kip (4.5 ksi, 31 MPa stress) until yielding occurred. Loading was stopped either upon pullout of the reinforcing bar or upon reaching 125% to 140% of the yield strength of the bar. At each load increment, load was maintained for a short period until the slip movements stabilized. A pictorial view of the test setup is shown in Figure A.20.

6.8.2 Specimen Preparation

The C-S bond test specimens were cast with the No. 6 bar at 2.5 in. (63 mm) from the bottom of the concrete beam with a concrete cover of 3 in. (76.2 mm) on each side. Polyvinyl chloride pipe sleeves with a 1-in. (25-mm) inner diameter surrounded the reinforcing steel bar on either end of the designed embedment length of 15 in. (375 mm). This minimized the local effect from the point loading. The embedment length used for the No. 6 bar was computed using the ACI 318 equation (1993c) based on a design strength of 5,000 psi (35 MPa) and a steel yield strength of 60,000 psi (420 MPa).

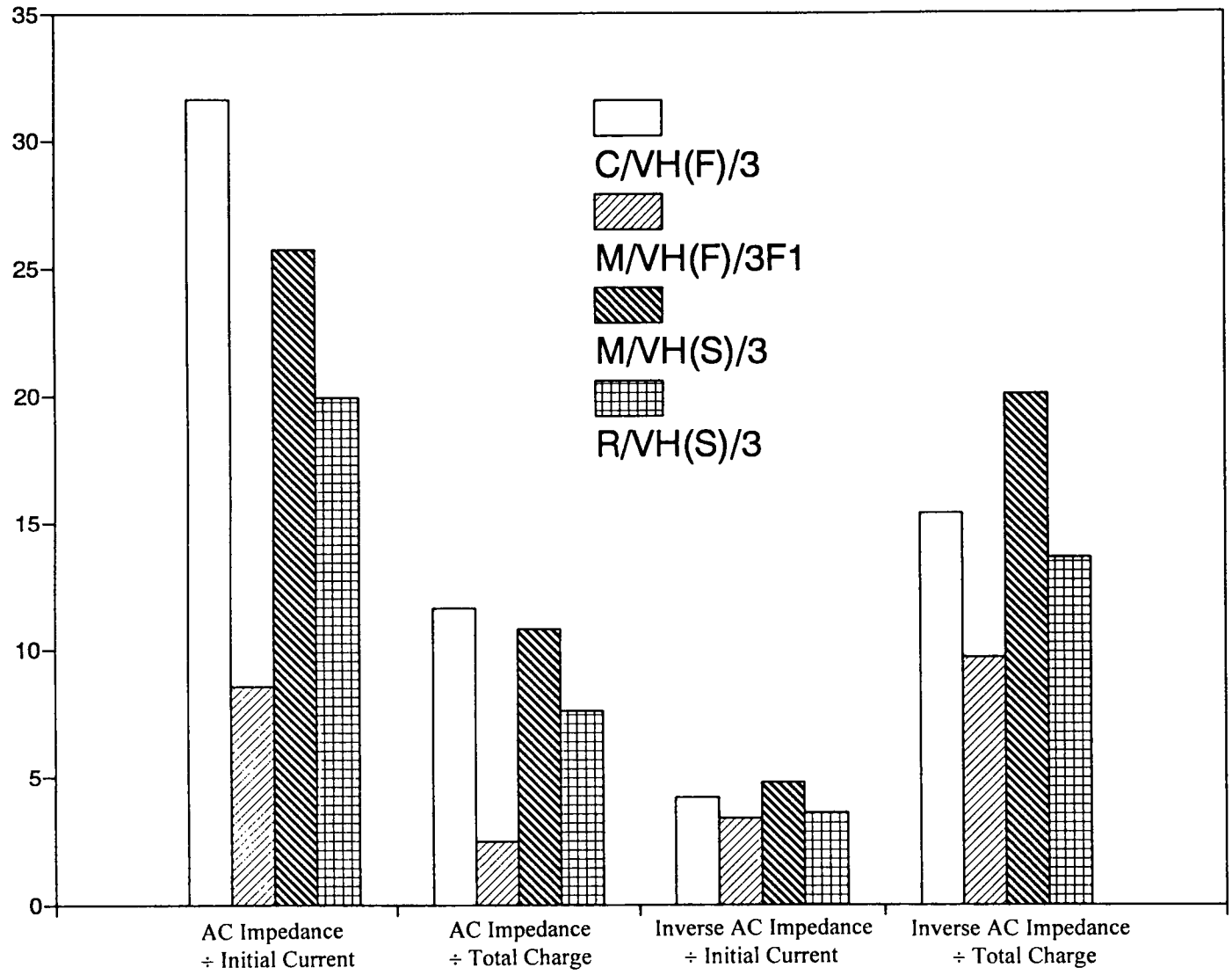

Figure 6.20 **Comparisons of results from AC impedance test and RCPT**

6.8.3 *Test Results and Discussion*

The results of the C-S bond tests are reported in Table 6.13. The values of concrete strength at the design age of 28 days are the average compressive strength of two 4 x 8 in. (100 x 200-mm) replicate specimens. The steel stress versus net slip at the pulling end for two replicate specimens of VHS (F) and VHS (S) concretes with CG is shown in Figures 6.21a and 6.21b. The bars reached a stress of 60,000 psi (420 MPa) at roughly 0.014 in. (0.36 mm) for the VHS (F) concrete and at 0.005 in. (0.20 mm) for the VHS (S) concrete. Therefore, the ACI 318 provisons (1993c) for the development length are adequate in this case. Note that although the ACI 318 equation was developed for normal strength concretes that reach their design strength at 28 days (f_c' less than 6,000 psi, 42 MPa), the equation is also applicable for VHS concrete.

Table 6.13 Summary of test results of concrete-to-steel bond tests for VHS (F) and VHS (S) concretes

Coarse Aggregate Type	Specimen ID	Age at Testing (days)	Air content (%)	Slump (in.)	Concrete Temp. (^{0}F)	f_c' of HPC at Testing (psi)
CG	VHS (S)/5S1	28	6.5	6.0	72	10,100
CG	VHS (S)/5S2	28	6.8	6.7	72	10,350
CG	VHS (F)/5S1*	28	4.5	9.5	80	10,200
CG	VHS (F)/5S2*	28	7.2	10.0	80	9,430

* Blue Circle cement (Type I) from Ravena, New York was used instead of Blue Circle cement from Harleyville, South Carolina.

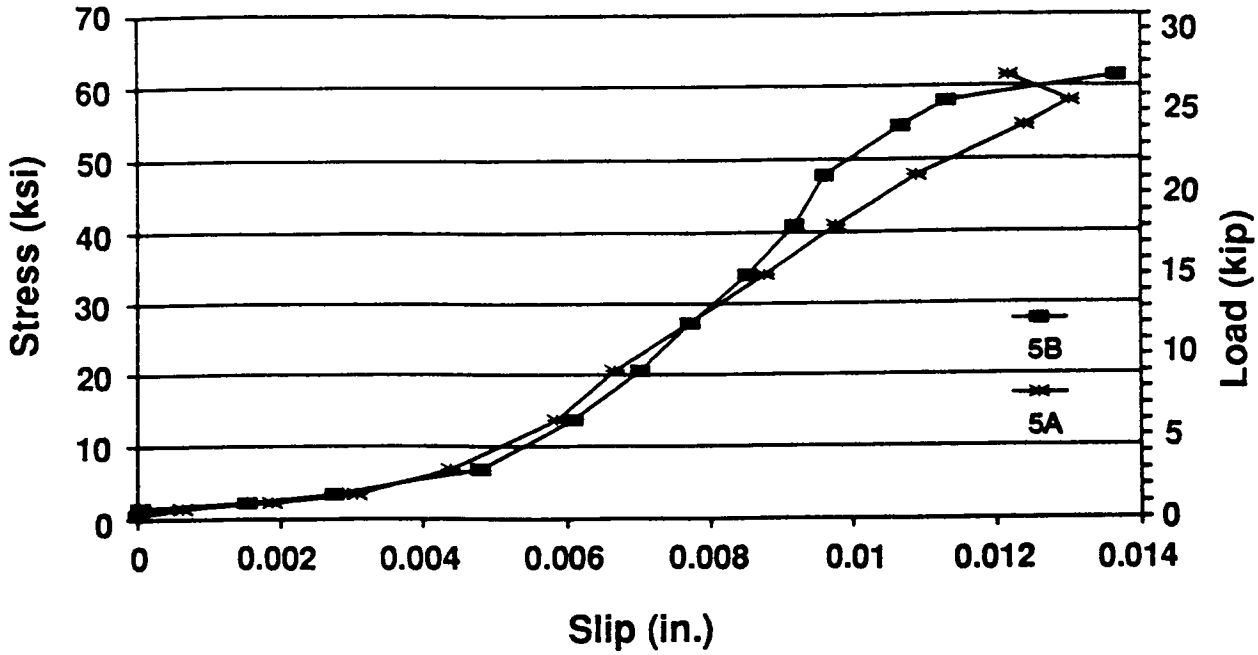

Figure 6.21a Stress versus net slip for VHS (F) concrete in C-S bond test

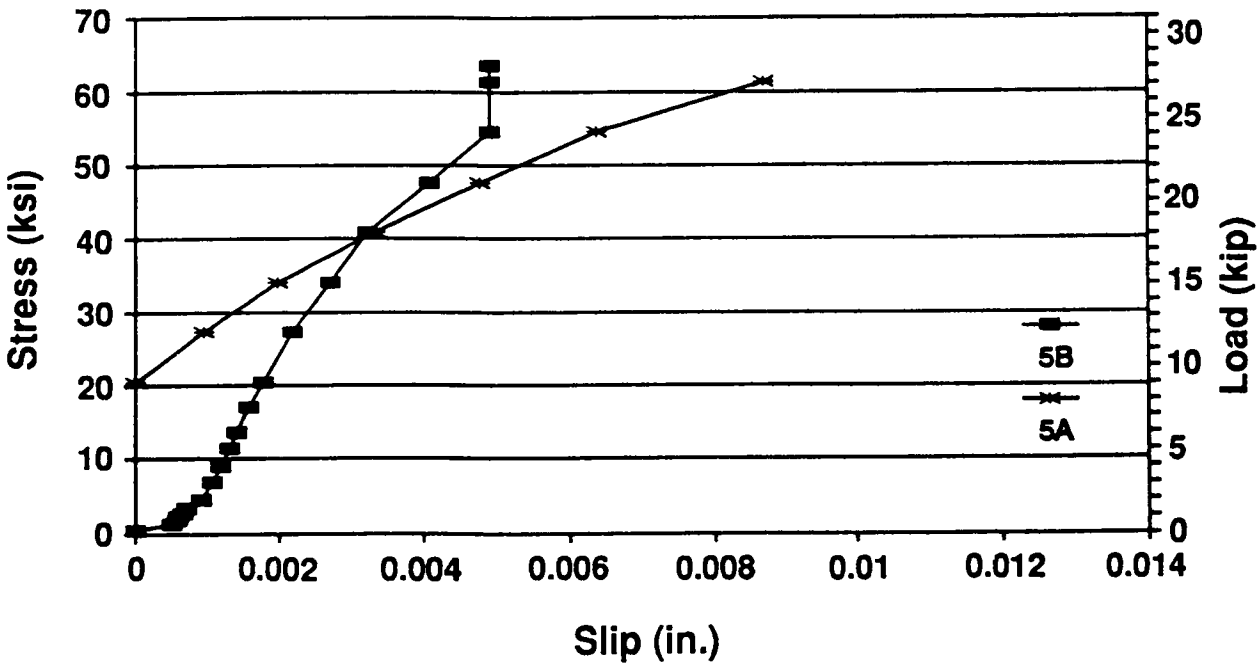

Figure 6.21b Stress versus net slip for VHS (S) concrete in C-S bond test

7

Conclusions

This report has documented the results of an extensive program of laboratory studies on the performance of very high strength (VHS) concrete, which is a class of high performance concrete designed for highway applications. The laboratory studies included eight different types of test: compression, flexural and split tension, shrinkage, creep, freezing-thawing, rapid chloride permeability, AC impedance, and concrete-to-steel bond. Based on the results of this investigation, the following conclusions can be drawn:

1. Using conventional materials and equipment, but with more care than needed for conventional concrete, VHS concrete with either fly ash or silica fume as the mineral admixture can be produced that will achieve a minimum compressive strength of 10,000 psi (70 MPa) in 28 days. Such concretes can be produced with either crushed granite or dense crushed limestone as coarse aggregate. However, with weaker aggregates such as marine marl and washed rounded gravel, the compressive strength would be slightly lower for comparable mixture proportions.

2. Because the demand for early strength gain is not critical for VHS concrete, it is not necessary to use insulation for curing under normal conditions.

3. Because of a larger amount of Type I cement plus fly ash or silica fume used in the VHS concrete mixtures along with a relatively low W/C, the strength development of the concretes is much more rapid in the first 7 days than predicted by the current recommendation of ACI Committee 209 (1993a) based on conventional concrete. The subsequent rate of strength growth is greatly reduced and is comparable to that predicted by the ACI method.

4. The modulus of elasticity increases with time in the same manner as the compressive strength. The same is true of the flexural modulus.

5. Because the design strength of VHS concrete is not too much higher than the upper ranges of conventional concrete, the mechanical behavior of VHS concrete, such as the modulus of elasticity and the compressive and tensile strain capacities, is similar to that of conventional concrete. The modulus of elasticity, the flexural modulus, and

the splitting tensile strength can still be predicted reasonably well by the ACI Code equations (1993c).

6. As VHS concrete ages, its stress-strain relationship becomes more linear.

7. VHS concrete with silica fume [VHS (S)] appeared to be slightly stiffer than VHS concrete with fly ash [VHS (F)] as measured by the modulus of elasticity. The modulus of elasticity is lower for concrete with softer aggregates such as marine marl.

8. The observed compressive strain capacity ranged from 1,000 to 2,500 microstrains. The VHS (F) concrete exhibited slightly higher compressive strain capacity than the VHS (S) concrete. The tensile strain capacity varied from 120 to 180 microstrains. The VHS (F) concrete exhibited lower tensile strain capacity than the VHS (S) concrete. These strain capacities are comparable to those of conventional concrete.

9. Even with a very low W/C, VHS concrete should have an adequate amount of air entrainment to enhance its freezing-thawing resistance. The results of this investigation indicate that the VHS concrete will meet the stringent requirement of a durability factor of 80% (in contrast to 60% commonly expected of quality conventional concrete) after 300 cycles of freezing and thawing according to ASTM C 666, procedure A, if the concrete contains at least 5% entrained air.

10. VHS concrete produced with washed rounded gravel from Memphis, Tennessee failed the freezing-thawing test according to ASTM C 666, procedure A, because of the deterioration of the aggregate, even though the concrete contained 8% entrained air. The aggregate had an absorption of about 5% and pore size of about 0.10 microns (as observed from scanning electron micrographs), the worst possible condition for freezing-thawing deterioration (Hansen 1993).

11. Shrinkage of VHS concrete follows the general trend of conventional concrete. The average shrinkage strain of the VHS (F) concrete with crushed granite aggregate was 521 microstrains at 90 days, which is about 70% of the ultimate shrinkage strain recommended by ACI Committee 209 (1993a) for the conventional concrete. On the other hand, the average 90-day shrinkage strains of VHS (S) concrete varied from -72 microstrains for concrete with washed rounded gravel aggregate to 361 microstrains for concrete with crushed granite aggregate, which indicates that VHS (S) concrete has even less shrinkage potential than VHS(F) concrete.

12. The observed creep strains of the different groups of VHS concrete ranged from 20% to 50% of that of conventional concrete. The creep strains were especially low for concretes with a 28-day strength in excess of 10,000 psi (70 MPa). The specific creep of the concrete with marine marl was much higher than that of the concrete with either crushed granite or washed rounded gravel.

13. With very low W/C and using silica fume or fly ash as mineral additive, VHS concrete after 14 days of moist curing exhibited fairly low chloride permeability based on the rapid chloride permeability test (RCPT).

14. The initial current (in amperes) flowing through the concrete specimen in the RCPT correlates consistently with the total charge measured in 6 hours. Therefore the initial current, which is an indirect measure of the concrete conductance, can be used as an alternate measurement for the RCPT. The total testing time can thus be shortened by 6 hours.

15. The AC impedance test measures the total resistance (in ohms) of a concrete specimen. This test method is simpler and faster than the RCPT, and has the potential to be used as a substitute for the RCPT. The best correlation between the two test methods is to express the inverse impedance (reciprocal of impedance) in terms of the initial current measured in the RCPT.

16. A "beam" type concrete-to-steel bond test showed that by using the ACI 318 requirement for development length (1993c), sufficient bond strength was developed by VHS concrete such that the steel reinforcement yielded before any significant bond slip occurred.

References

ACI Committee 209. 1993a. Prediction of Creep, Shrinkage and Temperature Effects in Concrete Structures (ACI 209R-92). *ACI Manual of Concrete Practice*, part 1, 47 pp.

ACI Committee 211. 1993b. Standard Practice for Selecting Proportions for Normal, Heavyweight, and Mass Concrete (ACI 211.1-91). *ACI Manual of Concrete Practice*, part 1, 38 pp.

ACI Committee 318. 1993c. Building Code Requirements for Reinforced Concrete (ACI 318-89) and Commentary (ACI318R-89), (Revised 1992). *ACI Manual of Concrete Practice*, part 3, 347 pp.

ACI Committee 363. 1993d. State-of-the-Art Report on High Strength Concrete (ACI 363R-92). *ACI Manual of Concrete Practice,* part 1, 55 pp.

Ahmad, S. H., and Shah, S. P. 1985. Structural Properties of High Strength Concrete and its Implications for Precast Prestressed Concrete. *PCI Journal*, vol. 30, no. 6, Nov-Dec, pp. 91-119.

America's Highways: Accelerating the Search for Innovation. 1984. Special report 202, Transportation Research Board, National Research Council, Washington, D.C.

Carrasquillo, R. L.; Slate, F. O.; and Nilson, A. H. 1981. Microcracking and Behavior of High Strength Concrete Subjected to Short Term Loading. *ACI Journal*, vol. 78, no. 3, May-June, pp. 179-186.

Cook, J. E. 1989. Research and Application of High-Strength Concrete: 10,000 PSI Concrete. *Concrete International*, vol. 11, no. 10, October, pp. 67-75.

Hansen, M. R. 1993. *Durability of High Peformance Concrete*. Ph.D. Dissertation, North Carolina State University, Raleigh, N.C., May, 224 pp.

Jobse, H. J., and Moustafa, S. E. 1984. Applications of High Strength Concrete for Highway Bridges. *PCI Journal,* vol. 29, no. 3, May-June, pp. 44-73.

Leming, M. L. 1988. *Properties of High Strength Concrete: An investigation of High Strength Concrete Characteristics Using Materials in North Carolina.* Report no. FHWA/NC/88-006, Department of Civil Engineering, North Carolina State University, Raleigh, N.C, July, 202 pp.

Mindess, S., and Young, J. F. 1981. *Concrete* Prentice Hall, Inc., Englewood Cliffs, New Jersey, 671 pp.

Moreno, J. 1990. The State-of-the-Art of High-Strength Concrete in Chicago: 225 W. Wacker Drive. *Concrete International*, vol. 12, no. 1, January, pp. 35-39.

Zia, P.; Leming, M. L.; and Ahmad, S. H. 1991. *High Performance Concretes: A State-of-the-Art-Report.* SHRP-C317, Strategic Highway Research Program, National Research Council, Washington, D.C., 250 pp.

Zia, P.; Schemmel, J. J.; and Tallman, T. E. 1989. *Structural Applications of High Strength Concrete*. Report no. FHWA/NC/89-006, Center for Transportation Engineering Studies, North Carolina State University, Raleigh, N.C., June, 330 pp.

Appendix

List of Figures

Figure A.1 Device for mounting transducers on 4 x 8-in. cylinders 82
Figure A.2 Steel jackets for protecting transducers during compression testing 83
Figure A.3 Compression test setup 84
Figure A.4 Transducer mounting device for flexural testing 85
Figure A.5 Beam support for flexural testing 86
Figure A.6 Frame mounting on flexural test beams for recording midspan deflection 87
Figure A.7 Loading arrangement for flexural test 88
Figure A.8 Flexural test setup 89
Figure A.9 Freezing-thawing chamber 90
Figure A.10 Measurement of dynamic modulus of elasticity 91
Figure A.11 Shrinkage test setup 92
Figure A.12 Rapid chloride permeability test (RCPT) vacuum saturation setup 93
Figure A.13 RCPT specimens sealed in two test cells 94
Figure A.14 RCPT test cells attached to power supply 95
Figure A.15 RCPT output being recorded 96
Figure A.16 RCPT output recorded on strip chart 97
Figure A.17 AC impedance test setup 98
Figure A.18 AC impedance test in progress 99
Figure A.19 Loading arrangement for concrete-to-steel bond test 100
Figure A.20 Concrete-to-steel bond test setup 101

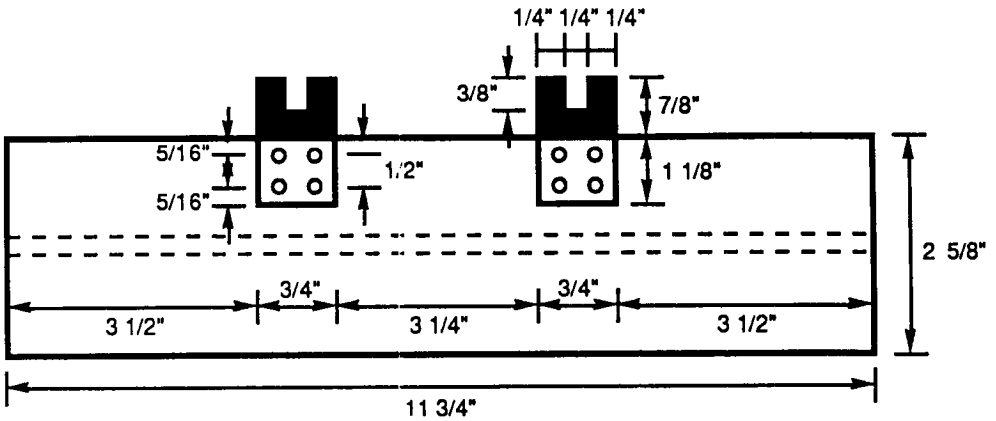

Elevation

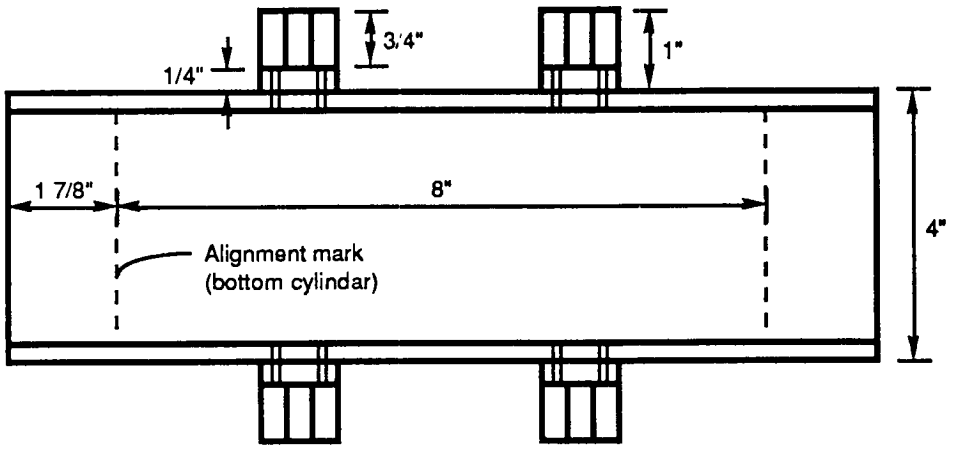

Top View

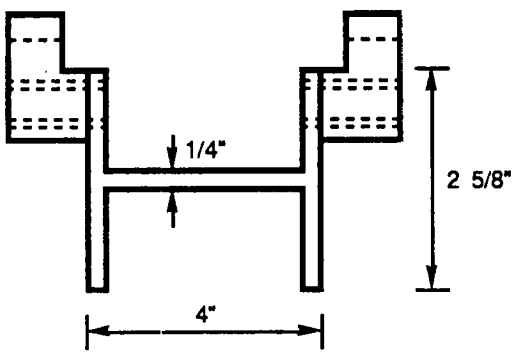

Side View

Figure A.1 Device for mounting transducers on 4 x 8-in. cylinders

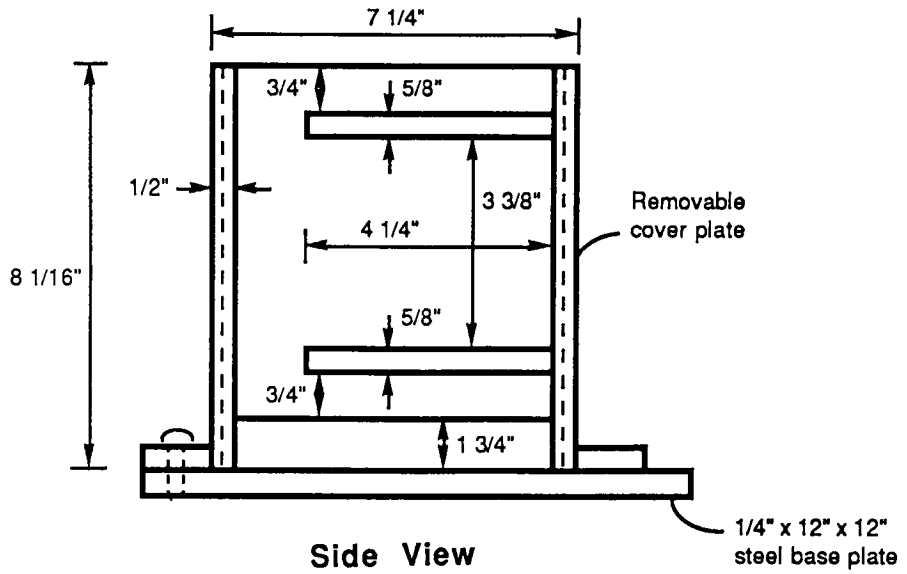

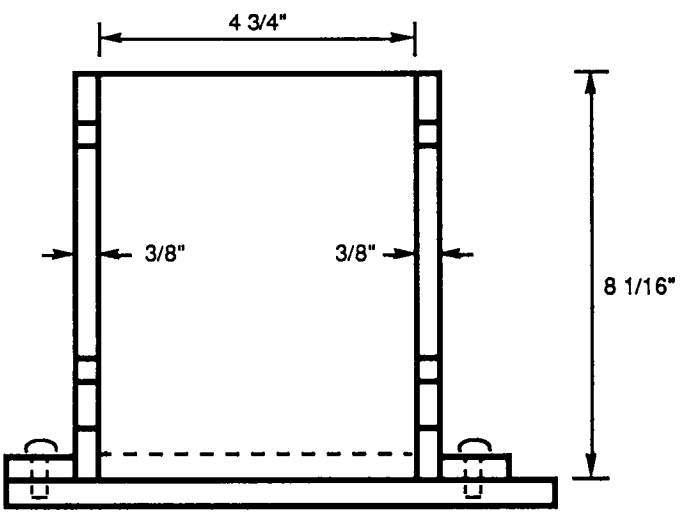

Figure A.2 Steel jackets for protecting transducers during compression testing

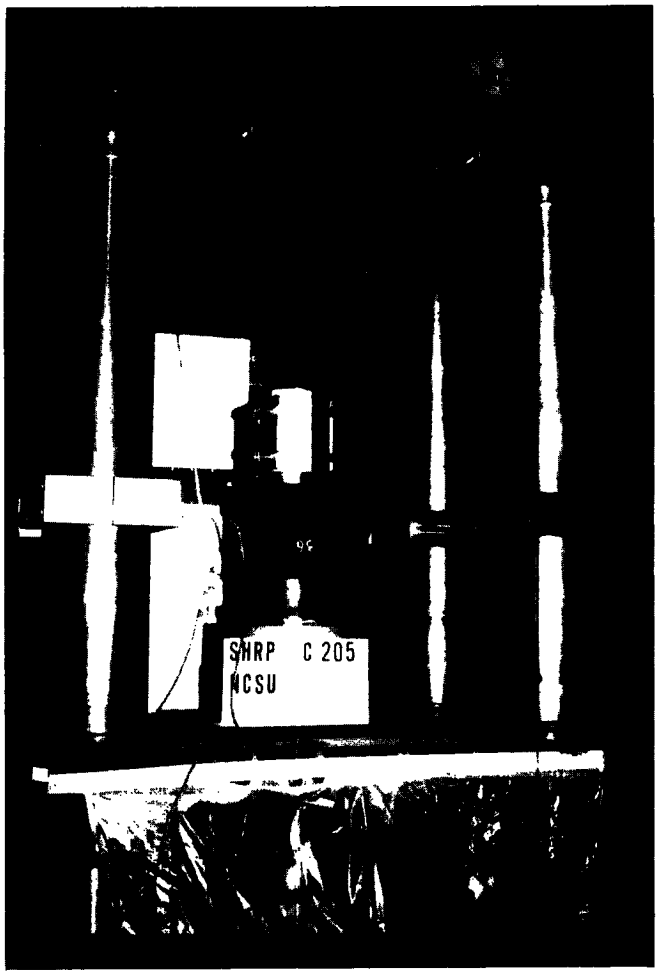

Figure A.3 Compression test setup

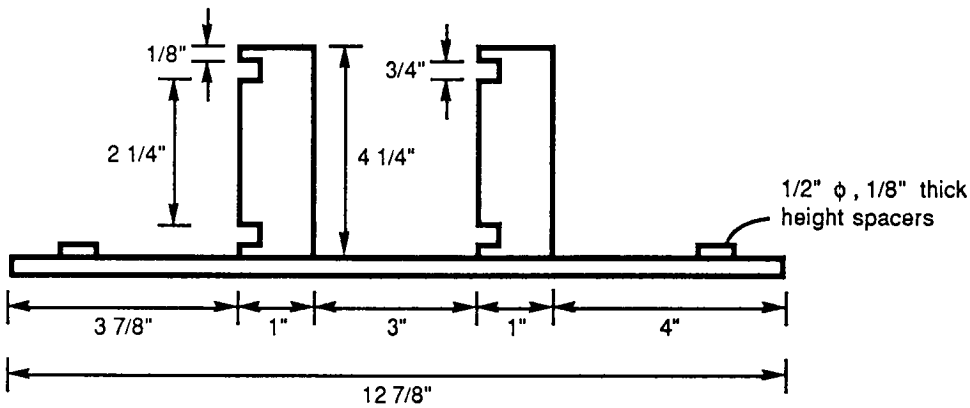

Front View

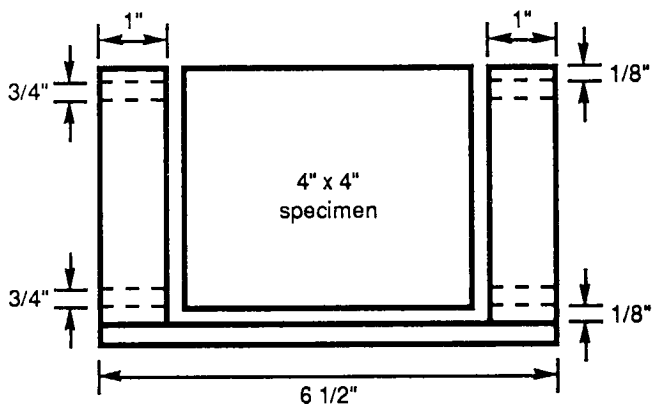

Side View

Figure A.4 Transducer mounting device for flexural testing

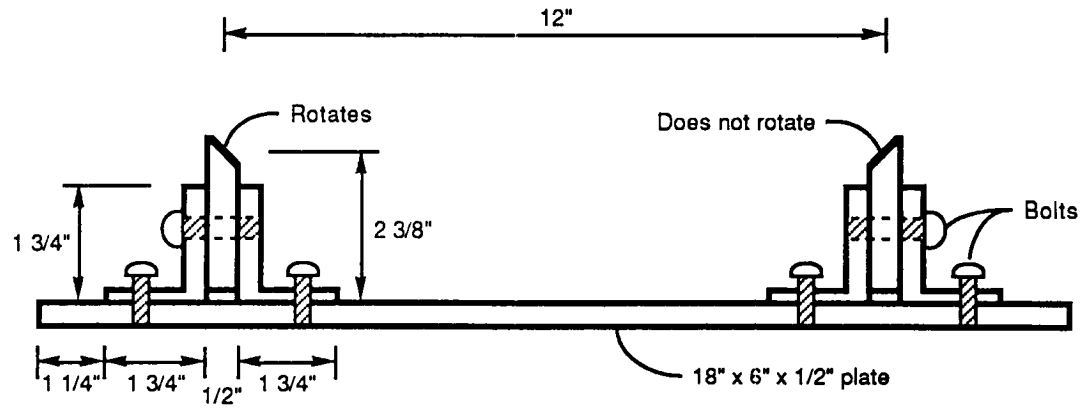

Side View

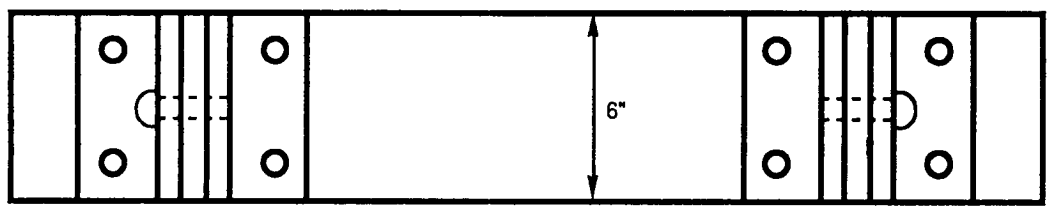

Plan View

Figure A.5 Beam support for flexural testing

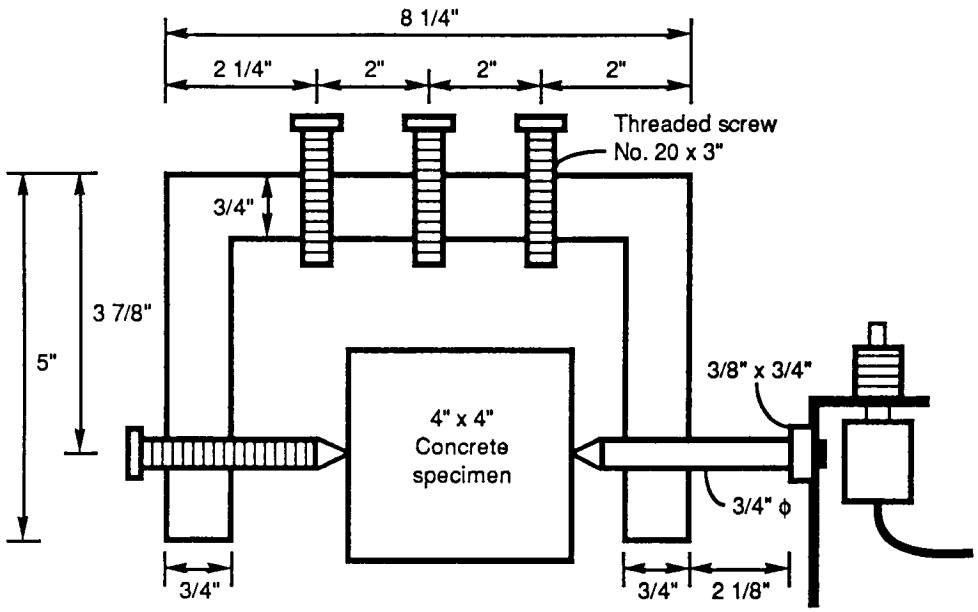

Side View

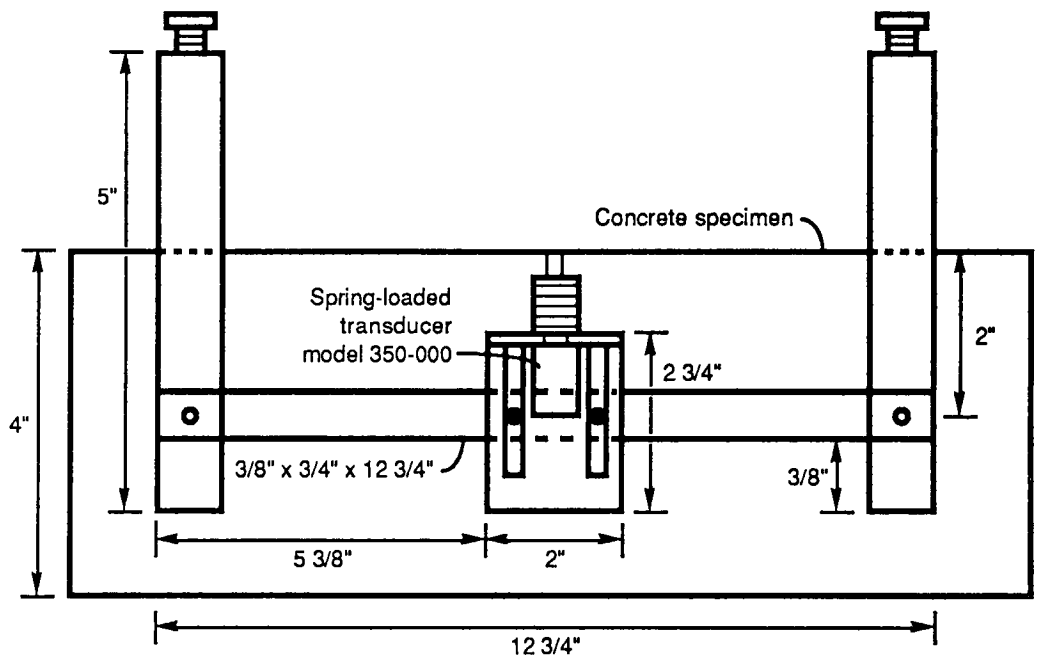

Front View

Figure A.6 Frame mounting on flexural test beams for recording midspan deflection

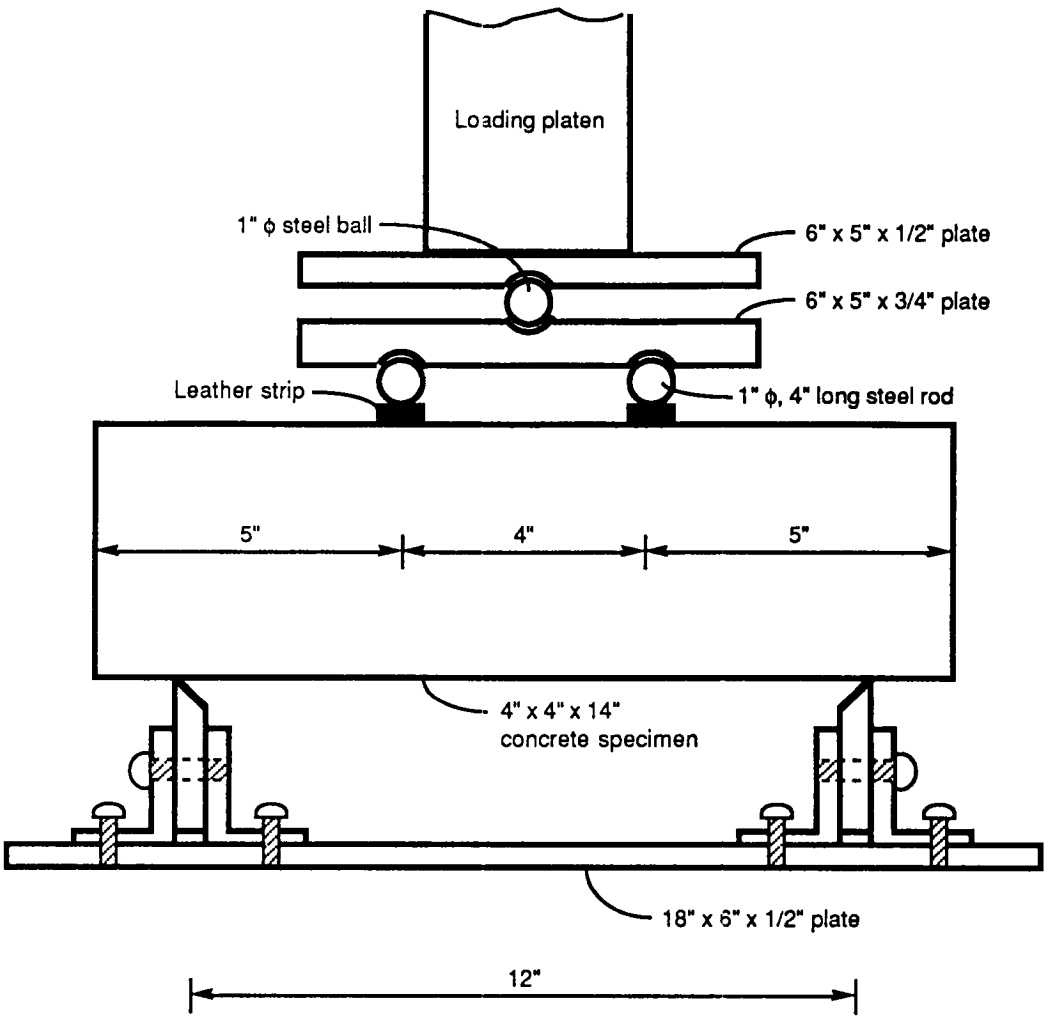

Side View

Figure A.7 Loading arrangement for flexural test

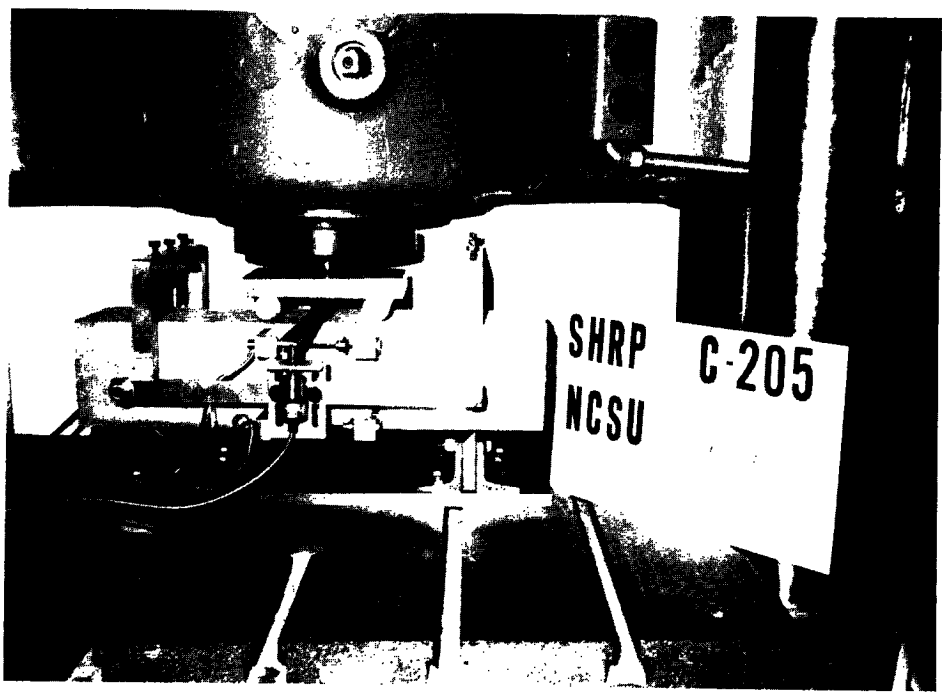

Figure A.8 Flexural test setup

Figure A.9 Freezing-thawing chamber

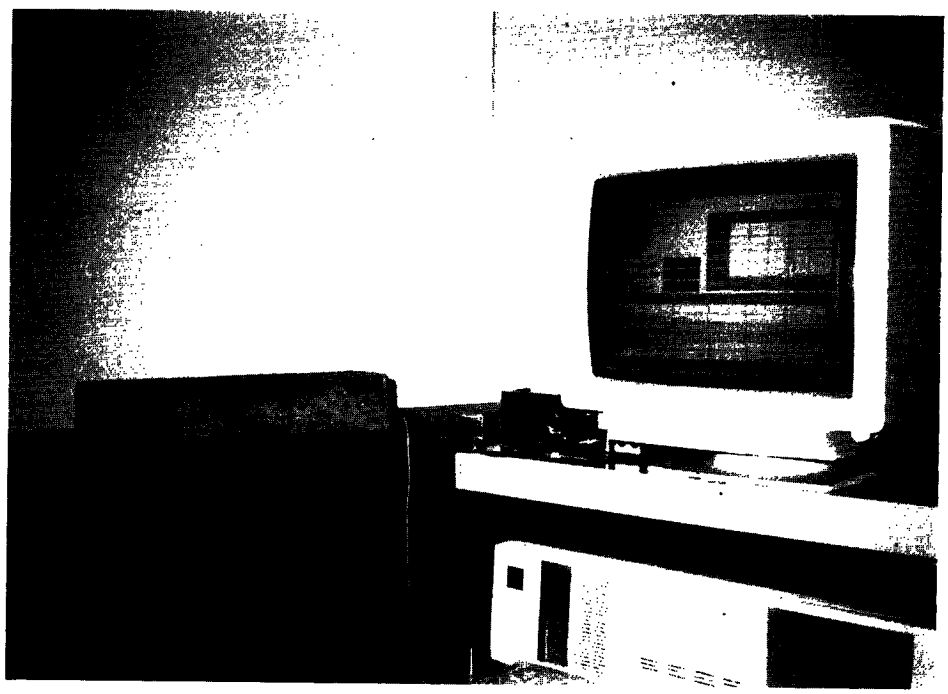

Figure A.10 Measurement of dynamic modulus of elasticity

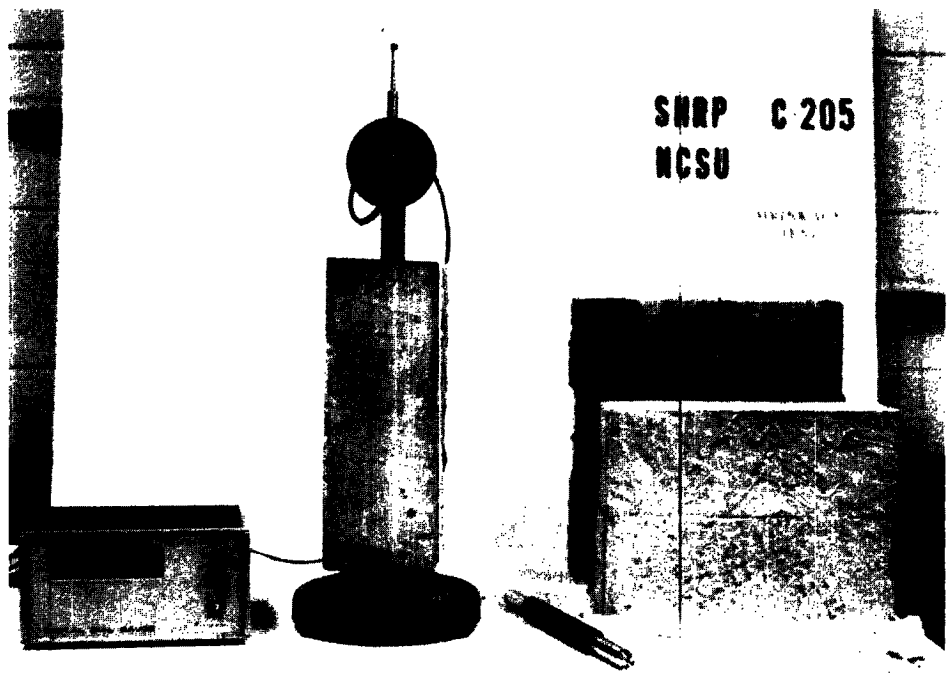

Figure A.11 Shrinkage test setup

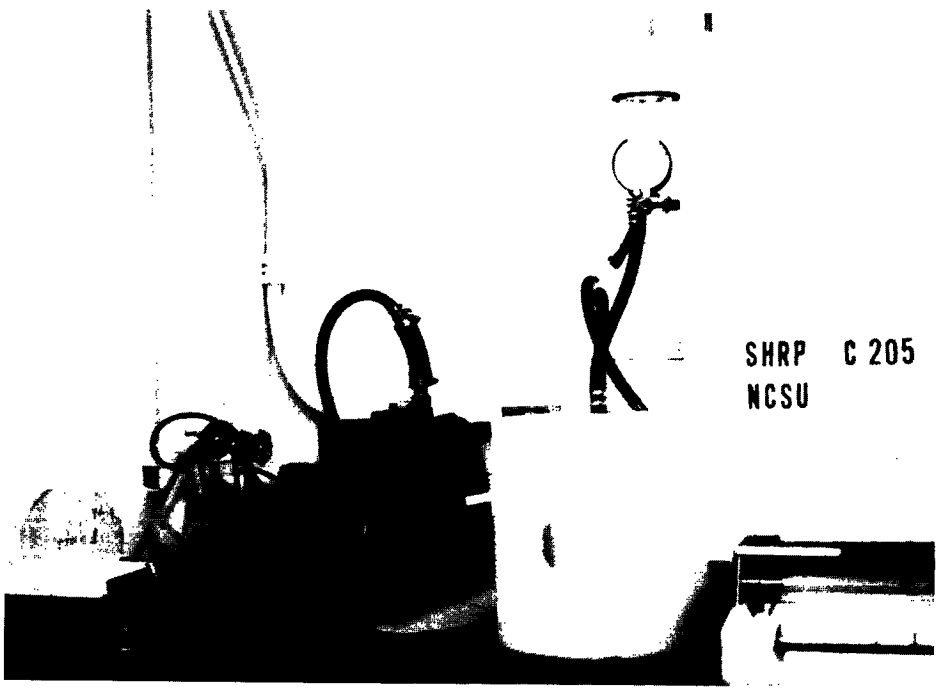

Figure A.12 Rapid chloride permeability test (RCPT) vacuum saturation setup

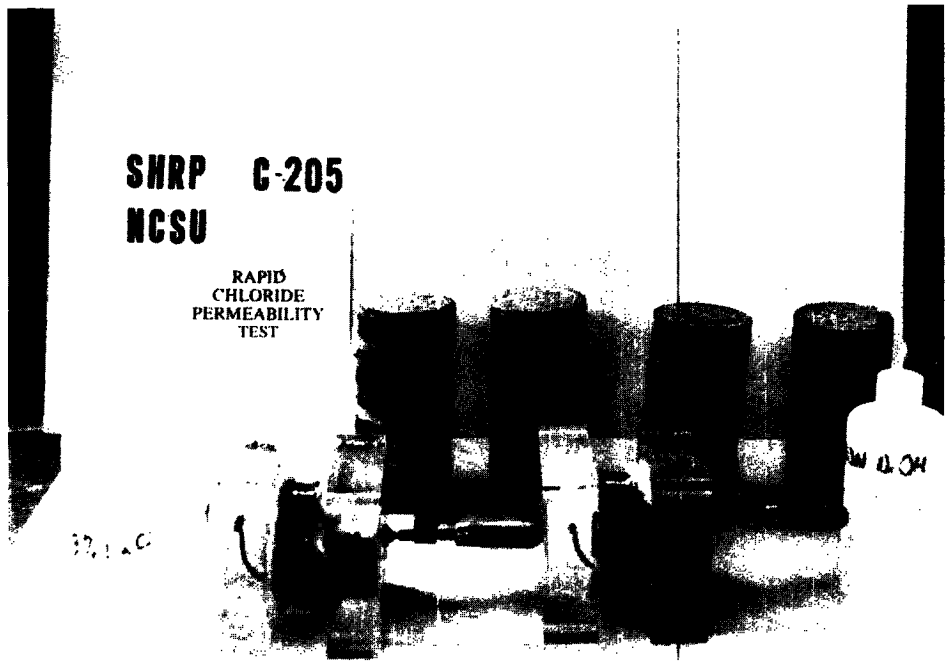

Figure A.13 RCPT specimens sealed in two test cells

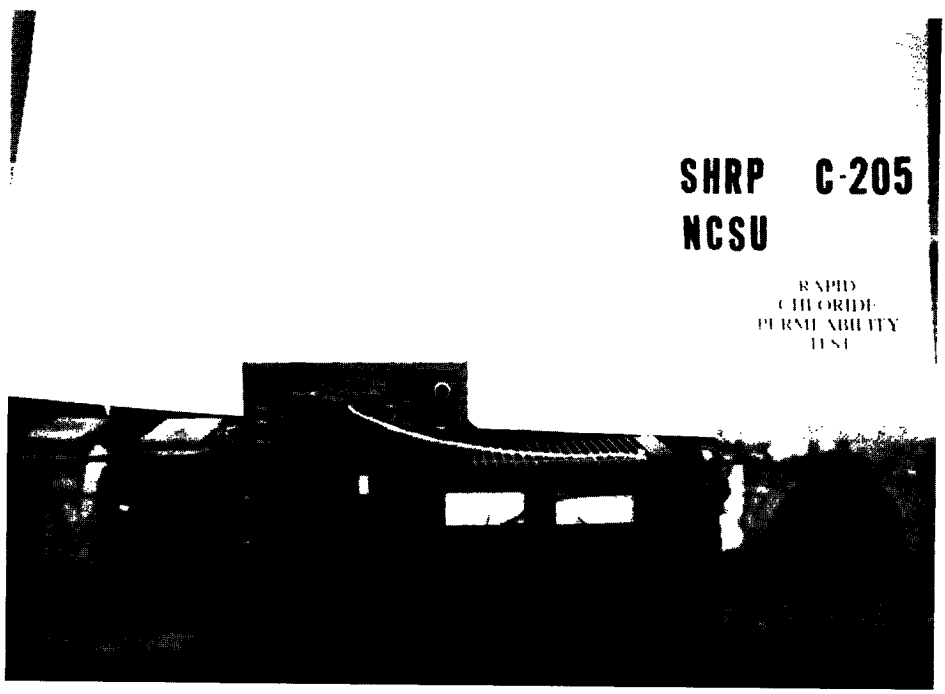

Figure A.14 RCPT test cells attached to power supply

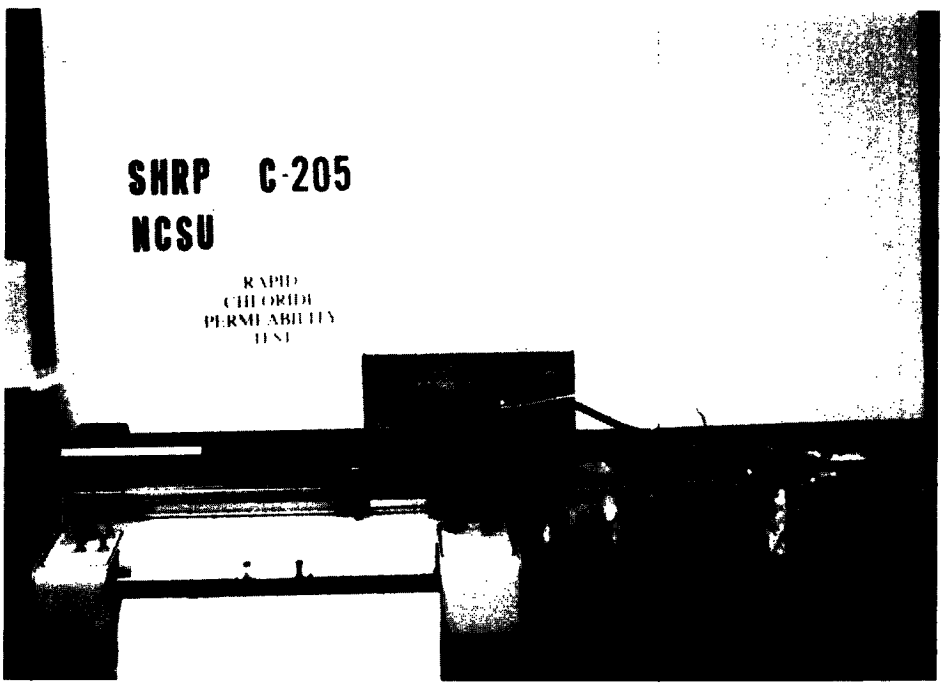

Figure A.15 RCPT output being recorded

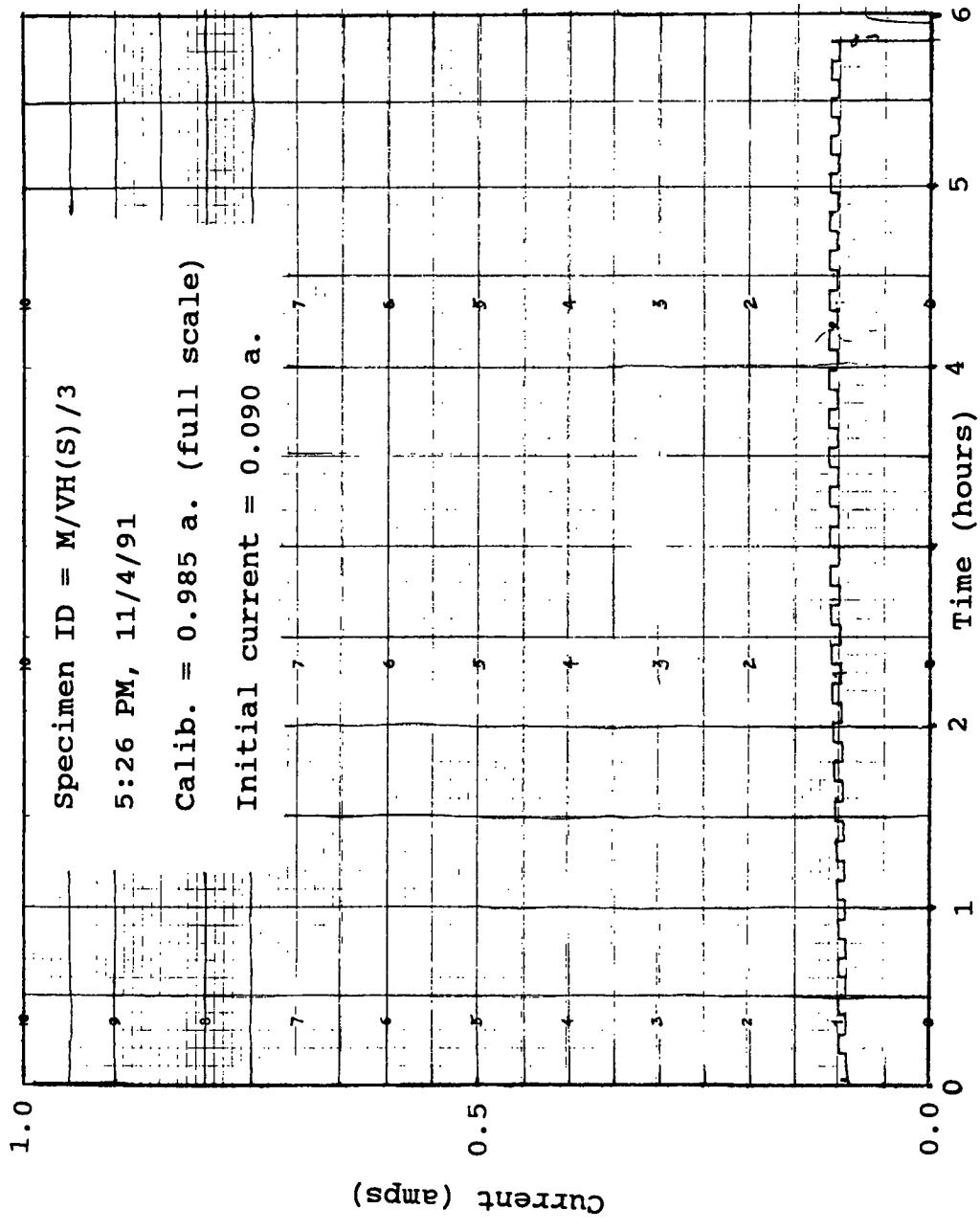

Figure A.16 RCPT output recorded on strip chart

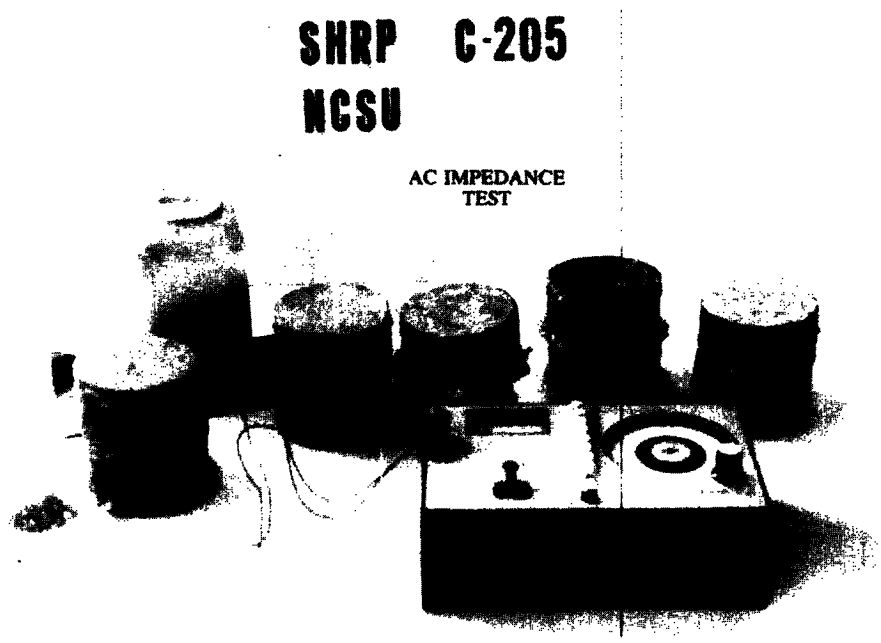

Figure A.17 AC impedance test setup

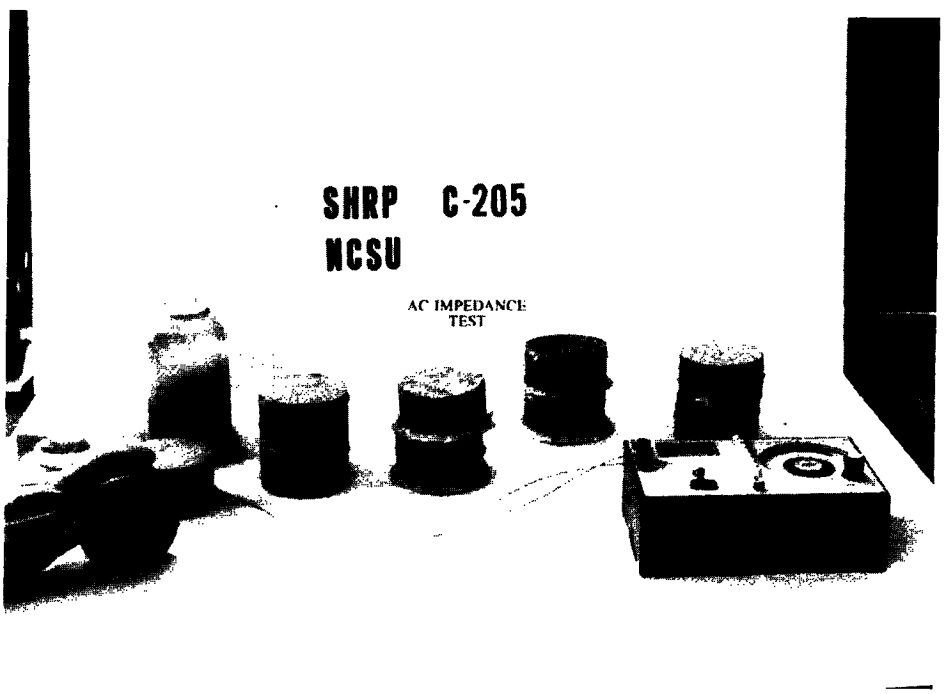

Figure A.18 AC impedance test in progress

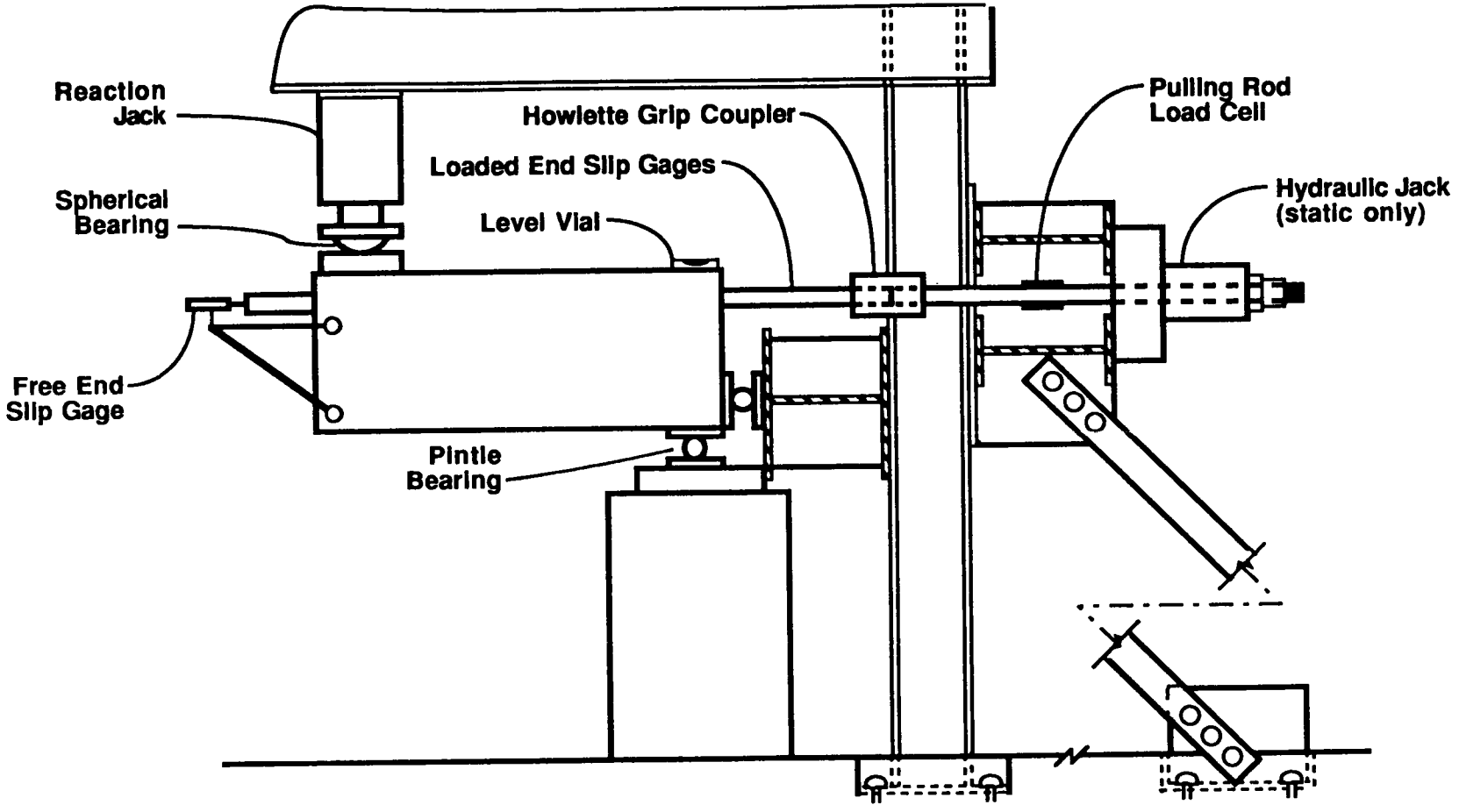

Figure A.19 Loading arrangement for concrete-to-steel bond test

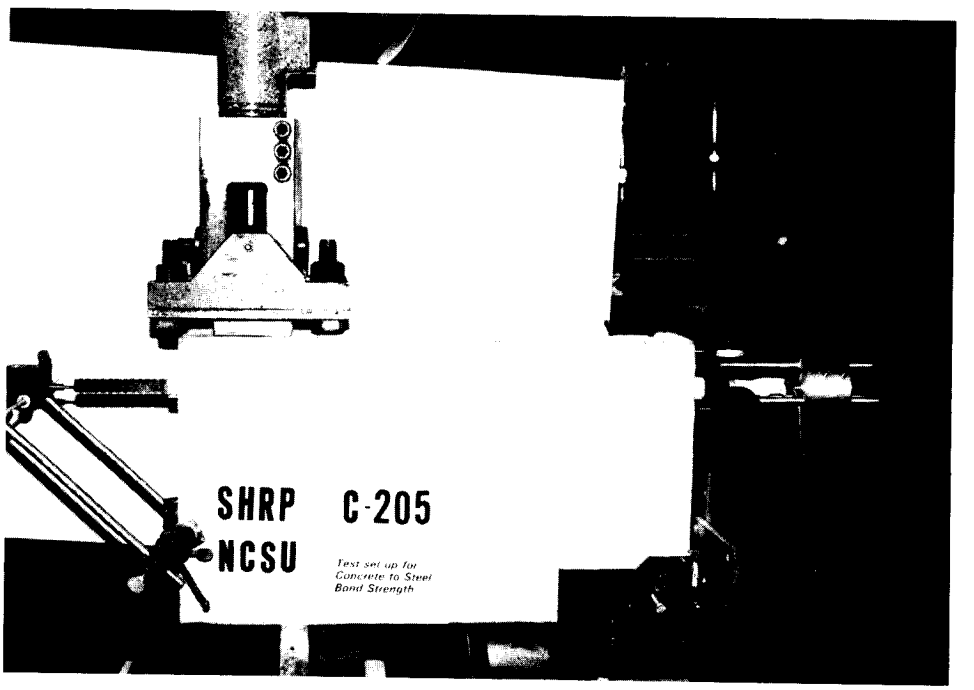

Figure A.20 Concrete-to-steel bond test setup

Concrete and Structures Advisory Committee

Chairman
James J. Murphy
New York Department of Transportation (retired)

Vice Chairman
Howard H. Newlon, Jr.
Virginia Transportation Research Council (retired)

Members

Charles J. Arnold
Michigan Department of Transportation

Donald E. Beuerlein
Koss Construction Co.

Bernard C. Brown
Iowa Department of Transportation

Richard D. Gaynor
National Aggregates Association/National Ready Mixed Concrete Association

Robert J. Girard
Missouri Highway and Transportation Department

David L. Gress
University of New Hampshire

Gary Lee Hoffman
Pennsylvania Department of Transportation

Brian B. Hope
Queens University

Carl E. Locke, Jr.
University of Kansas

Clellon L. Loveall
Tennessee Department of Transportation

David G. Manning
Ontario Ministry of Transportation

Robert G. Packard
Portland Cement Association

James E. Roberts
California Department of Transportation

John M. Scanlon, Jr.
Wiss Janney Elstner Associates

Charles F. Scholer
Purdue University

Lawrence L. Smith
Florida Department of Transportation

John R. Strada
Washington Department of Transportation (retired)

Liaisons

Theodore R. Ferragut
Federal Highway Administration

Crawford F. Jencks
Transportation Research Board

Bryant Mather
USAE Waterways Experiment Station

Thomas J. Pasko, Jr.
Federal Highway Administration

John L. Rice
Federal Aviation Administration

Suneel Vanikar
Federal Highway Administration

11/19/92

Expert Task Group

Stephen Forster
Federal Highway Administration

Amir Hanna
Transportation Research Board

Richard H. Howe
Pennsylvania Department of Transportation (retired)

Susan Lane
Federal Highway Administration

Rebecca S. McDaniel
Indiana Department of Transportation

Howard H. Newlon, Jr.
Virginia Transportation Research Council (retired)

Celik H. Ozyildirim
Virginia Transportation Research Council

Jan P. Skalny
W.R. Grace and Company (retired)

A. Haleem Tahir
American Association of State Highway and Transportation Officials

Lillian Wakeley
USAE Waterways Experiment Station

7/22/93